PneuScape

Towards High Resolution MR Safe Actuation

S.J. Neevel

Technische Universiteit Delft

TU Delft Delft University of Technology

Challenge the future

PNEUSCAPE

TOWARDS HIGH RESOLUTION MR SAFE ACTUATION

by

S.J. Neevel

in partial fulfillment of the requirements for the degree of

Master of Science
in Mechanical Engineering

at the Delft University of Technology,
to be publicly presented on Wednesday October 30th, 2019 at 14:00.

Student number:	4232623	
Project duration:	May 26th, 2018 – October 30th, 2019	
Supervisor:	Prof. dr. ir. Paul Breedveld	
Thesis committee:	Dr. ir. Hans Goosen,	TU Delft
	MSc. Fabian Trauzettel,	TU Delft
	Dr. ing. Roel Penterman,	Demcon Advanced Mechatronics
	MSc. Pieter Wiskerke,	Demcon Advanced Mechatronics

This thesis is confidential and cannot be made public until October 30th, 2020.

TU Delft Delft University of Technology

ABSTRACT

A future version of the DEMCON Needle Placement System (NPS) for use in the Magnetic Resonance Imaging (MRI) scanner requires accurate and small actuators that are MR (Magnetic Resonance) safe; actuators that can safely operate without interfering with the MR environment. The pneumatic stepper motor was chosen for actuation of the aiming segments of the future NPS. The pneumatic stepper motor can be made out of MR safe materials and its actuation principle is MR safe. MR safe, small size pneumatic stepper motors that produce high resolution motion however, do not exist. The goal of this thesis is to design and prototype such a pneumatic stepper motor and test its performance.

An MR safe, high resolution pneumatic stepper motor was designed. This motor, called the PneuScape, was designed to fit in the orientation module of the NPS. The design of the PneuScape consists of dual gear escapement mechanisms, connected with a differential mechanism. Ratchets apply a torque to move the output either clockwise or counterclockwise and the escapement anchors index the movement, creating a step. The PneuScape currently has the smallest designed step size $s_t = 0.83^o$ of any MR safe pneumatic stepper motor.

A prototype of the Pneuscape was developed using rapid prototyping techniques and its performance was evaluated. The total prototype did not meet all design requirements, in particular the requirement of maximum positioning error. The ratchets do not work reliably and result in the motor skipping steps, diminishing the motor's accuracy. The escapement anchors however, show promising results in their performance. Recommendations were given to improve the prototype. If the prototype is improved with aid of the recommendations, a future version of the PneuScape is expected to meet the design requirements. Finally, the work in this thesis has made science take a step towards high resolution MR safe actuation.

PREFACE

This thesis is about a mechanism. This thesis is about a pneumatic stepper motor for use inside an MRI scanner. The motor will be incorporated in the Needle Placement System (NPS), developed by Demcon, the company for which I did this work.

In the beginning when Pieter Wiskerke of Demcon first asked me to help redesign the NPS for use in the MRI scanner, I had no clue that I would have the chance to really come up with intricate and fundamental mechanisms and design them. Later, it was decided I would design the motor of the NPS for use in an MRI scanner. Designing actuators for use in an MRI scanner proved to be challenging, but it was the right amount of challenging. Ultimately, the total combination of creative design, 3D CAD drawing, producing parts, building a prototype and programming the motor was one that I thoroughly enjoyed.

The future of the Demcon NPS is uncertain at this moment, though I really see value in further development of the system. Finally, I hope that one day my work could benefit healthcare, all be it ever so slightly.

I would like to thank my professor Paul Breedveld for his advice and guidance through this thesis. We have spent some good time together discussing all sorts of mechanisms and brainstorming to find new solutions. The mechanisms and tools he invented and mechanical calculators he owns always were an inspiration for a new discussion.

Furthermore, I want to thank Demcon for the good environment and opportunity to do this work, for this thesis and the internship leading up to it. Thanks to Pieter for selecting me to work on the NPS in my internship and for offering me the opportunity to continue my work during this thesis.

I would like to thank Julian for the numerous discussions and advice about the core mechanical engineering aspects of the design. I want to thank Jurriën for reading through my literature review. Thanks to my parents, for supporting me during this thesis. Thanks to Sherin for letting me learn the value and difficulty of my work by showing me that it is impressive, even if I sometimes did not see it myself.

Finally, I would like to thank Roel Penterman for his guidance in this project as the main supervisor. I would like to thank him too for the career advice he gave, the guidance in my previous internship, the Friday afternoon chats and the fun in our side quest of preparing the water rockets!

S.J. Neevel
Enschede, October 2019

CONTENTS

1 Introduction **2**
- 1.1 Background of Magnetic Resonance Imaging . . . 2
- 1.2 DEMCON Needle Placement System . . . 2
- 1.3 Actuation Principle for NPS . . . 3
  - 1.3.1 Continuous Pneumatic Motors . . . 3
  - 1.3.2 Pneumatic Stepper Motors . . . 3
- 1.4 State of the Art in Pneumatic Stepper Motors . . . 5
- 1.5 Problem Definition . . . 5
- 1.6 Goal of the Study . . . 5
- 1.7 Structure of the Report . . . 5

2 Design Requirements **6**
- 2.1 Introduction . . . 6
- 2.2 Primary Requirements . . . 6
- 2.3 Design Conditions . . . 6
- 2.4 Wishes . . . 6

3 Conceptual Solutions **7**
- 3.1 Introduction . . . 7
- 3.2 Functions . . . 7
- 3.3 Selection of Best Conceptual Solutions . . . 7
  - 3.3.1 Provide High Positioning Resolution . . . 8
  - 3.3.2 Providing Discrete Motion . . . 10
  - 3.3.3 Provide Force . . . 12
  - 3.3.4 Ensure Correct Execution of Rotary Motion . . . 13

4 Integrated Concepts **14**
- 4.1 Introduction . . . 14
- 4.2 Dual Gear Stepper . . . 14
- 4.3 Dual Escapement with Vane . . . 15
- 4.4 Dual Escapement with Ratchets . . . 16
- 4.5 Concept Selection . . . 16

5 Final Design in Detail **17**
- 5.1 Introduction . . . 17
- 5.2 Final Design: PneuScape . . . 17
- 5.3 Anchor Geometry: Force Analysis . . . 18
- 5.4 Selection of Number of Teeth . . . 20
  - 5.4.1 Design Space & Upper Bound on Rotation of Gear 1 . . . 20
  - 5.4.2 Results & Conclusion . . . 21
- 5.5 Point-to-Point Movement: Step Planning & Execution . . . 22
  - 5.5.1 Step Planning . . . 22
  - 5.5.2 Step Execution . . . 22
- 5.6 Software . . . 22
- 5.7 Prototype . . . 23

6 Testing **25**
- 6.1 Introduction . . . 25
- 6.2 Escapement Mechanism . . . 25
  - 6.2.1 Goal of Tests, Method & Setup . . . 25
  - 6.2.2 Results & Discussion . . . 26

6.3 Escapement at 5 m Distance . . . 26
6.3.1 Goal of Tests, Method & Setup . . . 26
6.3.2 Results & Discussion . . . 27
6.4 Total Motor . . . 27
6.4.1 Goal of Tests, Method & Setup . . . 27
6.4.2 Total Motor: Results & Discussion . . . 27

7 Discussion **29**
7.1 Performance . . . 29
7.1.1 Primary Design Requirements . . . 29
7.1.2 Design Conditions . . . 29
7.1.3 Wishes . . . 29
7.2 Recommendations for Future Work . . . 30
7.2.1 Improving Accuracy & Precision . . . 30
7.2.2 Improving Speed & Torque . . . 31
7.2.3 New Research Directions . . . 31
7.3 Additional Fields of Application . . . 31

8 Conclusion **32**

Bibliography **33**

A Draft of Paper 'Actuation principles in the magnetic resonance environment: A review of the patent literature' **35**

B Overview of the State of the Art in PSMs **54**

C Positioning Error of Aiming Segments **56**

D Geometry Variables of Escapement Anchors **57**

E Step Planning: Table of Actions **58**

F MATLAB Code **59**

G Beckhoff Code **67**

H Technical Drawings **78**

1

INTRODUCTION

1.1. BACKGROUND OF MAGNETIC RESONANCE IMAGING

Magnetic Resonance Imaging (MRI) is a technique used to capture 3D images of the human body. MRI offers good contrast resolution to accurately detect anatomic features [1, 2]. Surgical interventions in the human body can be guided by MRI. These interventions include, among others, MRI-guided brachytherapy, MRI-guided prostate biopsy and MRI-guided neurosurgery [2]. Typically, in such MRI-guided interventions, a needle or instrument has to be positioned in the body to reach a specific target, for instance a tumor. It is key that this needle or instrument reaches the target accurately, and mechatronic systems in surgery can significantly improve surgeons' technical capabilities to perform these interventions [3]. Different types of mechatronic devices have been developed to assist in positioning the needle or instrument. Multiple reviews of the scientific literature on mechatronic devices in MRI-guided surgery have been done [2, 4, 5].

MRI scanners consist of electromagnets and Radio Frequency (RF) coils. Scanners with a field strength of 1.5 T to 3 T are typically used in hospitals. However, clinical trials are being conducted with high resolution 7 T scanners. Any instrument or device used in the Magnetic Resonance (MR) scanner room must comply with the electromagnetic effects of the MRI scanner; it must be safe for use in the MR environment. Three terms regarding MR safety have been defined by the ASTM F2503 standard [6]: a device can be MR safe, MR conditional or MR unsafe. As described by Shellock et al.[7]: "A device is MR safe if it poses no known hazards in the MR environment. MR safe devices are nonconducting, nonmetallic, and nonmagnetic. A device may be determined to be MR safe by providing a scientifically based rationale rather than test data." In contrast, a device can be MR conditional: it poses no known hazards in a specified MR environment. Testing of the device must be performed in order to specify the conditions of usage. For example, conditions can be set on the distance from the device to the MRI scanner, or on the time the device can be used close to the MRI scanner. MR unsafe devices pose safety risks to the patient or user and cannot be used in the MR environment.

Figure 1.1: DEMCON Needle Placement System, from: Arnolli [8]

1.2. DEMCON NEEDLE PLACEMENT SYSTEM

Arnolli [8] developed a system for CT-guided needle placement in the thorax and abdomen, see Figure 1.1. This Needle Placement System (NPS) was developed at DEMCON Advanced Mechatronics B.V. in collaboration with the University of Twente. The system assists in ablation or biopsy procedures by guiding the manual insertion of the needle in the correct direction towards the target lesion. The NPS consists of an arm and an orientation module (OM). The OM incorporates two aiming segments and a pointer, see Figure 1.2. The arm allows for placement of the pointer at the position of the entry point for the needle. Subsequently, the system automatically aims the pointer at the right angle(s) towards the target in the patient, based on CT scans of the patient and the NPS together. Afterwards, the pointer is removed and the needle is attached to the system as in Figure 1.1. Finally, the needle can be manually inserted.

The NPS is designed to be used in clinical intervention and is CT scan compatible: materials are used that only minimally obstruct the X-rays. Any metal is placed in the foot of the robot, far from the CT scan

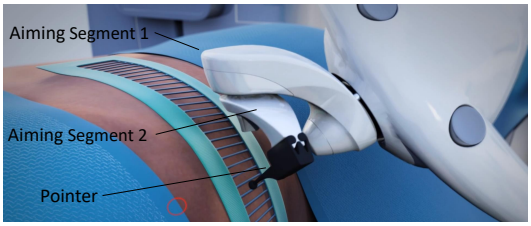

Figure 1.2: NPS orientation module (OM) and its aiming segments and pointer, adapted from: Arnolli [8].

region of interest. In the NPS, electromagnetic motors are used to actuate the aiming segments. These motors are placed near the foot of the NPS, and motion is transferred with a cable system to the aiming segments. The cable system uses endless dynamo cables and pulleys that require special manufacturing, making the system complex and expensive. Currently, DEMCON is in the process of further developing the NPS for use in the MRI scanner. An improvement DEMCON wants to make is to place the motors in the OM or directly in the aiming segments, thus removing the complex cable system. Furthermore, in the future, DEMCON wishes to attach an MR safe biopsy module to the aiming segments, to automate the process of taking biopsies. The module remains to be developed, so the exact details of this module are yet unknown.

A key challenge in designing the NPS for use in the MRI scanner is making sure its actuators are MR safe or conditional. The currently used electromagnetic motors are not MR safe, because they will be attracted by the field of the MRI scanner [9]. Moreover, during operation, these motors will produce electromagnetic rays, creating artifacts in the MR image. The artifacts can hinder identification of abnormal tissue or diagnostics with MRI in general. The future version of the NPS for use in the MRI scanner must be able to operate and adjust the position of the aiming segments without disturbing the imaging process, so a proper MR safe actuator must be chosen.

1.3. ACTUATION PRINCIPLE FOR NPS

There are multiple actuation principles used in the MR environment. In order to find a fitting MR safe actuator for the NPS, a patent review on the actuation principles used in the MR environment was done, see Appendix A. A categorized overview of actuation principles in the MR environment is given in Figure 1.3. There are two main categories of actuators, the first category consists of actuators that have their kinetic energy externally induced and transmissioned by means of pneumatic, hydraulic or mechanic transmissions. The second category induces their kinetic energy internally in the actuator. The group of MR safe actuation principles contains actuators that have their kinetic energy transmissioned; pneumatic, hydraulic and mechanic transmissions. Furthermore, actuators that rely on heating of a gas or liquid, chemicals or light to induce kinetic energy also belong to the group of MR safe actuation principles.

Hydraulic transmissions can suffer from leakage and mechanic transmissions are not flexible in placement of the NPS on the patient bed. Actuators relying on heating of a gas or liquid must use a controllable heating process which is not based on electricity. Parts close to the patient may heat up, and exhaust gasses could leak into the MR room. Chemical actuators and their chemical processes are complex to accurately control. Light activated polymers show a low power-density ratio, and slow response times. Pneumatics are selected as the most promising actuation solution. Pneumatic actuators can be made of MR translucent materials and do not rely on electromagnetism to operate, so they are MR safe and produce little image distortion is. Moreover, pressurized, treated medical instrument air is available in most operating theaters, which can be used as a convenient energy source. Furthermore, a shift towards the use of MR safe and purely pneumatic actuators is justified, since more powerful MRI scanners will be used in the future [2].

1.3.1. CONTINUOUS PNEUMATIC MOTORS

Pneumatic rotational actuators can be divided into two groups: continuous motors and stepper motors. In continuous motors, a stream of air spins a central rotor. Examples of continuous motors are vane or turbine type motors. Regulating the pressure and flow of the air with valves influences the speed of the rotor, and can be used to position the actuator. MR unsafe control systems and valves can be placed outside of the MR room, in order not to influence the imaging process. Long tubes must then be used to transmission the kinetic energy from the valves to the actuator. Due to the pneumatic losses in the long tubes, pneumatic continuous motors present complicated dynamic behaviors, including compressibility, viscosity, turbulence, throttling, friction and leakage [10]. This affects the controllability and accuracy of the actuator.

1.3.2. PNEUMATIC STEPPER MOTORS

A pneumatic stepper motor (PSM) relies on the timed sequence of a series of pneumatic actuators to turn a rotor stepwise. The control signals are discrete Boolean pulses. Typically in pneumatic stepper motors, a first actuator contracts fully, and the next actuator extends fully, creating a step of the rotor. The individual position of the actuators needs not be controlled accurately, since a full extension and retraction of the actuators creates a step of the rotor.

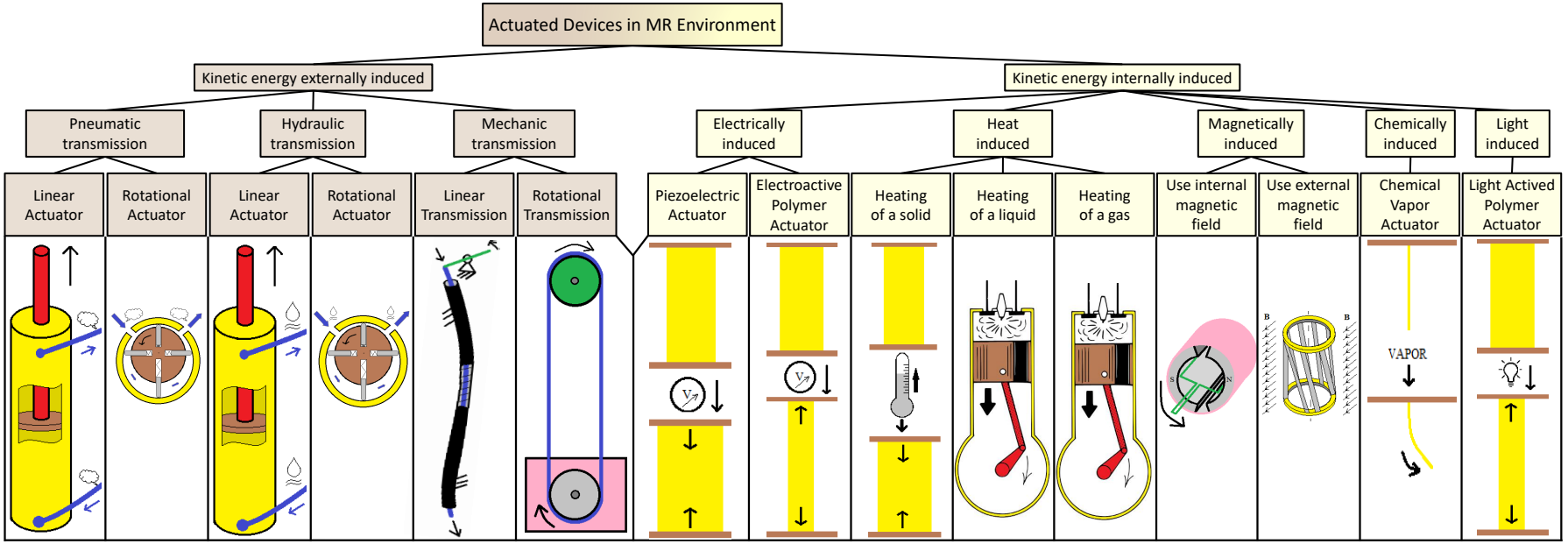

Figure 1.3: Classification of actuation principles. Two main categories of actuators exist: the first category consists of actuators that have their kinetic energy externally induced and transmissioned to the actuators. The second category induces their kinetic energy internally in the actuator. Figure adapted from the patent review in Appendix A.

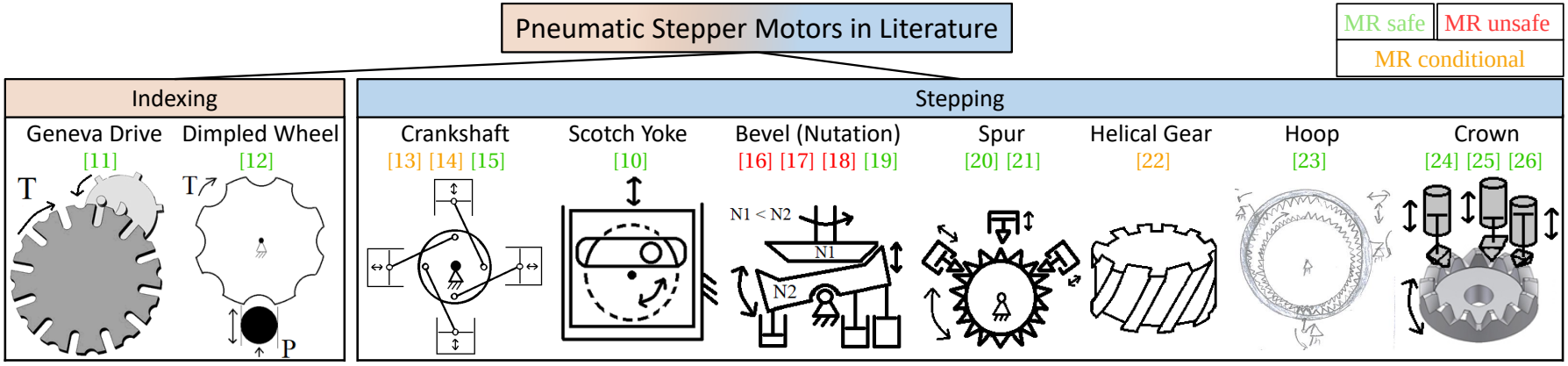

Figure 1.4: Categorization of pneumatic stepper motors in literature. The references to literature are below their respective category, and are colored to indicate their MR safety. Picture of crown gear adapted from: ASSAG [27].

Therefore, the pneumatic stepper motor does not suffer from complicated dynamic behaviors in the air tubes, resulting in higher accuracy in positioning and control. Furthermore, pneumatic stepper motors are tolerant for small air leakages, can be controlled with a standard pneumatic valve manifold, and allow for step wise position control without need for a position feedback system [21]. Therefore, the PSM is chosen as actuation principle for the NPS.

1.4. STATE OF THE ART IN PNEUMATIC STEPPER MOTORS

An overview of the literature on pneumatic stepper motors has been made by Groenhuis and Stramigioli [21] and Boland *et al.* [15]. They report on the size, step size, torque and speed characteristics of the motors. To extend the information on different designs, a literature search was done. PSMs in literature were included when the following definition applied: a PSM produces a discrete stepping motion, and is controlled by Boolean pulses of air. The Web of Science Core Collection was used with the following search query: "pneumatic* AND stepp* AND (motor* OR actuat*)". Furthermore, a search on Google with the query: "Pneumatic stepper motor" revealed one commercially available PSM [19]. These searches include motors which are MR safe, conditional and unsafe. Appendix B gives an overview of designs of pneumatic stepper motors, listing size and performance measures such as step size, power and speed. The appendix also indicates the MR safety of the motors. The development of the motor in this thesis should not infringe any patents, so the appendix shows if the motors in literature have been patented. Multiple types of PSMs can be identified in literature. Figure 1.4 gives an overview of the stepper motors.

There are two classes of PSMs; motors that perform stepping and motors that perform indexing. In indexing, a torque is applied to the output axle by an actuator that accelerates the output axle. A separate actuator provides a stopping force to decelerate the output axle. In order to stop the output axle at a known location, the stopping force is applied after the output axle has turned a specific indexing distance [1]. Indexing is done by Wineland *et al.* [11], a continuous air motor provides the actuating force and is indexed by a Geneva drive. Would no stopping force be provided by the Geneva drive, the output axle would continuously turn. Stepping consists of a sequence of discrete actuation actions on the output axle. These actuators both accelerate and decelerate the output axle. If no action is taken, the output axle does not turn, since it is held stationary by the force of the actuator. Stepping is done by, among others, Groenhuis and Stramigioli [21]: teeth are sequentially pushed into a spur gear to produce a stepping motion.

The highest resolution that has been reached with a PSM is a step size of 0.25° [16]. However, this motor is MR unsafe. There is a motor that reaches a step size of 0.5° [22] and is MR conditional. However, this motor has a power of $5.9 * 10^{-4}$ W, which is several orders of magnitude lower than other pneumatic stepper motors. The state of the art in pneumatic stepper motors is currently embodied by Groenhuis *et al.* [20], Baumgartner Maschinenbau AG [19] and Farimani and Misra [10]. Their motors deliver a reasonable amount of power compared to other motors ($10^0 - 10^1$ W), are MR safe and have a step size of 2.86° or 3°.

1.5. PROBLEM DEFINITION

The geometry of the NPS' aiming segments, combined with the maximum error tolerated in placing the needle require the aiming segments to be positioned with a maximum error of 0.46°. Appendix C explains the calculation of this error. The error means that a step size of less than $2 * 0.46 = 0.92°$ is required. Current state-of-the-art MR Safe PSMs have a step size of 2.86°. Furthermore, DEMCON wishes to have the motors placed in the OM or aiming segment in order to remove the current complex cable system. This OM and aiming segments have limited space, and a majority of PSMs in literature do not fit in this space. In conclusion: MR safe, small size and high resolution pneumatic stepper motors do not exist.

1.6. GOAL OF THE STUDY

The goal of this study is to design and prototype a high resolution MR safe pneumatic stepper motor for actuation of the aiming segments of the NPS. A subsequent goal is to evaluate the performance of this prototype.

1.7. STRUCTURE OF THE REPORT

This report is structured as follows: Chapter 2 introduces the design requirements of the motor. Chapter 3 states the functions of the design and discusses the conceptual solutions. In Chapter 4, integrated concepts are compiled from the conceptual solutions and a final integrated concept is chosen. The final design and its prototype are elaborated on in Chapter 5. Testing the prototype on the design requirements is described in Chapter 6. Chapter 7 discusses the performance of the PSM by reviewing which design requirements are met and gives recommendations for future work. Finally, Chapter 8 concludes the report.

[1] The indexing distance will be called a 'step' throughout this thesis.

2

Design Requirements

2.1. Introduction

This chapter introduces the requirements of the pneumatic stepper motor. The design requirements are split into three categories: primary design requirements, design conditions and the category of wishes. The primary design requirements cover criteria for the most important performance of the motor. The design process aims to maximize the performance on these requirements. The design conditions must also be met, but do not require the main design effort. Wishes are features that are nice to have, but are not necessary for the design to work.

2.2. Primary Requirements

P1 *Error < 0.46º.* Both aiming segments must be positioned with this maximum error. The sum of accuracy and precision of the movement must remain within this error. This follows from a target of 10 mm diameter needing to be hit at 250 mm depth, leading to 5 mm one sided error budget [8]. Appendix C uses the geometry of the aiming segments to calculate a worst case configuration and the maximum error in rotation.

P2 *Design space according to Figure 2.1.* The motors to actuate the aiming segments must fit in the OM. The body of the OM is a frustum with base 100x48 mm, a top of 40 mm diameter and a height of 100 mm. The aiming segments in the OM allow for a small extra design space.

P3 *Torque > 0.62 Nm.* The output torque of the motor. The value is the torque needed to hold a biopsy module of 0.5 kg mounted at 10 cm from segments 2's axis plus the hand of the operator (4N at 3 cm distance) resting on segment 2 during insertion of the needle [8].

P4 *Speed > 21 º/s.* Any motion must be completed within 15 seconds in order not to slow down the procedure of taking biopsies. The geometry of segment 2 allows for a maximum rotation of 310º, resulting in the specified speed.

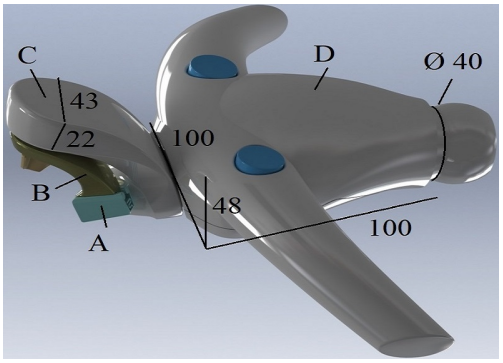

Figure 2.1: The OM with approximate dimensions of design space and indications of parts. Aiming segment 1 (C) is connected to the main body of the OM (D). A needle clip (A) is used to attach the needle to aiming segment 2 (B). Dimensions are in mm.

2.3. Design Conditions

C1 *MR safe.* The motor must be MR safe; it must not disturb the imaging process. The motor can thus not contain any metallic, magnetic or electrically conductive materials.

C2 *Sterile.* The device shall support sterile operation.

C3 *Stiffness.* The motor should be stiff enough to satisfy the error of P1 when the torque of P3 is applied as a load on the output and movement is executed.

C4 *Vibrations.* After execution of a step, any vibration on the output should dampen out to meet the error of P1 before a new step is taken, when the motor runs with the speed of P4.

C5 *Range of motion of 135º & 310º.* The motor for segment 1 must provide at least 135º movement. The motor for segment 2 must provide movement for at least 310º.

2.4. Wishes

W1 *Sound < 50 dB.* Sound produced by operation of the motors. Based on not disturbing speech.

3

Conceptual Solutions

3.1. Introduction

This chapter describes the conceptual design process of the pneumatic stepper motor. First, functions that the design must fulfill will be defined. In Section 3.3, solutions are conceptualized that provide ways to solve the functions and a choice of the best conceptual solutions per function is made. The choice is based on how well each solution fulfills the design requirements and additional design criteria. Chapter 4 compiles three integrated concepts from the best conceptual solutions.

3.2. Functions

The pneumatic stepper motor has to fulfill certain functions. For the following functions, multiple solutions will be conceptualized in the next section.

- Provide high positioning resolution
- Provide discrete rotary point-to-point motion
  - Provide actuating force
  - Provide stopping force
- Ensure correct execution of rotary motion

The first function is to provide a high resolution of the motion. As discussed in Chapter 1, the highest resolution reached by a state-of-the-art MR safe PSM is a step size of 2.86°. Since the maximum error allowed is $\alpha = 0.46°$, the step size $s_t \leq 2 * 0.46 = 0.92°$.

For the second function, the PSM must provide a discrete rotary point-to-point motion on an output axle. Any point-to-point movement can be split into two functions: provide an actuating force that accelerates that output axle and load, and provide a stopping force to stop the motion at a predefined point.

The final function is to ensure a correct execution of the rotary motion. In normal practice, the positioning of the stepper motor is done by feed forward control; by counting how many steps are taken the position of the output axle is known. However, there could be failure scenarios in which the position of the output is changed without the controller being aware of it. For instance, the user could hit the aiming segments by accident and make the stepper motor skip steps. The output would move uncontrollably. When this peak force disturbance is applied during motion, the motor should still reach its position set point. It is therefore necessary to ensure the motion was correctly executed. Furthermore, at standstill, the motor must keep its position.

3.3. Selection of Best Conceptual Solutions

Having defined the functions of the design, conceptual solutions can be formed for each function. The solutions to each function will be described in separate subsections. All subsections start with a short description of the main strategies and solutions. A figure will be presented displaying all solutions. Afterwards, a selection is made of the most promising conceptual solutions for each function. Finally, the subsection is summarized and concluded. Throughout the subsections, the terms central gear and teeth will be used. A central gear in this sense means any circular body with teeth; teeth being geometric local minimums or maximums.

The selection of the best conceptual solutions is made based on how well each solution will fulfill the primary design requirements, supplemented with additional design criteria of simplicity of design and ease of control. The list of the total design criteria is the following:

- Ability to have small positioning error
- Ability to fit in design space
- Ability to provide torque
- Ability to be fast
- Simplicity of design
- Ease of control

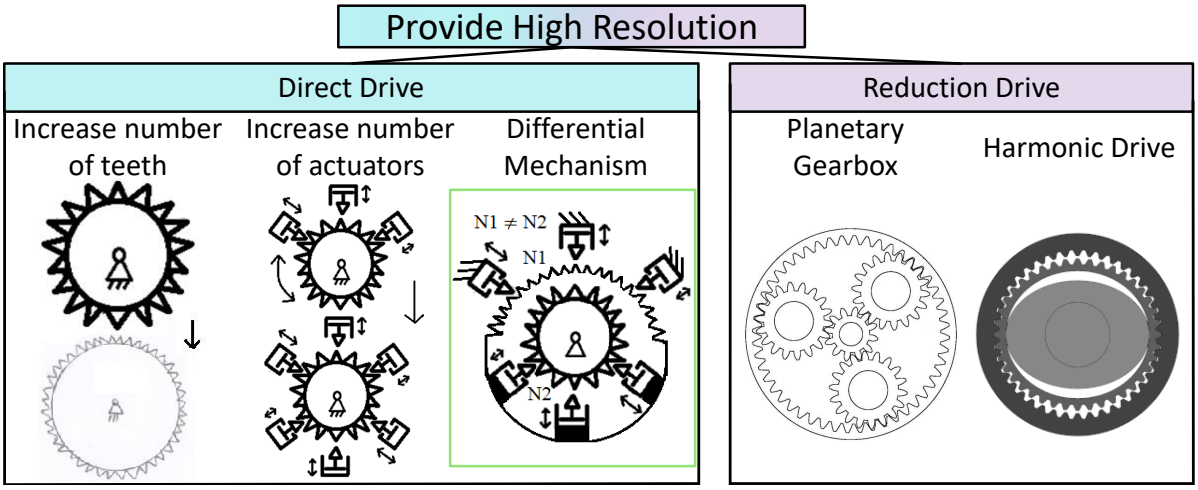

Figure 3.1: Strategies and solutions for increasing the resolution. Pictures of planetary gearbox from [28] and harmonic drive from [29]. The selected best solution is indicated by a green rectangle.

3.3.1. PROVIDE HIGH POSITIONING RESOLUTION

There are two main strategies to provide a high resolution of the motion. All the concepts for each strategy are in Figure 3.1. An increase in resolution can be done by adding a reduction drive such as a planetary gearbox. However, there also exist solutions that do not have a reduction drive, thus are direct drive. These solutions involve adding more actuators or increasing the number of teeth on actuated gears. Furthermore, a carrier can be added as a differential mechanism between the input actuators and the output axle. This carrier allows the motor to subtract the positions of two gears. If the two gears have different step sizes, the differential mechanism produces a smaller nett step size s_t. For instance; step sizes of 10° and 9° result in a $s_t = 10 - 9 = 1°$.

SELECTION

For the selection of the best solution for this function, the primary design requirements of maximum error, speed and design space play an important role. A general trade-off exists between the step size and design space. In order to make smaller steps, the number of teeth on a gear can be increased, as in the left solution in Figure 3.1. There is a limited design space so the central gear cannot be enlarged. Adding more teeth will thus make the teeth smaller. Smaller teeth can transfer less torque, since they approach their yield strength faster. So there is a limit on the amount of teeth that can be on the gear. The step size in degrees of a gear is calculated as in Equation 3.1, where a is the number of actuators working on the gear, and n is the number of teeth on the gear.

$$s = \frac{360}{a * n}. \tag{3.1}$$

In order to have an $s_t < 0.92°$, a gear of 98 teeth is needed, when 4 actuators are working on it. Increasing the number of actuators working on the central gear has the benefit that the teeth can remain the same size. The downside is that more actuators take more design space, more tubing and more complex control. A good option is to combine the solutions of increasing the number of teeth and increasing the number of actuators.

Adding a reduction drive, as on the right side of Figure 3.1 does not need an increase of teeth on the main gear, and so does not suffer from teeth reaching their stress limit. For instance, adding a gearbox with a ratio of 4 to 1 to the example in the previous paragraph will lower the number of teeth on the central gear to $98/4 \approx 24$. Since a quarter of the teeth need to fit on the same circumference, the teeth can be 4 times as large, resulting in stronger teeth. If a central gear of 24 teeth is used, with 4 actuators working on it and a gearbox ratio of 6 to 1, a step size of 0.62° is achieved. Two types of reduction drives are depicted in Figure 3.1: the planetary gearbox and the harmonic drive. Planetary gearboxes suffer from backlash when precise positioning is required. When a force disturbance is applied in the opposite direction of the previous rotation direction, there is play on the output axle. For example, a step size of 0.62° leaves room for $b_t = 0.92 - 0.62 = 0.30°$ or 18 arc minutes of backlash to stay within the error specified. High precision planetary gearboxes do exist that have this little backlash, but these are all made from ferromagnetic metals, so they cannot be used. There exist methods to overcome this backlash, for instance introducing spring-loaded split gears on the output axle. A custom made, high precision MR safe gearbox with or without MR safe backlash-decreasing methods would need to be designed, increasing the com-

plexity of the design. Harmonic drives use a compliant ring and can have less than 18 arc minutes of backlash when made from ferromagnetic materials. However, no MR safe harmonic drives exist that have little backlash, so this gearbox would need custom design as well.

The last important design criteria is speed. The requirements state that any motion must be completed in 15 seconds and that a rotation of at least 310º is required. For every step, a valve has to switch to send air to an actuator or release from it. This takes time; high speed switching valves exist that have a switch time of less than 10 ms, for instance from FESTO [30]. At 5 m distance, the air needs approximately 70 ms to leave or fill the tubes to the actuator [21], so a total time per step of around 80 ms is achieved. The differential mechanism can be used with two gears of slightly different step size. This solution will be called a dual gear motor. Steps can be taken with larger step sizes, and due to the differential mechanism still have a resulting smaller step size. Equation 3.2 shows the step size when two gears are used. In order to have $s_t < 0.92º$ and the least amount of actuators and teeth on the gears, gears with 14 and 15 teeth can be chosen. These have step sizes of $s_1 = 12°$ and $s_2 = 12.86°$. This results in $s_t = 0.86°$. In order to rotate 310°, the dual gear motor can take 26 steps forwards of 12.86°, and 2 steps backwards of 12°. The motor thus needs a total of 28 steps or 28*0.08 = 2.24 seconds to rotate 310°, well within the requirements. So the dual gear motor with a differential mechanism is fast. In contrast, the single gear motor with 98 teeth, 4 actuators and step size of 0.92° needs 310/0.92 = 337 steps and 337*0.08 = 27 seconds to complete its motion. This is slower than the required time of 15 seconds. Even slower is the single gear motor with a gearbox of 6:1 ratio, 4 actuators and 18 arc minutes of backlash with a step size of 0.62º. In order to rotate 310° it would need 500 steps, resulting in 400 seconds of rotation time, which is too slow.

$$s_t = s_2 - s_1, s_1 = \frac{360}{a * n_1}, s_2 = \frac{360}{a * n_2}. \tag{3.2}$$

CONCLUSION

In conclusion, the differential mechanism produces the required fast motion and still offers a small step size. Gears with few teeth can be used, resulting in teeth that are large and can withstand the torque specified. Therefore, the differential mechanism is chosen as the best solution for this function.

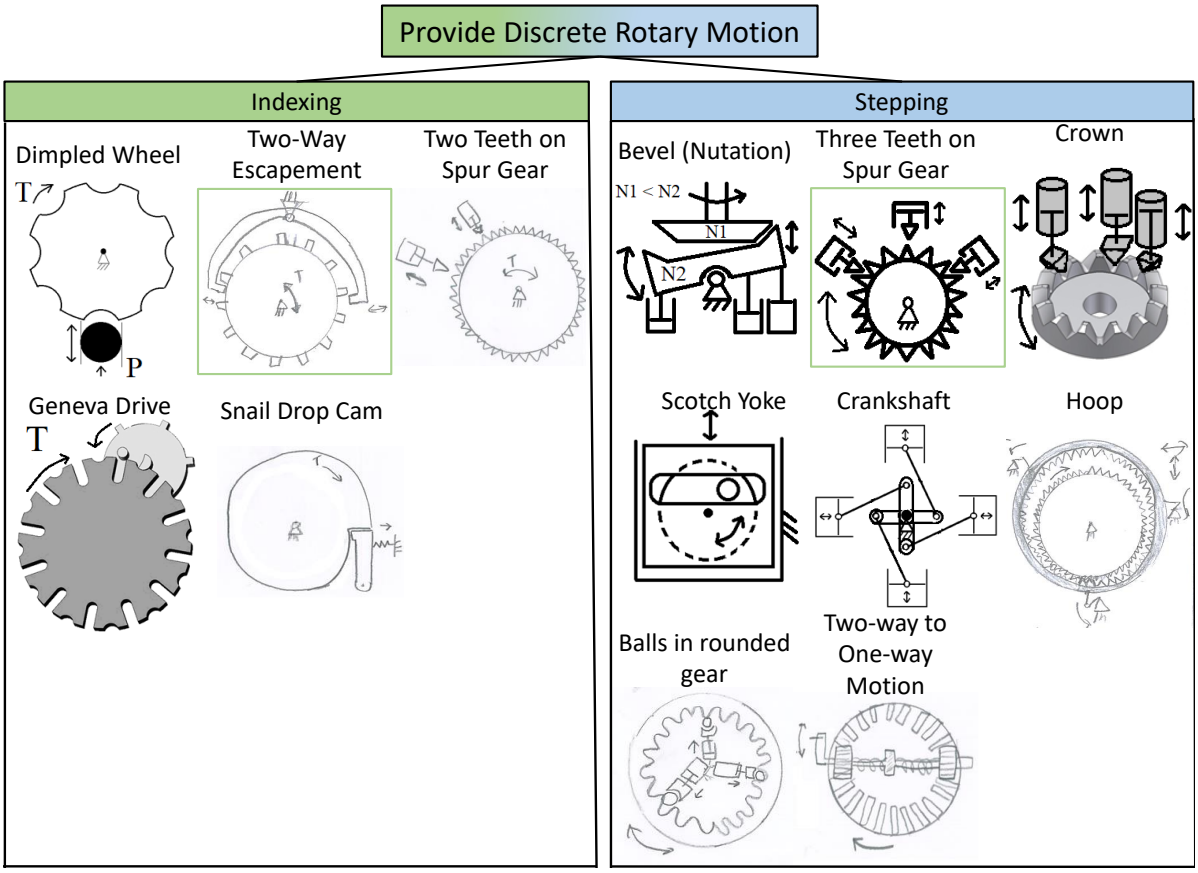

Figure 3.2: Strategies and solutions for providing discrete rotary motion: Indexing and Stepping. The selected best solutions are indicated by green rectangles. Picture of crown gear adapted from: ASSAG [27].

3.3.2. PROVIDING DISCRETE MOTION

For the function of providing discrete motion, two opposing strategies are defined: indexing and stepping. In indexing, as stated in Chapter 1, a torque on the output axle is counteracted at predefined intervals. In indexing, the functions providing actuating force and stopping force are separately solved: different mechanism provide these functions. In contrary, stepping combines the actuating and stopping force into the same mechanism. In order to produce a motion, stepping consists of a sequence of discrete actuation actions on the output axle. If no action is taken, the output does not turn, since it is held stationary by the actuation/stopping force. Mechanisms for indexing and stepping are conceptualized for both strategies and are summarized in Figure 3.2.

SELECTION

The selection of the best solutions for the function of providing discrete rotary motion is done based on primary design requirements and the additional criteria of simplicity of design and ease of control. If a solution can be used to produce motion in two directions, it scores higher in simplicity of design. If a solution can only produce motion in one direction, a mirrored version of the solution can be added to create motion in two directions or a reversible gearing can be added. Both solutions would decrease the simplicity of design. All solutions in this section will be combined with the differential mechanism, thus producing a dual gear motor. Therefore, all solutions in this section must be able to make a step as small as 12° in order to reach the required resolution, as described in Section 3.3.1. In indexing, the actuating torque T is applied to turn the output and a stopping force is supplied to counteract the torque. In general, the actuators that supply the stopping force can be small. By designing the geometry of the locking mechanism correctly, the small force produced by the actuators is amplified and is sufficient to counteract the actuating torque T. Furthermore, it is important that the position is correctly locked when no motion is intended. The latter makes sure that the solution is accurate.

The upper left solution in Figure 3.2 is the dimpled wheel as used by Wei *et al.* [12]. The solution works by applying a pressure P and pushing a ball into the dimpled wheel. When the pressure is at a maximum, the torque T is counteracted and the wheel stops rotating. When the pressure is between certain thresholds $p_{low} < p < p_{high}$, the ball is pushed in and out of the wheel with a natural frequency. Adjusting the pressure p within the thresholds regulates the speed of the wheel. When the pressure is below p_{low}, the wheel is free to accelerate. Since 5 m long tubes with complex dynamics are being used and the pressure needs to be regulated, the control over this motor is hard. Therefore, this solution is disregarded.

The two-way escapement is an adaption of the escapement mechanism from a grandfather clock. The latter works only in one direction, while the two-way escapement is symmetrical and works in two directions. The escapement mechanism consists of an escapement anchor with two teeth, and an escape gear. The anchor has two positions, if the left tooth is engaged, the right is disengaged. If a step needs to be made, the anchor changes to the other position. During this transition, the left tooth moves away from the gear, still making contact with the gear. When contact is finally lost, the right tooth has fully moved towards the gear and will engage the next teeth on the gear. The latter results in a high guarantee that the escape gear is correctly locked when no motion is intended. The actuator to move the anchor needs only an on-off pressure signal to operate, which simplifies the control over the motion.

The solution of two teeth on the spur gear consists of two actuators with teeth working on the central gear. A torque is applied on the central gear. When a step is taken, one actuator retracts and the other engages. This solution is a variation on the two-way escapement. In the two-way escapement the two teeth are mechanically connected, in such a way that when one retracts, the other engages. The mechanical connection between the teeth lacks in the two teeth solution, so there is a higher chance that steps are missed when the central gear starts moving. This solution is thus inferior to the two-way escapement.

The Geneva Drive is a classical indexing mechanism. It consists of a drive wheel with a drive pin and locking pin, and a driven wheel with slots. The driven wheel is locked in position by the locking pin on the center of the drive wheel. This locking pin is circular with a cutout at the position of the drive pin, resembling a half-moon shape. The driven wheel only rotates when the drive wheel is turned and advances the driven wheel. This a benefit for accurately positioning. However, in order to reach s_1 = 12°, 360/12 = 30 slots on the driven wheel would be needed. The driven wheel becomes very large in comparison to the drive wheel. This means that the locking pin becomes small, and cannot withstand the torque needed. An extra reduction drive would be needed, increasing the complexity and design space.

The snail drop cam mechanism is used in many devices, including mechanical calculators. It comprises a spiral-shaped cam, and a pawl. A torque is applied on the cam. When the pawl is retracted, the central wheel can turn. After re-engagement of the pawl, the cam is stopped, completing one rotation. This mechanism only works in one direction, so a second mirrored version of the mechanism, or a reversing gearbox would need to be added.

Table 3.1: Selection of Function Providing Discrete Rotary Motion. Conceptual solutions are scored from negative - - to positive ++.

	Accuracy & Precision	Design Space	Speed	Simple Design	Ease of Control
Dimpled Wheel	+	-	+	+	–
Two-Way Escapement	+	+	+	+	+
Two Teeth on Spur Gear	- -	+	+	++	+
Geneva Drive	+	+	-	-	+
Snail Drop Cam	+	-	+	-	+
Bevel	+	-	+	+	+
Three Teeth on Spur Gear	-+	+	+	+	+
Crown	-+	-	+	-+	+
Scotch Yoke	-	-	-	+	+
Crankshaft	-	-	-	+	+
Hoop Gear	+	-	+	-	+
Roller in Face Cam	+	+	+	-	+
Two-way to One-way Motion	-	-	-	-	+

In the category of stepping, all solutions work by a sequence of discrete actuating actions. There is no external torque on the central gear. The bevel gear solution has two bevel gears, one with a slightly different amount of teeth than the other. The solution works by nutation; the lower bevel gear tilts on the ball joint. This tilting causes the upper bevel gear to rotate. Actuation of the lower bevel gear can be done with three linear actuators. This solution has been used in the only commercially available PSM by Baumgartner Maschinenbau AG [19].

The solution of three teeth on a spur gear works by sequential pushing of the teeth in the gear. The solution is a simple design and can be designed to fit in the compact design space. To produce $s_t < 0.92°$, the required 12 and 13 teeth on the gears can fit. However, the actuators must supply large forces in order to move the gear. A large friction force occurs between the teeth of the gear and the teeth of the actuators. This can wear the teeth down. The crown gear solution works the same as the spur gear, but the teeth are not in the same plane as the actuators. This makes the crown gear solution less compact.

The scotch yoke mechanism has a central wheel with a pin. A slotted body pushes down on the pin and rotates the central wheel. Three of these slotted bodies and three pins on the central wheel can generate a full rotation on the wheel, as done by Farimani and Misra [10]. The crankshaft is similar to the scotch yoke mechanism, but the pistons are directly linked with rods to the crankshaft. Three actuators can generate steps of $s = 360/3 = 120°$. However, in order to reach $s_1 = 12°$ as specified in Section 3.3.1, a total of 30 actuators or a reduction drive would be needed, both increasing the design space needed.

The hoop gear solution consists of two gears with a slightly different amount of gears. The hoop gear translates in a circular motion around the central gear. The central gear will rotate in the opposite direction, but with a slower speed than the hoop gear. This creates an increase in resolution. The hoop gear is actuated with three linear actuators. The total design is quite complex, since the hoop gear must have bearings that allow for the translation in a circular motion.

The solution of the balls in the rounded gear is similar to the three teeth on a spur gear solution. Three balls are pushed in a sequential fashion into rounded 'teeth' of the central gear. Since the balls can roll, they produce less friction than the sliding teeth of the three teeth on a spur gear solution. However, the balls need to be encapsulated, so a race in the central gear is needed, adding complexity to the design.

The two-way to one-way motion mechanism converts any motion on the input into a clockwise (CW) rotation on the central gear. For example, a spring loaded linear pneumatic cylinder on the input can be used. When pressure is applied to the cylinder, the output moves CW. When pressure is released, the spring pushes it back, resulting in CW motion on the output. Since both on extension and retraction of the piston the output moves, the motor is fast. However, the central gear is only locked for rotation in the counterclockwise (CCW) direction, so an extra locking mechanism would need to be added locking the CW movement.

CONCLUSION

Table 3.1 scores and summarizes the selection of the solutions. The two best conceptual solutions for providing discrete rotary motion are the two-way escapement mechanism and the three teeth on spur gear solutions. They both score positive on all design criteria. They both have the benefit that a small force on the anchor can be used to switch a significantly larger actuating force. Furthermore, the mechanisms have easy control, and are able to lock their position reliably in both directions. Moreover, movement of the output is possible in both directions. The designs are flat, and can be made to fit in the design space.

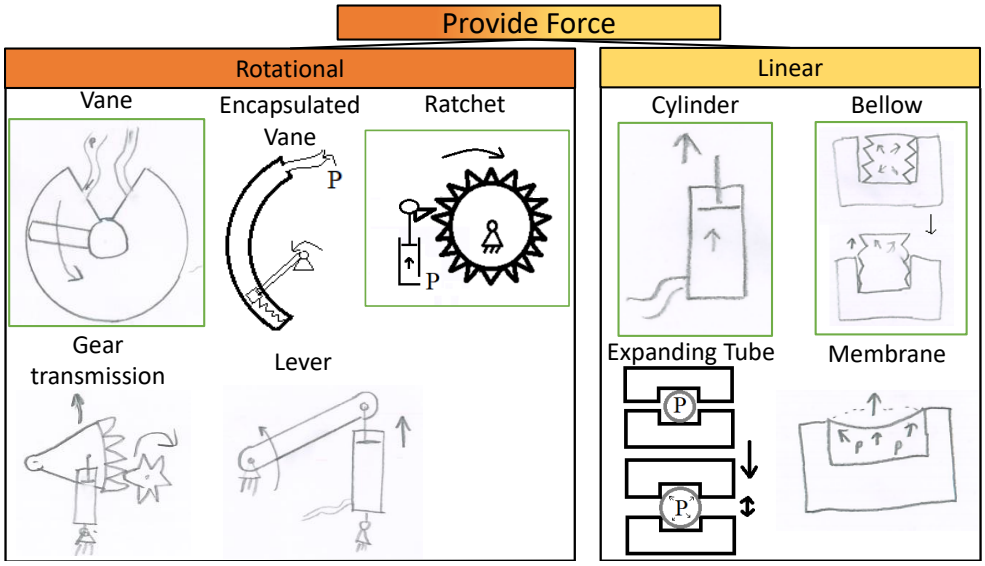

Figure 3.3: Strategies for providing force split into rotational and linear force. The selected best solutions are indicated by green rectangles.

3.3.3. PROVIDE FORCE

The previously described mechanisms need force to work, and the source of the force must be pneumatic. Multiple concepts are synthesized to transfer the air pressure into a force, these concepts are displayed in Figure 3.3. Solutions for the strategy of indexing require a torque to rotate the output. The actuators in stepping are generally of linear nature, and require a conversion of pressure into linear force. Therefore, the concepts for providing force are divided into solutions that provide rotational torque and linear force.

SELECTION

The most important design criteria to select the best concepts is the ability to provide torque. Furthermore, the design space and simplicity of design are important design criteria.

The vane solution consists of a circular housing with two inlets. A vane is located inside the housing, the former can turn CW or CCW depending on which inlet is pressurized. In order to have a compact design space, the inlets are located in the same plane as the vane. The latter means that the vane cannot make a full rotation, but it can still rotate the required 310°.

The encapsulated vane is an adaption of the vane solution. The solution comprises a vane which runs in a circular housing. The vane is connected to a rotation point that is outside the housing. Furthermore, the vane returns with a spring, so there is only one inlet on the housing. The housing is harder to seal than the one on the normal vane, so this solution is inferior to the normal vane.

The ratchet solution converts linear into rotational force. The solution comprises a cylinder with a ratchet that engages on the central gear when pressure is supplied. The central gear will rotate. When the cylinder has reached its travel limit, the pressure is released and the ratchet can move back without rotating back the central gear.

The lever and gear transmission solutions both convert a linear force into a torque. With only one actuator working on the lever, the lever has a limited stroke. The gear transmission can produce torque over more than a full rotation.

The linear solution of the cylinder is a classic solution. Pressure is applied on the piston head, so the former can translate inside the cylinder. The piston head is easy to seal, since a standard O-ring can be used inside the cylinder. The bellow solution comprises a body and a bellow. When a pressure is supplied, the bellow inflates and extends. However, the bellow must be properly guided in its extension in order for the force to work in the desired direction.

The expanding tube solution comprises a thin-walled tube that is located between two movable bodies. When a pressure is applied, the tube expands and pushes the bodies away. The membrane solution consists of a u-shaped body and a membrane. The membrane expands when a pressure is applied. This solution has limited travel, since the membrane can only deflect a limited amount before it yields.

CONCLUSION

The vane solution is selected as it can be made into a flat design. Furthermore, the ratchet solution is selected as it provides a high torque and is easily sealable, since the solution contains a standard pneumatic cylinder. The bellow solution is selected for linear force required for stepping, since the solution is compact and can still allow for a large travel.

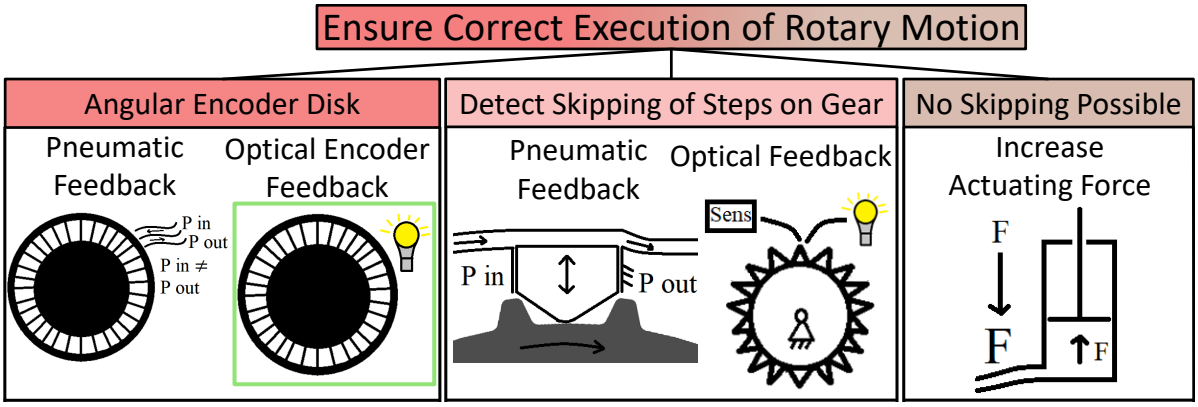

Figure 3.4: Strategies to ensure the correct execution of motion. The selected best solution is indicated by a green rectangle.

3.3.4. ENSURE CORRECT EXECUTION OF ROTARY MOTION

Correct execution of the motion can be ensured by the solutions in Figure 3.4. The solutions can be split into three strategies; the first is to add an encoder disk for angular feedback. The position can be monitored continuously. If a step is skipped due to an unforeseen disturbance force, compensatory steps can be taken. The signal to transfer the data must be MR safe, so for example, light signals can be used. Moreover, pneumatic signals can be used. The second strategy is to detect skipping of steps directly on the central gear. A mechanical follower can be placed on the gear. This follower blocks an air flow in a tube when a tooth passes. The blocking of the air flow can be detected by pressure sensors at the end of the 5 m long tubes. When skipping of steps is detected, the motor can take steps to compensate. Light can also be used to detect teeth passing. The last strategy is to incorporate a mechanism to ensure that steps cannot be skipped, even with a force disturbance. One solution is to increase the actuating force, making the motor more robust against force disturbances.

SELECTION

For this function the design criteria of speed and design space play an important role. An incremental encoder can be added to measure the position of the output axle. If a peak force on the output makes the motor skip a step, the encoder can measure how much the position deviates from the set point. Then, the motor can take steps to compensate and reach its set point again. The exact position of the output is continuously measured. Any other inaccuracies in the placement due to, for instance, geometrical inaccuracies in the motor can also be measured with the encoder and compensated for.

With the strategy of detecting skipping of steps, it is known how many steps are skipped. Measurement is carried out directly on the gears. For a dual gear motor, two measurement systems are needed to detect skipping of steps on both gears, making it rather complex. For the optical feedback, the measurement system is designed in such a way that it can accurately count the amount of skipped steps even if they occur in fast succession. In this way, the motor can take steps back to compensate and reach the position set point. The pneumatic feedback concept will be slow in the detection of skipped steps due to 5 m long tubes to the pressure sensors. In this case, it is only known that steps are skipped, but not how many steps are skipped. When the disturbance force ceases to be applied, the motor can home again and the motor can restart to step towards its set point.

With increasing the actuating force, the motor is inherently robust against higher force disturbances. There is less need for an active compensation. This is the least complicated solution. However, it requires stronger parts to withstand the extra force, so in general would result in a design requiring more space.

CONCLUSION

Adding an optical encoder is chosen as the best solution. If a disturbing force acts on the output, the motor can directly take steps to compensate for it. The latter improves the speed of the motor.

4

Integrated Concepts

4.1. Introduction

In the previous chapter, the best conceptual solutions were chosen. This chapter combines these solutions into integrated concepts. Three integrated concepts will be presented. Section 4.5 at the end of the chapter describes the choice of the best integrated concept. Chapter 5 will go into detail about the final design compiled from the best integrated concept. The legend in Figure 4.1 indicates the colors for inputs, output, world and carrier and is used in the figures of the integrated concepts.

Figure 4.1: Legend for figures of integrated concepts.

4.2. Dual Gear Stepper

The dual gear stepper concept consists of the differential mechanism with six teeth working on two spur gears. It uses bellows to generate force. An optical encoder is used to provide feedback of rotation, so any skipping of steps can be corrected for. See Figure 4.2, there is an outer gear, carrier and a central spur gear. The motor has an in-plane configuration: the outer gear is placed around the central gear. This is done to make the motor thin, in order to make it fit in segment 1. The inputs of the motor are six bellows located in the carrier. Three bellows actuate the teeth working on the outer gear, and three bellows work on teeth for the central gear, thus needing a total of six actuators. The central spur gear is the output of the stepper motor. The carrier in the middle is used as the differential mechanism between the outer and the central gear. The outer gear has 13 teeth producing steps of 9.23° and the central gear has 12 teeth producing steps of 10°. This results in a step size $s_t = 0.77°$ as in Equation 4.1, which complies with the design requirements.

$$s_t = \frac{360}{3*12} - \frac{360}{3*13} = 10 - 9.23 = 0.77°. \tag{4.1}$$

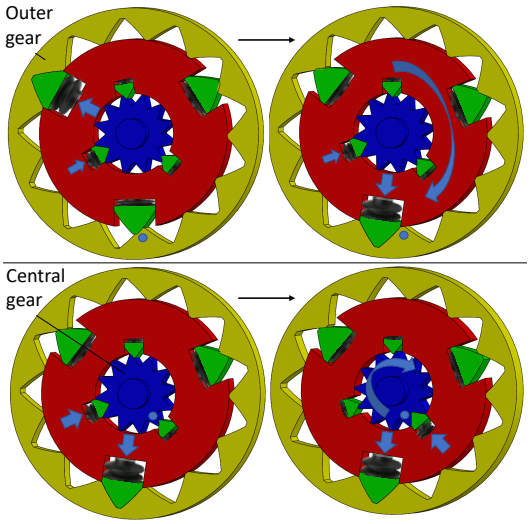

Figure 4.2: Dual Gear Stepper and its stepping functions. Actuation of the teeth is done with bellows. The top images depict operation of the outer gear. The bottom images depict operation of the central gear. Picture of bellow from [31].

The stepping procedure for the outer gear is depicted in the top images of Figure 4.2: sequential pushing of teeth in the outer gear moves the carrier with respect to the world. In this operation, one tooth is continuously engaged between the carrier and the central gear, so the movement on the outer gear is transferred to the output. The bottom images in Figure 4.2 show the stepping procedure for the central gear. Sequential pushing of teeth in the central gear moves the output with respect to the carrier. In this operation, one tooth is continuously engaged between the carrier and outer gear, so the carrier remains stationary with respect to the world.

This motor is a stepper; the functions of providing actuating force and stopping force are combined in the same mechanism. The bellows and teeth are used to hold the output in place and to provide torque to move the output. Air pressure is used to actuate the bellows; 5 m long tubes connect the valves to the motor and its bellows. Since the bellows are attached to the carrier that rotates, the tubes will bend and rotate.

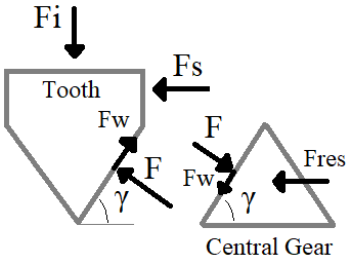

Figure 4.3: Free body diagrams from the integrated concept of dual gear stepper. A tooth of the central gear is shown, and a tooth that is actuated by the bellow with force F_i.

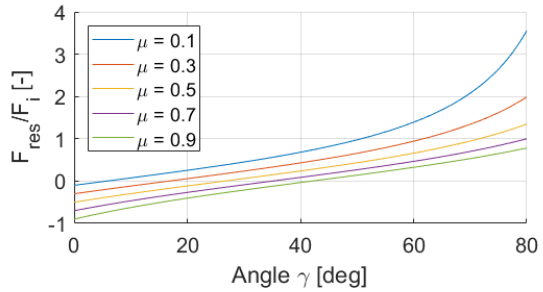

Figure 4.4: Amplification factor between the supplied force by the below F_i and the resulting output force F_{res}, from Equation 4.2. Different values of friction coefficient μ between the teeth are plotted. Amplification factor is desired to be higher than 1, which can be achieved by lowering the friction coefficient or increasing the angle γ between the teeth.

This limits the total rotation of the motor, in order not to entangle the tubes. It is therefore not possible to rotate more than one revolution.

A design parameter in this concept is the angle γ between the input teeth and the teeth in the gears, see Figure 4.3. The force F_s is the contact force between the tooth and its housing in the carrier. The input force F_i is transferred via force F to supply a force F_{res} to turn the central gear. The angle γ works as a transmission; the input force F_i is amplified to a force F_{res} . This amplification factor is stated in Equation 4.2. A certain angle is needed to overcome the friction force F_w between the teeth and have a positive transmission ratio. Equation 4.2 is plotted in Figure 4.4, using the code in Appendix F.1. A high transmission ratio can be achieved when γ approaches 90°. However, high γ would mean long teeth, needing more design space. A lower value of γ must be selected for a final design.

$$\frac{F_{res}}{F_i} = \frac{\sin\gamma - \mu\cos\gamma}{\mu\sin\gamma + \cos\gamma}. \tag{4.2}$$

4.3. DUAL ESCAPEMENT WITH VANE

This integrated concept consists of two escapement anchors and an outer and central gear. The central gear is the output of the concept. A carrier is used as a differential between the gears. See Figure 4.5 for an overview of the integrated concept. The outer gear has 15 teeth, and the central gear has 14 teeth. This results in a step size of $s_t = 0.86°$, as in Equation 4.3. The two escapement anchors are positioned in-plane. Actuation of an escapement anchor is done with a bellow on one side and a return spring on the other side of the escapement anchor. A vane provides the torque to rotate the output. The vane is directly connected to the output and can rotate up to 310°. A total of four tubes is needed to control the motor; two for the escapement anchors and two for the vane.

$$s_t = s_c - s_o = \frac{360}{2*14} - \frac{360}{2*15} = 0.86°. \tag{4.3}$$

The upper images of Figure 4.5 show indexing with the outer gear. First, pressure is applied to the bellow of the central gear's anchor. This pressure makes sure that the carrier and the output are connected. Pressure is applied to the vane in the direction of rotation that is desired. Finally, indexing with the outer gear is done by releasing pressure of the bellow of the outer anchor. The anchor springs back to its other position. The carrier and the output rotate to the next tooth in the outer gear.

The bottom images of Figure 4.5 show indexing with the central gear. Pressure is continuously applied to the bellow on the outer gear in order to lock the position of the carrier with respect to the world. Indexing with the central gear is done by releasing pressure on the bellow of the central anchor. Due to the pressure on the vane, the output rotates to the next tooth on the inner gear.

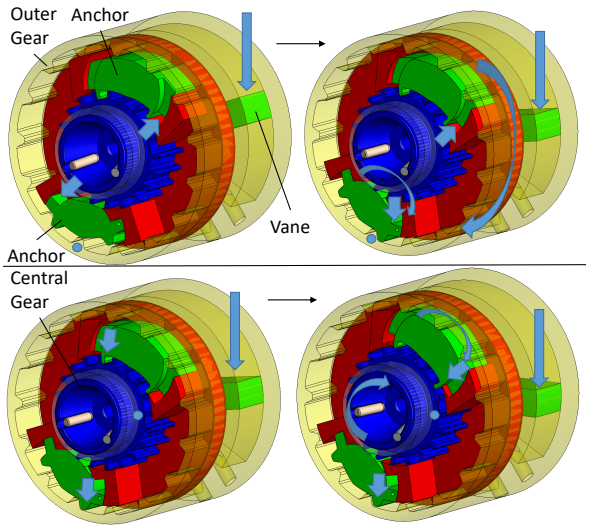

Figure 4.5: Dual Escapement with Vane and its indexing functions. Bellows and return springs are not shown. The top images show indexing with the outer gear. The bottom images show indexing with the central gear.

4.4. DUAL ESCAPEMENT WITH RATCHETS

The integrated concept of the Dual Escapement with Ratchets comprises two gears with escapement mechanisms, two ratchets and a carrier. The carrier is used as a differential mechanism. The integrated concept is depicted in Figure 4.6. There are two ratchets and pawls, one for CW rotation, and the other for CCW rotation. The gears are not positioned in the same plane, but behind one another. Gear 1 has 22 teeth, and gear 2 has 20 teeth, resulting in a step size of $s_t = 0.82^o$, as in Equation 4.4. Actuation of an anchor is done with a cylinder and a return spring, as in Figure 4.7. The anchor has two defined positions. A total of four actuators is needed for this integrated concept; two for the escapement anchors and two for the ratchet cylinders.

$$s_t = s_2 - s_1 = \frac{360}{2*20} - \frac{360}{2*22} = 0.82°. \tag{4.4}$$

The operation of the motor is similar to that of the Dual Escapement with Vane. However, in the present concept, torque is applied with ratchets. Pressure is converted into force in the ratchet cylinder. When the piston extends, the ratchet engages on the ratchet wheel. When the piston reaches its travel limit, pressure in the ratchet cylinder can be released. A spring in the ratchet cylinders pushes back the ratchet. In doing so, the ratchet pawl can rotate and disengage from the ratchet wheel, allowing the piston to move back. Afterwards, the ratchet pawl springs back.

Indexing is done by applying a pressure to the ratchet cylinder of the desired direction of rotation. For indexing with gear 1, anchor 1 moves to its other position by switching the pressure state of anchor 1's piston. During indexing with gear 1, the anchor of gear 2 remains pressurized, connecting the carrier with the output. Anchor 1, carrier and the output rotate to the next tooth on gear 1 over a distance of s_1 by the torque applied with the ratchet cylinder. The top images of Figure 4.6 indicate this procedure.

Indexing with gear 2 is depicted in the bottom images of Figure 4.6. The anchor of gear 2 is moved to its other position by switching the pressure state of anchor 2's piston. The output moves to the next tooth on gear 2 over a distance s_2. During this operation, the anchor of gear 1 remains in the same position, fixing the carrier with respect to the world.

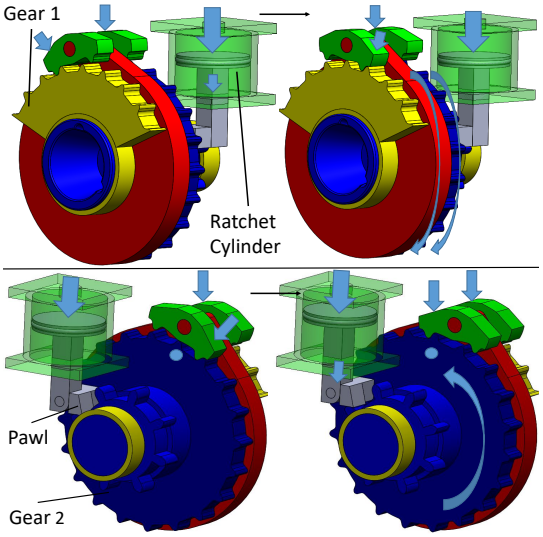

Figure 4.6: Dual escapement with ratchets. Only one of the two ratchets is displayed. Actuation of the anchors is shown in Figure 4.7. The top images indicate indexing with gear 1. Indexing with gear 2 is depicted in the bottom images.

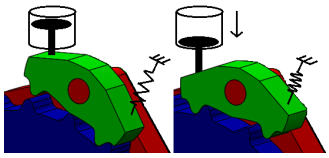

Figure 4.7: Actuation of anchor with return spring.

4.5. CONCEPT SELECTION

The choice for the best integrated concept is mainly based on the design criteria of simplicity of the design and the ability of the concepts to fit in the design space. The integrated concepts with an escapement mechanism need only four actuators and four tubes conducting the pneumatic control signals: one actuator for each anchor, one for CW motion, and one for CCW motion. The Dual Gear Stepper needs 6 actuators. The concepts with the escapement mechanism thus score higher in terms of simplicity of design.

When comparing the two integrated concepts with escapement mechanisms; in the in-plane configuration of the Dual Escapement with Vane, there is little room for the bellows to work on the escapement anchors. Furthermore, there is little room for tubing to supply pressure to the bellows, since both anchors are located inside the outer gear. In the out-of-plane configuration of the gears as in the Dual Escapement with Ratchets, there is more room for the actuators to operate on the anchors. Moreover, tubing to supply the pressure to the anchors is easier to install, since both anchors are located on one side of the motor. Furthermore, the ratchets can more easily be sealed than the vane. This is because the vane motor requires complex sealing around the vane's perimeter, and the ratchets cylinders can be sealed with a simple o-ring.

In conclusion, the dual escapement with ratchets is chosen as the best integrated concept, as it fits best in the design space, can more easily be sealed and has the least amount of actuators and tubes.

5

Final Design in Detail

5.1. Introduction

The best integrated concept called Dual Gear Escapement with Ratchets as chosen in Section 4.5 has been worked out into a final design. The first section of this chapter introduces the final design and discusses the differences between the integrated concept as introduced in the previous chapter. Next, the chapter explains the design choices made to form the final design: the geometries of the escapement anchors are defined by an analysis of the forces working on their teeth in Section 5.3. The number of teeth on both gears are chosen in Section 5.4. The last part of this chapter explains the working principles of the final design in detail: the planning and execution of the indexing sequence in order to reach a position set point is elaborated on in Section 5.5. Section 5.6 elaborates on the software structure and GUI used for operation of the motor. Finally, a prototype of the motor was made and is presented in Section 5.7. Parts in the figures in this chapter are colored according to the legend in Figure 5.1.

Figure 5.1: Legend for figures of the final design.

5.2. Final Design: PneuScape

The final design of the pneumatic stepper motor with dual escapements and ratchets has been made. See Figure 5.2 for a 3D CAD overview of the design and its parts. The final design will be called 'PneuScape' from now on. There are some differences between the integrated concept as presented in Chapter 4 and the PneuScape. One difference is the configuration of the escapement anchors with respect to the world. In the integrated concept from Figure 4.6, the actuators of both escapement anchors rotate with respect to the world. The final design has been made more compact and made to fit the design space better. In the PneuScape, the actuators of the anchor of gear 1 are fixed to the world. Moving actuators means

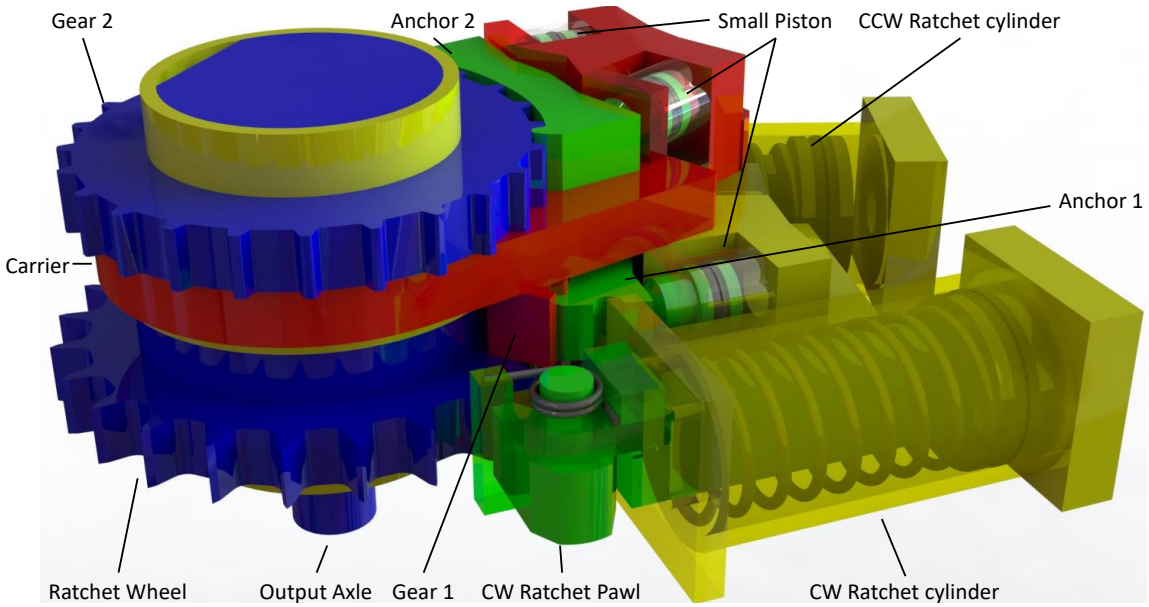

Figure 5.2: 3D CAD model of the PneuScape, without casing and tubing. Parts are colored according to the legend in Figure 5.1.

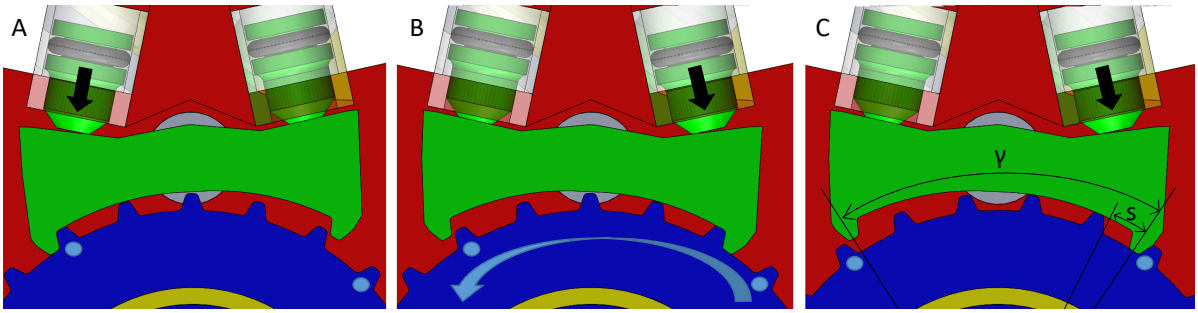

Figure 5.3: Sequence of actions to index and indication of step size s and angular width γ of the anchor. A: pressure is on the left piston. B: the left piston is depressurized, and pressure is put on the right piston. Movement of the gear starts. C: the gear has made a step.

that the tubes to the actuators need space as well, so having more actuators fixed to the world makes for a more compact design. The new configuration means that gear 1 is attached to the carrier. Furthermore, the axes of the ratchet cylinders are placed closer to the carrier and the ratchet wheel has been placed on the front of the motor. Figure 5.4 shows an impression of the PneuScape incorporated in segment 1. The motor positions segment 2. In a future version of PneuScape, the curvature of segment 1 can be taken into account, in order to fit the motor exactly in the segment. A second PneuScape incorporated in the OM positions segment 1. An encoder was not yet added in the final design.

A final difference with the integrated concept from Figures 4.6 and 4.7 is the number of actuators in the motor. In the integrated concept, one cylinder with a return spring works on the anchor. In the final design, two small cylinders with pistons of 5 mm diameter operate on one escapement anchor. The cylinder in the integrated concept must be big enough to counteract the spring and supply force on the anchor, making it have twice the area as a small cylinder in the final design. The two small cylinders are chosen because they are flatter than one big cylinder, allowing for a flatter design. The total number of actuators and tubes for the final design is six: twice two for the anchors, and two for the ratchets cylinders. Simplicity of design has thus been sacrificed to allow for a smaller design space.

Indexing with the PneuScape works as follows: only one piston per anchor is pressurized at a given time. In order to move, the opposing piston on the anchor is pressurized and the escapement anchor moves to its other position. This is depicted in Figure 5.3 in position A and B. The torque to move the motor is exerted by one of the two ratchet cylinders; one for CW rotation and one for CCW rotation. If a ratchet cylinder is pressurized, the ratchet exerts a force on the ratchet wheel. When an anchor changes position, the force of the ratchet moves the gear to position C in Figure 5.3. Indexing with gear 1 makes the carrier move with respect to the world with a step

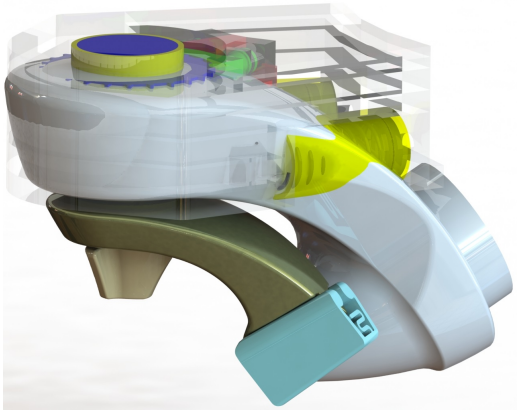

Figure 5.4: PneuScape with its housing, incorporated in segment 1. The motor sticks out from some parts of the segment.

size s_1. With anchor 2 holding its position, the output will also move with step size s_1. On the contrary, when anchor 1 hold its position, the carrier does not move. Next, if anchor 2 indexes on gear 2, the output will move with step size s_2.

The ratchet has limited travel, because of the limited design space. For every third step in the same direction of rotation, the ratchet cylinder must be reset. During the reset, the cylinder is depressurized and the spring pushes the ratchet back. Afterwards, the cylinder is pressurized again and the ratchet makes contact with the ratchet wheel. During a reset, the position of the output is not known; any disturbing force can position the output between the positions B and C in Figure 5.3. However, after the reset, the cylinder is pressurized again and the position is known to be position C in Figure 5.3.

5.3. ANCHOR GEOMETRY: FORCE ANALYSIS

The anchors and their teeth need to have a certain geometry in order to fulfill their function of indexing the gears. Firstly, the anchors and gears must be symmetrical because they must work the same in rotating both directions. Secondly, the geometry of the an-

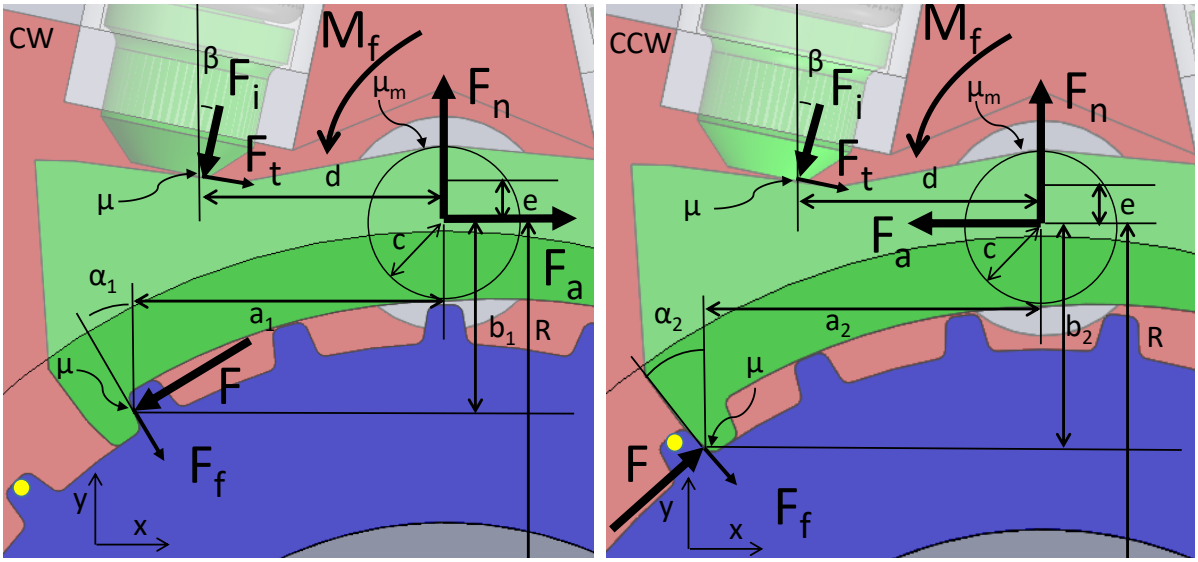

Figure 5.5: Forces working on the escapement anchor of gear 2, when a force F_a is supplied by the ratchet. Furthermore, all geometry variables of the anchor are defined. The left image depicts the CW ratchet applying a torque on the carrier, which is resisted by force F on gear 2. The right image depicts the CCW ratchet applying a torque on the carrier, which is resisted by force F on gear 2.

chor is influenced by the angular width γ that the anchor spans in its two positions. This distance γ must allow for a whole number of teeth to fit under the anchor in its two positions, see Figure 5.3. The latter makes sure the anchor can move from position A to B in Figure 5.3 and that teeth of the gear can pass underneath the anchor when moving from position B to C. Figure 5.5 shows the forces on the escapement anchor in the two positions of the anchor. When disregarding friction forces, force F needs to work on the line passing through the axis of the anchor to make sure the gear cannot push up the anchor when a torque is applied. To allow force F to work on the line passing through the axes of the anchor in both CW and CCW situations, the angular width γ is chosen such that five teeth fit under the anchor.

An elaborate force analysis is carried out to identify all the forces on the anchor, including the friction forces. The goal of the force analysis is to calculate the force F_i by choosing geometry variables $\alpha_1, \beta, a_1, b_1, c$ and e. Because of the symmetry of the anchor, α_1 is dependent on α_2. A pressure of $p = 3$ bar is used throughout the calculations. For a 5 mm diameter small anchor piston, this results in a maximum actuation force of $F_{max} = 5.9$ N. In both CW and CCW situations in Figure 5.5, the force F_i exerted by the anchor piston needs to be between $-F_{max}$ and F_{max}. If F_i is calculated to be larger than zero, the piston must exert a force in order to hold the gear stationary. When a step needs to be taken, the pressure on the piston is released and the anchor starts moving. On the contrary, if the force F_i is less than zero, the system is self-locking: When a step needs to be taken, the pressure on the piston is released, but only when the other piston is pressurized the gear starts to move. The radius c of the anchors axis is set to 2 mm, in order to reduce b_1, and make the design more compact. The ratchet cylinders have an internal diameter of 12 mm and have a normal distance of 22 mm to the ratchet wheel's axis. A torque of $T = 0.72$ Nm is produced by the ratchet cylinder and used in the calculations. The friction coefficient $\mu = 0.3$ between piston and anchor and between the teeth is used. The axle of the anchor is supported by a plastic bush bearing with a friction coefficient of $\mu = 0.25$. The remainder of the geometry variables are in Appendix D. This section continues with the calculations of forces working on escapement anchor: the Equations 5.1 through 5.9 are used. The MATLAB code for the force calculations is in Appendix F.2.

The applied force F_a on the anchor due to the torque produced by the ratchet:

$$F_a = \frac{T}{R}. \tag{5.1}$$

The friction forces:

$$F_f = \mu F,\ F_t = \mu F_i, \tag{5.2}$$

$$M_f = c * \mu_m \sqrt{F_a^2 + F_n^2}. \tag{5.3}$$

Forces in CW situation in Figure 5.5:

$$\overset{+}{\rightarrow} \sum F_x = 0 \Rightarrow$$
$$-F_i \sin\beta + F_t \cos\beta + F_a - F\cos\alpha + F_f \sin\alpha = 0 \Leftrightarrow$$
$$F = \frac{F_a - F_i \sin\beta + \mu * F_i \cos\beta}{-\mu \sin\alpha + \cos\alpha}, \tag{5.4}$$

$$+\uparrow \sum F_y = 0 \Rightarrow$$
$$F_n - F_i\cos\beta - F_t\sin\beta - F\sin\alpha - F_f\cos\alpha = 0 \Leftrightarrow$$
$$F_n = F_i\cos\beta + \mu * F_i\sin\beta + F(\mu\cos\alpha + \sin\alpha), \quad (5.5)$$

$$\overset{+}{\curvearrowleft} \sum M = 0 \Rightarrow$$
$$M_f + d * F_i\cos\beta + e * F_i\sin\beta - b * F\cos\alpha + a * F\sin\alpha$$
$$+a*F_f\cos\alpha + b*F_f\sin\alpha + d*F_t\sin\beta - e*F_t\cos\beta = 0 \Leftrightarrow$$
$$F_i = \frac{M_f + F((-b+\mu*a)\cos\alpha + (\mu*b+a)\sin\alpha)}{(-e-d*\mu)\sin\beta + (e*\mu-d)\cos\beta}. \quad (5.6)$$

Forces in CCW situation in Figure 5.5:

$$\overset{+}{\rightarrow} \sum F_x = 0 \Rightarrow$$
$$-F_i\sin\beta + F_t\cos\beta - F_a + F\cos\alpha + F_f\sin\alpha = 0 \Leftrightarrow$$
$$F = \frac{F_a + F_i\sin\beta - \mu * F_i\cos\beta}{\mu\sin\alpha + \cos\alpha}, \quad (5.7)$$

$$+\uparrow \sum F_y = 0 \Rightarrow$$
$$F_n - F_i\cos\beta - F_t\sin\beta + F\sin\alpha - F_f\cos\alpha = 0 \Leftrightarrow$$
$$F_n = F_i\cos\beta + \mu * F_i\sin\beta + F(\mu\cos\alpha - \sin\alpha), \quad (5.8)$$

$$\overset{+}{\curvearrowleft} \sum M = 0 \Rightarrow$$
$$M_f + d * F_i\cos\beta + e * F_i\sin\beta + b * F\cos\alpha - a * F\sin\alpha$$
$$+a*F_f\cos\alpha + b*F_f\sin\alpha + d*F_t\sin\beta - e*F_t\cos\beta = 0 \Leftrightarrow$$
$$F_i = \frac{M_f + F((b+\mu*a)\cos\alpha + (\mu*b-a)\sin\alpha)}{(-e-d*\mu)\sin\beta + (e*\mu-d)\cos\beta}. \quad (5.9)$$

There exist no closed-form solution for the forces F, F_n, M_f and F_i due to the square root in Equation 5.3, but the problem is solved with an iterative scheme until F_i converges with less than 0.1%. For anchor 1, for the CW and CCW situations as in Figure 5.5, the force F_i is 2.4 N and 4.9 N, respectively. For anchor 2, for the two situations, the force F_i is 1.4 N and 4.9 N, respectively. The forces are below the maximum force of F_{max} = 5.9 N which the pistons can supply, so the escapement anchors can keep the output axle stopped. The MATLAB code for calculation of the forces is in Appendix F.2.

5.4. SELECTION OF NUMBER OF TEETH

In the motor, the escapement mechanisms index the two gears. The number of teeth on each gear define the smallest step that can be made. As stated in Chapter 3; adding more teeth to the gears will result in small teeth, which will limit the torque they can transfer. Furthermore, adding more teeth will increase the total steps needed, thus slowing down the movement of the motor. A selection of the number of teeth on each gear must be made.

There are two pistons operating on the anchor, the latter therefore has two defined positions. A gear with number of teeth n has step size s, which is calculated in Equation 5.10. By taking steps with step sizes s_1 and s_2, a given position α can be approximately reached. The smallest step reachable is s_t; the difference between s_2 and s_1. The position α_d that can be reached is calculated by rounding off α to the nearest reachable position α_d with step size s_t, see Equation 5.11. The number of teeth n_1 and n_2 must be chosen such that $s_t \leq 0.92°$. The latter assumes that the motor is perfectly accurate and precise; α_d is always reached. However, in a real life prototype, there will be some inaccuracies in the production of parts, which will introduce errors in reaching α_d. It is therefore chosen to design for $s_t \leq (0.92 - e)°$, to allow for some errors. The commercially available motor by Baumgartner Maschinenbau AG [19], has a step size of 3° with 0.15° accuracy, or 5 % maximum error. It is decided to take this error percentage as a guide and to design for $s_t \leq 0.85°$.

$$s_t = s_2 - s_1, s_1 = \frac{360}{2n_1}, s_2 = \frac{360}{2n_2}, \quad (5.10)$$

$$\alpha_d = \text{round}(\frac{\alpha}{s_t}) * s_t. \quad (5.11)$$

5.4.1. DESIGN SPACE & UPPER BOUND ON ROTATION OF GEAR 1

The design space for the escapement mechanism is limited. The carrier moves with respect to the casing of the motor by making steps with gear 1. In order to save space, the amount of rotation of gear 1 for any α needs to be minimized. This upper bound ub_1 on the rotation of gear 1 depends on the choice of n_1 and n_2, which in turn influences s_t. The upper bound ub_1 on the rotation is defined in Equation 5.12. It is necessary to find how many steps with each gear must be taken to reach any α, in order to find the maximum rotation of gear 1. Therefore, Equation 5.13 needs to be solved, where the positions k_1 and k_2 are integers. This last equation assumes that the current position of the gears is zero. This equation has infinite solutions. As an example, $s_1 = 9°$, $s_2 = 10°$. Three example solutions are in Equations 5.14, 5.15 and 5.16.

$$ub_1 = \max(2 * k_1(\alpha) * s_1), \ \forall\alpha \in \mathbb{R}, \quad (5.12)$$

$$\alpha_d = k_1 * s_1 + k_2 * s_2, \quad (5.13)$$

$$341 = 34 * 10 + 1 * (10 - 9) = -1 * s_1 + 35 * s_2, \quad (5.14)$$

$$346 = 34 * 10 + 6 * (10 - 9) = -6 * s_1 + 40 * s_2, \quad (5.15)$$

$$346 = 35 * 10 - 4 * (10 - 9) = 4 * s_1 + 31 * s_2. \quad (5.16)$$

In the example of Equation 5.15, $|k_1| = 6$. In the example of 5.16 $|k_1| = 4$, so there is a difference in the number of steps k_1 for the same α_d. In order to save design space, ub_1 needs to be minimized, so k_1 needs to be minimized. When minimizing the movement of gear 1, a closed-form solution for 5.13 can be devised. The motor will reach its set point by taking k_2 big steps of s_2 and a limited number of steps k_1 with smaller step size s_1.

CLOSED-FORM SOLUTION

The closed-form solution of Equation 5.13 arises from a general form of Equations 5.14 and 5.16, as in Equation 5.17. When comparing 5.17 with 5.13, the coefficients from Equation 5.18 are found. Further observation of examples from Equations 5.14 and 5.16 yields $a = 34$ when $\alpha_d / s_2 < 34.5$ and $a = 35$ when $\alpha_d / s_2 > 34.5$. The expression for a is thus as in Equation 5.19. Finally, rewriting 5.13 gives the closed-form solutions for k_1 in 5.20 and k_2 in 5.21. Equation 5.20 can be used to calculate the upper bound ub_1 on the rotation of gear 1 according to Equation 5.12.

$$\alpha_d = a * s_2 + b(s_2 - s_1) = -b * s_1 + (a + b) * s_2, \quad (5.17)$$

$$k_1 = -b, \; k_2 = a + b = a - k_1, \quad (5.18)$$

$$a = \text{round}(\frac{\alpha_d}{s_2}), \quad (5.19)$$

$$k_1(\alpha) = \frac{\alpha_d - k_2 * s_2}{s_1} = \frac{\alpha_d - (a - k_1)s_2}{s_1} = \frac{a * s_2 - \alpha_d}{s_t}, \quad (5.20)$$

$$k_2(\alpha) = a - k_1. \quad (5.21)$$

5.4.2. RESULTS & CONCLUSION

To summarize, the selection of n_1 and n_2 must be such that the $s_t \leq 0.85°$, n_1 and n_2 are minimized, and ub_1 is minimized. In order to facilitate for $s_t \leq 0.85°$, n_1 is almost equal to n_2. Using the equations in Section 5.4.1, plots of ub_1 are made for differences of 2, 3 and 4 teeth between gear 1 and 2, see Figure 5.6. The time to reach one revolution is plotted in Figure 5.7. The time scales linearly with the number of steps taken, and thus becomes larger with higher number of teeth n. A step time of 80 ms is used, equal to the one used in Chapter 3. There are three candidates for an optimum solution: points A, B and C in Figures 5.6 and Figure 5.7. Point B has a better ub_1 than point A. Point C does have a better ub_1 than point B, but has a worse time and needs an increase in the number of teeth, which in turn lowers the strength of the teeth. Finally, point B is chosen as the best optimum. It has $n_1 = 27$, $n_2 = 24$, $s_1 = 6.67°$, $s_2 = 7.5°$, $s_t = 0.83°$ and $ub_1 = 53.33°$. This ub_1 means gear 1 needs to take a maximum of 4 steps to either side. The code to plot Figure 5.6 and Figure 5.7 is in Appendix F.3 and F.4.

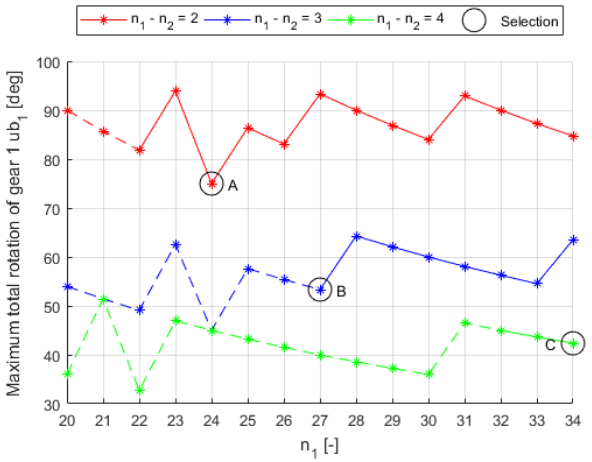

Figure 5.6: Maximum rotation ub_1 of gear 1 for different number of teeth n_1 and n_2. A dotted line indicates unfeasible $s_t > 0.85°$, a solid line indicates feasible $s_t \leq 0.85°$. Selected optimum is point B with $n_1 = 27, n_2 = 24$, resulting in $s_t = 0.83°$.

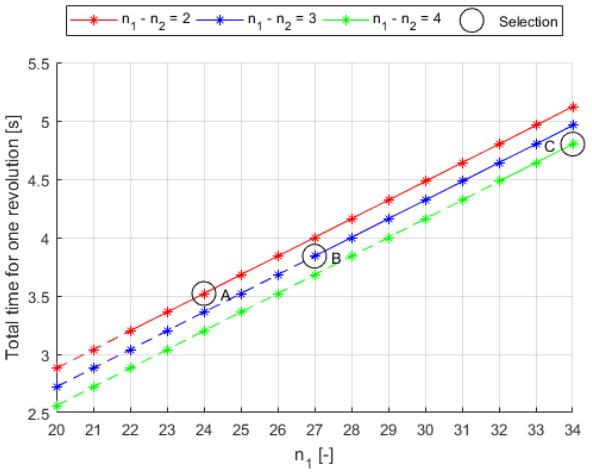

Figure 5.7: Time to make one revolution, for different number of teeth n_1 and n_2. The step time is 80 ms. A dotted line indicates unfeasible $s_t > 0.85°$, a solid line indicates feasible $s_t \leq 0.85°$. Selected optimum is point B with $n_1 = 27, n_2 = 24$, resulting in $s_t = 0.83°$.

5.5. POINT-TO-POINT MOVEMENT: STEP PLANNING & EXECUTION

In the previous section, step planning was described for the case that the current position of the gears is zero. For any point-to-point movement the procedure is more extensive due to the following: when the escapement mechanism switches from rotation direction, which will be called a turn-around, one ratchet is depressurized and the other is pressurized. This results in the output moving until the teeth of the gear hit the other side of the escapement anchor. The yellow dot and the neighboring tooth in Figure 5.5 illustrate the turn-around. This movement effectively makes both gears move a step, thus resulting in a movement of $s_1 + s_2$ on the output. Whenever a point-to-point movement is required in the opposite direction as the previous movement, this turn-around takes place. This turn-around needs compensation, otherwise the output would move too far.

5.5.1. STEP PLANNING

The desired planned positions of gear 1 and gear 2 are denoted by k_1 and k_2, respectively. The current positions of the gears are denoted by p_1 and p_2. The procedure for planning a movement to a position α is as follows; the position is discretized as in Equation 5.11. Next, planned gear positions k_1 and k_2 are solved from Equation 5.13 as described in Section 5.4.1. Afterwards, the steps d_1 and d_2 needed to get from the current positions to the planned positions for the gears are as in Equation 5.22.

$$d_1 = k_1 - p_1, d_2 = k_2 - p_2. \tag{5.22}$$

Finally, the steps d_1 and d_2 need compensation if a turn-around occurs. Their exist multiple compensation cases, depending on the previous direction of rotation, and the current positions p and planned positions k of gear 1 and gear 2. Furthermore, it is convenient to start the indexing with a gear that is planned to move in the same direction as the previous. All cases of taking steps, including turn-around compensation and indexing order are in Tables E.1 and E.2 of Appendix E.

A few of the compensation cases will be discussed here as an example. The simplest compensation arises for output movement that requires one or more steps with both gears in the opposite direction as the previous. In this case, both gears need to take one less step. Another case involves gear 1 needing to take one or more steps in the same direction as the previous movement, and gear 2 in the opposite direction. Then gear 1 first needs to take one extra step, so $|d_1|+1$ steps, than the turn-around should occur, and next gear 2 should take one extra step, so $|d_2|+1$ steps.

5.5.2. STEP EXECUTION

Execution of a step is done by switching the state of the 5/2 valve connected to pistons of the escapement anchor of the first gear. After execution of two steps in one direction, the ratchet has reached its travel limit and must move back. Pressure is released and reapplied. If a turn-around must occur, one ratchet is moved back and pressure is applied on the other ratchet. Finally, if needed, steps are executed with the other gear. The motor always ends its movement with pressure applied to one of the ratchets in order to maintain position.

5.6. SOFTWARE

Software was written to control the valves and motor. The code can be found in Appendix G and was implemented in Beckhoff TwinCAT [32]. The user can input a desired position set point and adjust the speed of the motor with a Graphical User Interface (GUI). The speed of the motor is adjusted by modifying the time delay between the switching of the valves. Furthermore, the user can start the homing procedure of the motor, and start or stop the movement. The GUI is depicted in Figure 5.8. The software was written according to the State Machine Diagram in Figure 5.9. The software has six different

Figure 5.8: GUI for controlling the motor. The GUI depicts a state where the motor was just homed and the position was reset to zero. This state could be either of the 'Hold CCW' or 'Hold CW' states. On the left of GUI, the user has inputted a desired position set point. The measured position is for testing purposes only, and remains zero if no encoder for testing the motor is attached.

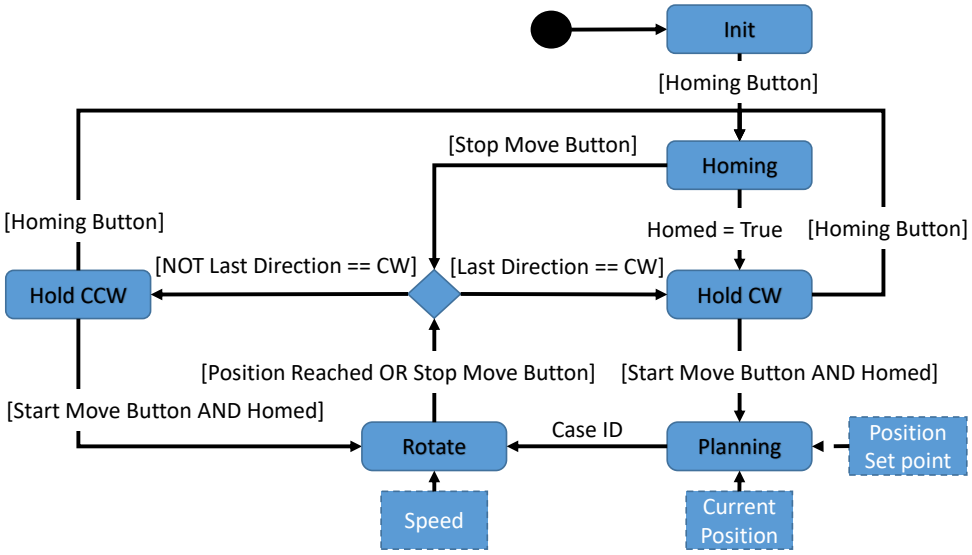

Figure 5.9: State Machine Diagram of software. States are in rounded-off rectangles. Squared rectangles define input variables. Texts in brackets belonging to a line are Boolean variable checks. Texts without brackets belonging to a line are outputs from a state. The Case ID corresponds to the step planning actions in Appendix E.

states. It starts in the 'init' state, and when the user presses the Home button, the motor starts homing. Homing consists of gear 1 centering itself. Homing of gear 2 and thus the output axle happens outside the design of the PneuScape. When the motor is incorporated in the NPS to move the aiming segments, aiming segments 1 and 2 provide a limited movement of 135° and 310°, respectively. Indexing with gear 2 can be executed for at least 18 steps to rotate 135° and 42 steps to rotate 310°, thus allowing the segments to reach their travel limit. With this information, the position of gear 2 is known. Homing of gear 1 involves movement towards the CCW direction, until the carrier hits the casing. Homing of gear 1 only needs indexing with a maximum of eight steps CCW, since that is the maximum travel range of the carrier within the casing. Afterwards, a turn-around occurs, and gear 1 steps three steps in CW direction to reach its central position: $p_1 = 0$. If the user decides to abort the homing by pressing the Stop button, the state changes to 'Hold CCW' or 'Hold CW'. If the last direction of movement was CCW, the motor holds its position with the CCW ratchet piston pressurized, and vice versa for 'Hold CW'.

If homing was successful, the Move button becomes visible. The user can input a position set point and press the Move button to start the 'Planning' state. In this state, step planning is done as described in Section 5.5. A step planning Case ID as in Appendix E is stored and the state is changed to 'Rotate'. The valves start to operate and the motor rotates to its position. If the user stops the movement, the motor stops and goes to either the 'Hold CCW' or 'Hold CW' state, as described above.

5.7. PROTOTYPE

A prototype of the PneuScape was build. See Figures 5.10 and 5.11. Most parts of the prototype were fabricated with rapid prototyping techniques. A Trotec Speedy 300 laser cutter [33] was used to cut parts in either 5, 6 or 8 mm cast PMMA. The escapement anchors were printed on a Felix Printers 3.0 3D printer with PLA filament. The main axle was turned on a lathe and milled. The four pistons in the small cylinders for actuation of the escapement anchors were turned on a lathe. The two piston heads in the ratchet cylinders were turned as well. All parts that were turned or milled are made of POM. The technical drawings of the main axle, pistons of the small cylinder and the piston head of the ratchet cylinder are in Appendix H. The prototype is almost entirely made out of plastics. Only the springs in the ratchet and in the ratchet cylinders are made of spring steel. In a future version of the motor, these can be replaced by plastic ones, or by an elastic member.

The ratchet cylinders need to be pressurized and depressurized, and this is done with fast-switching 3/2 valves (Festo MHE2-MS1H-3/2G-QS-4-K). The two escapement anchors and their two sets of small pistons have two defined states, so one set of small pistons is operated by one fast switching 5/2 valve (Festo MHE2-MS1H-5/2-QS-4-K). Controlling the valves is done with Beckhoff PLC modules [32]. Festo 4 mm outer diameter tubing of 5 m length is used to connect the PneuScape to the Festo valves. In order to support the rotation according to $ub_1 = 53.33°$ of the carrier with respect to the housing, flexible silicon tubes were used to connect to the anchor pistons of anchor 2.

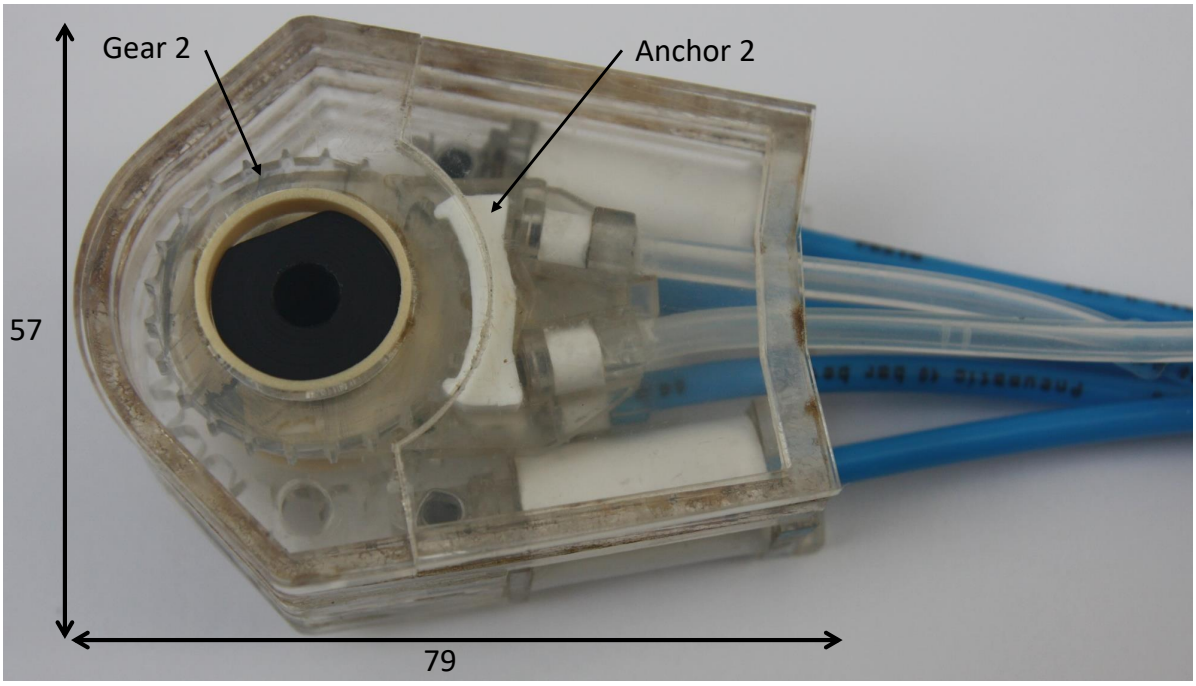

Figure 5.10: Prototype of the PneuScape with approximate dimensions in mm. The height of the prototype is 28 mm.

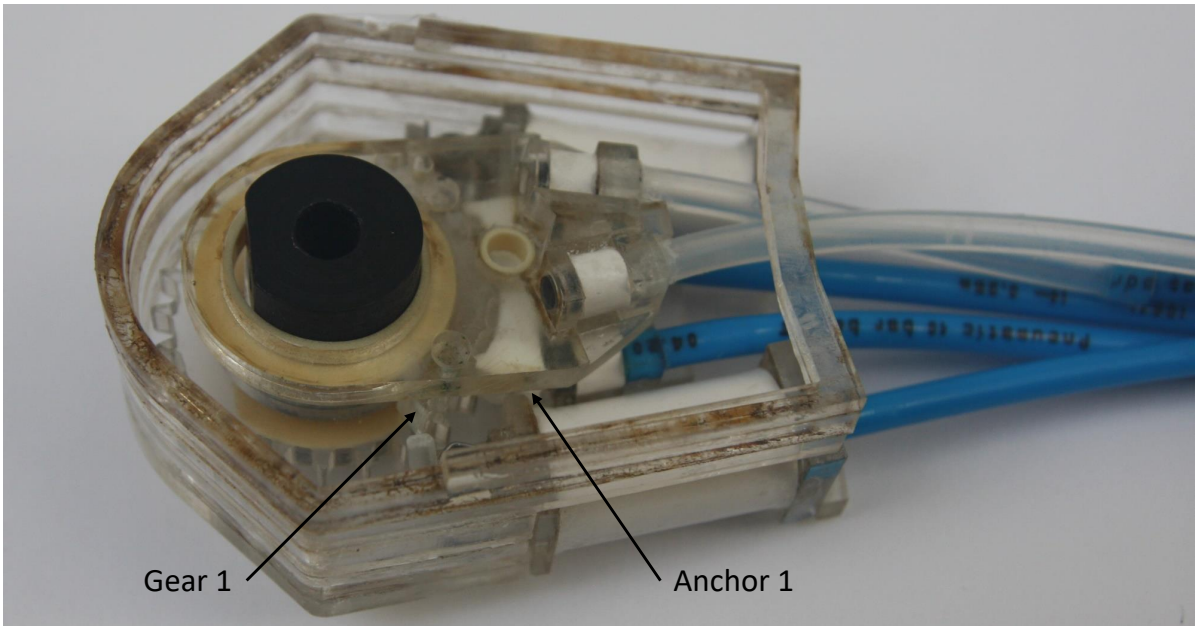

Figure 5.11: Prototype of the PneuScape with the back cover, gear 2 and anchor 2 removed, exposing gear 1 and anchor 1.

6

TESTING

6.1. INTRODUCTION

In this chapter, testing of the operation of the prototype is described. The testing is split into three parts. Testing of the escapement mechanism without operation of the ratchets will be described first. During indexing, pressure is released on one piston and applied to the opposing piston on the anchor. The pneumatic signals need time to travel from the valves to the motor and build up pressure on the anchor pistons. If the pressure is not build up in time, the anchor cannot withstand the torque applied to the output and steps are skipped. Therefore, there is a limit on the speed the motor can reach before steps are being skipped. This limit is influenced by the length of the tubes between the valves and the motor. In order to test the influence of the tube length on the speed and performance of the escapement, testing of the escapement mechanism was done with tubes of 0.2 m length and 5 m length between the valves and the motor. Finally, the total motor including operation of the escapement mechanisms and ratchets was tested with 5 m tube length.

6.2. ESCAPEMENT MECHANISM

6.2.1. GOAL OF TESTS, METHOD & SETUP

In this test, the operation of the escapement mechanism was tested. The ratchets providing the torque were disabled to solely test the escapement mechanism. The goal was to test the accuracy and speed of the output movement produced by operation of the escapement mechanism. An actuating torque was supplied by a weight on a pulley. Different valve delays were introduced in the software, in order to find the maximum speed the motor could turn before it started skipping steps. The test setup is depicted in Figure 6.1. A high resolution encoder (Inducoder ED 58-6-32000-05-D-SC12) was used to measure the rotation of the output of the motor. A pressure of 3 bar was supplied to the small anchor pistons. The tube length from the valves to the small pistons was 0.2 m and used to test the best performance of the escapement mechanism. The supply pressure was 3 bar. The weight on the pulley was 0.4 kg, resulting in 0.12 Nm torque on the output axle. The first test conducted consisted of rotations of $\alpha = 720°$ only with gear 2. The latter translates to 96 steps of $s_2 = 7.5°$. The second test involved the combination of both escapement anchors; 4 steps were done with s_1 and 12 with s_2, resulting in a rotation of $\alpha = 116.67°$.

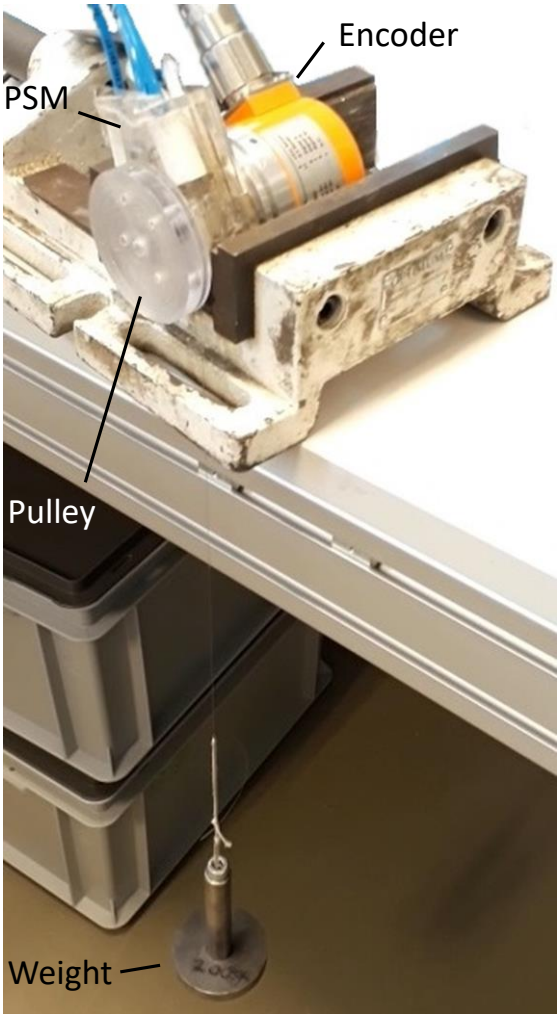

Figure 6.1: Test setup to test the escapement mechanism.

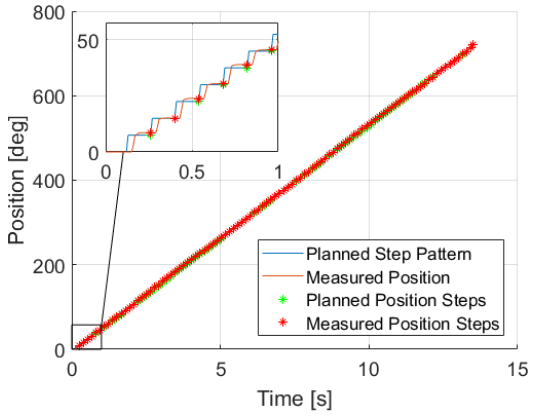

Figure 6.2: Step pattern of the escapement mechanism with 0.2 m tube length. Two full rotations were performed by the motor. Motor was set on the fastest possible speed before steps were skipped. In this trial, the final measured position is 719.89° and average speed is 53.3°/s.

6.2.2. RESULTS & DISCUSSION

Figure 6.2 shows the planned step pattern of the motor and the measured position for the first test. The code to plot the figure is in Appendix F.5. The final measured position was 719.9° for this trial. Other trials showed final measured positions ranging from 719° to 721°, thus within 1° of the planned position. The maximum speed found before the motor started skipping steps was $7 * 10^2$ °/s among the trails. This translates to a step time of 100 ms. The pneumatic valves have a switch time of 2 ms, which is negligible, so it takes 100 ms for the output to accelerate, rotate and decelerate in a step.

INDIVIDUAL STEPS PATTERN

The measured position did not always coincide with the planned pattern, so the individual steps taken were not exactly 7.5°. The latter is made visual by plotting the individual steps as function of the position in Figure 6.3. As can be observed, the mean of the measured step size coincides with the designed step size of 7.5°, and the individual steps differ from 5.7° to 8.9°. However, there is a pattern that repeats itself every revolution; the left and right side of the split line look similar. This repetition means that gear 2 is the main cause of the differing individual steps. The gear in the prototype is not produced with small enough tolerances, so the distance between the teeth is not 7.5° for every step. After a full revolution, the same tooth engages again with the anchor, so the prototype is the most accurate at this position. So after two full rotations, this accuracy manifests itself in measured positions ranging from 719° to 721°; the precision of the motor on this tooth is thus 1°. The origin of this precision error by re-engagement of the same tooth on the gear and anchor has not been further investigated. However, a possible cause could be that every time the teeth engage, they engage at slightly different places along their edge. This could be due to inaccuracies in the geometry of the teeth.

Another observation from Figure 6.3 is that every odd step is above the mean and every even step is below the mean step size. This pattern is caused by geometric inaccuracies in the escapement anchor. A possible cause could be that the anchor has one tooth that is larger than the other. Another cause could be that the angular width γ between the teeth of the anchor as defined in Figure 5.3 is too large. A final cause for this step pattern could be eccentric misalignment of the axes of the anchor or output gear, resulting in a larger distance between the anchor and gear.

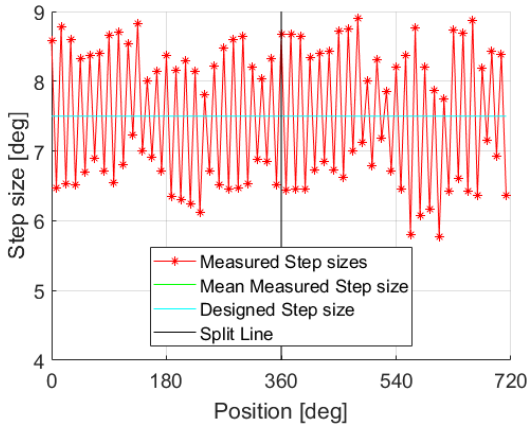

Figure 6.3: Individual steps taken by the escapement mechanism with tube length of 0.2 m.

The second test involved the combination of the two step sizes. It was found that the latter does not produce accurate movement. In many cases gear 1 skips steps. The latter can be caused by gear 1 or anchor 1 being produced with geometric inaccuracies. Furthermore, gear 1 and the carrier were produced as two separate parts, so misalignment in the attachment of gear 1 to the carrier could be a cause for gear 1 skipping steps. The best trail was one that ended in a measured position of 117.6°, where it should be 116.67°.

6.3. ESCAPEMENT AT 5 M DISTANCE

6.3.1. GOAL OF TESTS, METHOD & SETUP

In this test, the influence on the performance of motor with 5 m long tubes between the valves and the motor was tested. The test setup was the same as in Section 6.2.1, but the tubes to the escapement anchors had a length of 5 m. Furthermore, rotation was done with 47 steps with gear 2, resulting in a planned rotation of 352.5°. Different valve delays were introduced in the software, in order to find the maximum speed the motor could turn before it started skipping steps.

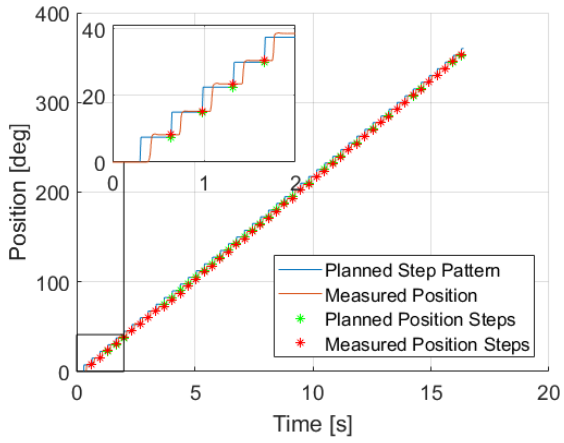

Figure 6.4: Step pattern of the escapement mechanism, with a tube length of 5 m. Rotation was done over 352.5°. In this trial, the final measured position was 353.6°, and an average speed of 21.6°/s was measured.

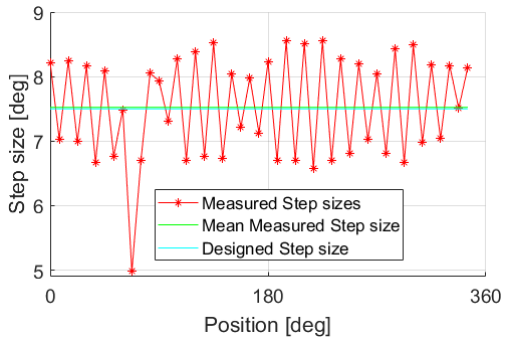

Figure 6.5: Individual steps taken by the escapement mechanism, with a tube length of 5 m.

6.3.2. RESULTS & DISCUSSION

The biggest influence of the longer tubes was the speed the motor could reach before it started skipping steps. The maximum speed measured during the tests was in the order of $2 * 10^2$ °/s. This translates to a step time of 370 ms. The step pattern for a trial is depicted in Figure 6.4. The slower speed is logical: it takes longer for the pressure to build up in the small anchor pistons.

The accuracy of the motor with 5 m long tubes is the same as in the test with 0.2 m; measured positions show a maximum of 1° error in the final position. This resemblance is logical, the length of the tubes only influences the time it takes to make a step, so the final error after a number of full rotations is a function of the geometry of the escapement mechanism. Furthermore, the individual measured steps show a similar pattern as in the test with 0.2 m long tubes: the plot of Figure 6.5 approximately coincides with position 165° to 525° in Figure 6.3. The latter is made visual in Figure 6.6, by plotting the two graphs together. This resemblance justifies the claim that gear 2 and anchor 2 are causes for errors.

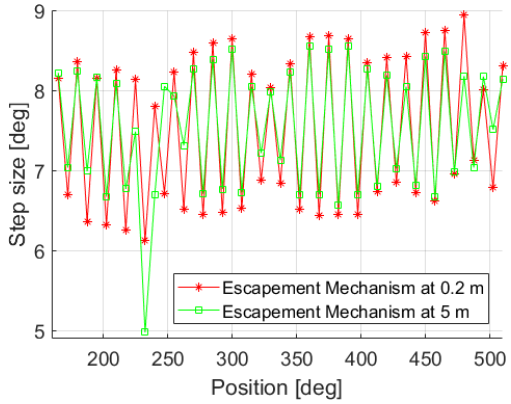

Figure 6.6: Resemblance in individual step pattern taken by the escapement mechanism, with a tube length of 0.2 m and 5 m.

6.4. TOTAL MOTOR

6.4.1. GOAL OF TESTS, METHOD & SETUP

In this test, the total motor including operation of the ratchets was tested. Both functions of providing torque with the ratchets and providing stopping force with the escapements anchors were tested. The test setup consisted of the motor and the Inducoder encoder. The tube length to the motor was 5 m. The supply pressure to the small cylinders of the escapement anchors was set to 3 bar. In order to perform the test, the supply pressure for the ratchets had to be set. This pressure was set such that the escapement mechanism could hold the force exerted by the ratchet, even during execution of steps. A pressure to high would result in the motor skipping steps. A position set point of 360° was used and different valve delays were introduced in the software, in order to find the maximum speed the motor could turn before it started skipping steps.

6.4.2. TOTAL MOTOR: RESULTS & DISCUSSION

The supply pressure found for operation of the ratchets was 1 bar, however this required delicate tuning. Just under 1 bar, the ratchets would not move due to internal friction. For a value slightly higher than 1 bar, the ratchets would move too fast and would make the escapement mechanism skip steps: After the escapement mechanism switches position and releases its gear, the ratchets start to move the output. When the output has rotated to the next tooth on the gear, the momentum of the ratchet pushes the gear through underneath the anchor and the motor skips a step, when the pressure is higher than 1 bar. If however, the ratchet is at standstill with a tooth of the gear pushing against the anchor, the pressure can be increased to values higher than 1 bar, before the anchor slips. The latter shows that the momentum of the ratchets plays an important role.

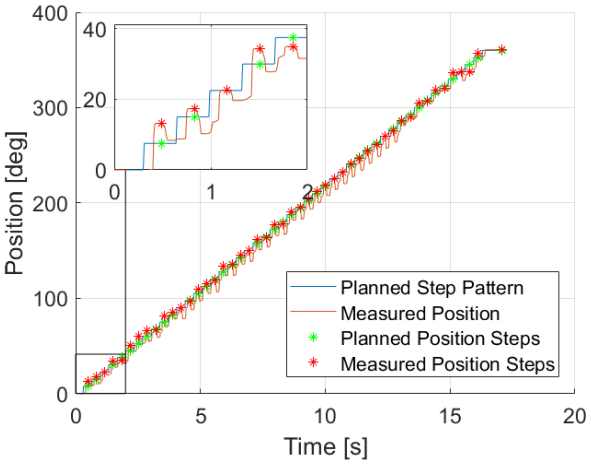

Figure 6.7: Step pattern of the total motor. Rotation was done over 360°. In this test, the final measured position was 360.7°, and an average speed of 21.1°/s was measured.

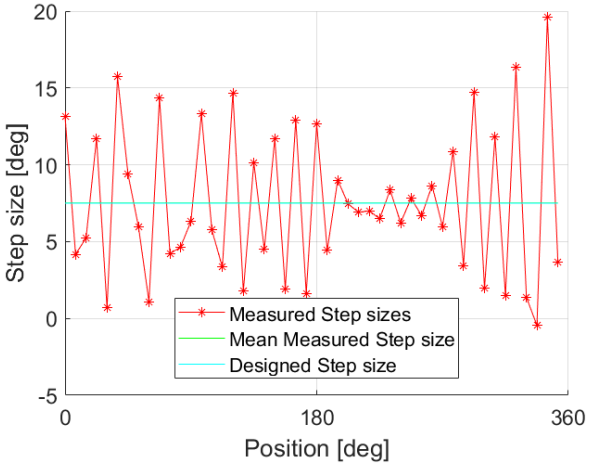

Figure 6.8: Individual Steps taken with the total motor. Results are for one trial, and do not represent average performance.

Even with the delicate tuning of the supply pressure, during the tests, it was found that the ratchets do not perform reliably. In many cases the ratchets make the motor skip steps, or take too little steps. The ratchets suffer from unreliable friction against the housing, resulting in them sometimes building up more speed before engaging. This unreliability in momentum makes tuning the pressure harder.

The ratchet cylinders have an internal diameter of 12 mm and are placed 22 mm from the center of the output axle. At 1 bar, the ratchets thus produce a torque of 0.25 Nm, which the escapement anchors can still withstand. Figure 6.7 shows the step pattern for the best test conducted, one that achieved the highest speed. The geometric pattern of gear 2 as observed in the previous tests from Section 6.3 and 6.4 is not observed in this test. The individual steps taken show values two or three times larger than the step size of 7.5°, indicating that steps are skipped numerous times. By chance the final measured position after a full rotation was 360.7°, within 1° from the set point. However, this accuracy was not achieved in other trails, so the result is not representative for all trails conducted. Furthermore, this result is only achieved after tuning of the supply pressure. An average speed of 21.1 °/s was measured, comparable to the test in Section 6.3 where the escapement mechanism with 5 m tubes was tested. This shows that ratchets retracting en reengaging are not a limiting factor in the speed of the motor.

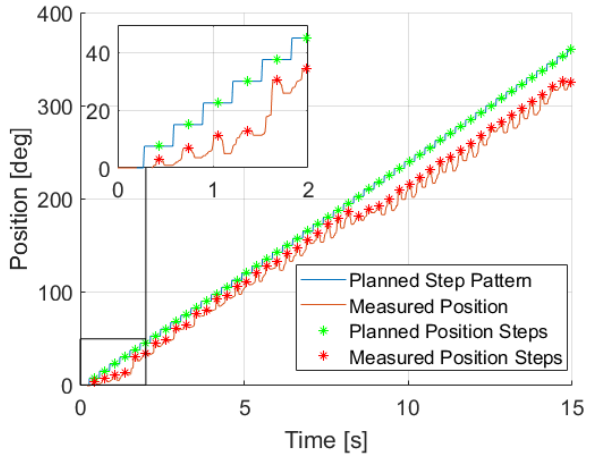

Figure 6.9: Step pattern of the total motor, showing a failed movement. Rotation was done over 360°. In this test, the final measured position was 324.8°, and an average speed of 21.7°/s was measured.

Figure 6.9 shows the step pattern of a movement with the ratchet that failed to reach its position set point. The final measured position was 324.8°, showing large definition from the set point of 360°. The individual steps in Figure 6.10 show a couple of steps that are negative. The latter means that no step was executed and the ratchet failed to reengage correctly.

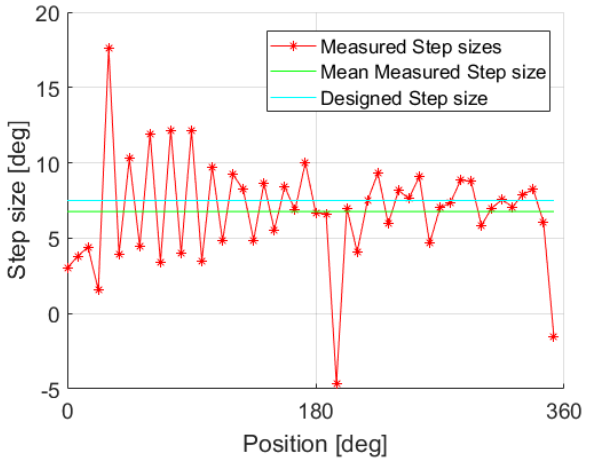

Figure 6.10: Individual steps taken with the total motor, showing a failed movement.

7

DISCUSSION

7.1. PERFORMANCE

With testing done, the performance of the prototype can be evaluated by reviewing the design requirements and stating which are met. The requirements that are met will be given a pass, those that were not met will be given a fail. In general, the total motor including operation of the ratchets does not fulfill the design requirements. However, the escapement mechanism itself shows promising results. Recommendations for future work are given in Section 7.2.

7.1.1. PRIMARY DESIGN REQUIREMENTS

P1 *Error ≤ 0.46°.* Fail. The general accuracy and precision of the total motor including operation of the ratchets is insufficient. The motor skips steps. Steps executed with just the escapement mechanism and without operation of the ratchets produce more accurate motion. However, gear 1 skips steps in most trials. Nonetheless, when only gear 2 is making steps, no steps are skipped. For a general point-to-point movement, gear 2 produces an error up to 3 degrees. This is due to inaccuracies in production of the escapement anchors and gears or eccentric misalignment of the gears and anchors. However, after any number of full revolutions with gear 2, the motor positions itself with a precision of 1°.

P2 *Design space.* Accepted Fail. Two PneuScapes to actuate both aiming segments approximately fit in the design space, with only a small portion sticking out, see Figure 7.1.

P3 *Torque ≥ 0.62 Nm.* Fail. The momentum of the ratchets during their movement in combination with the design of the teeth of the anchors and gears do not allow for a high supply pressure to the ratchets. The supply pressure to the ratchets is limited to 1 bar resulting in 0.25 Nm of torque.

P4 *Speed ≥ 21 °/s.* Pass. Movement of the total motor with ratchets with 5 m tube length runs at 21 °/s. The escapement mechanism itself with a tube length of 5 m can run at 21 °/s as well.

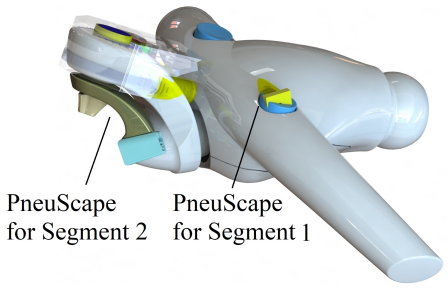

Figure 7.1: Two PneuScapes in the design space. One Pneuscape is incorporated in segment 1 for rotation of segment 2. The motor sticks out from some parts of the segment. The other Pneuscape is incorporated in the main body of the OM and fits almost entirely.

7.1.2. DESIGN CONDITIONS

C1 *MR Safe.* Pass. The operation principle of the PneuScape is MR safe. The prototype is largely MR safe, it only contains metal springs, that can be replaced with nonmagnetic counterparts in a future version.

C2 *Sterile.* Pass. The motor supports the sterility of the current NPS. Any leakage of gasses in the motor does not disrupt sterility since cleaned medical instrument air or nitrogen can be used to power the motor.

C3 *Stiffness.* Not evaluated. Stiffness could not be defined since the motor does not meet the error requirement P1 and torque requirement P3.

C4 *Vibrations.* Pass. When the escapement mechanism runs at 21°/s, the motion dampens out before a new step is taken, see Figure 7.2. The plastic materials used dampen out the vibrations.

C5 *Range of motion of 135° & 310°.* Pass. The PneuScape can produce unlimited range of motion.

7.1.3. WISHES

W1 *Sound < 50 dB.* Pass. Operation of the motor does not disturb speech, so the volume stays below 50 dB.

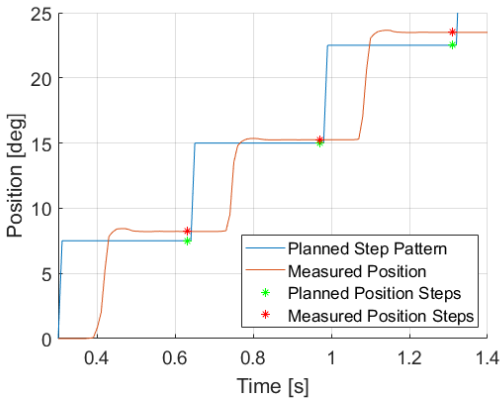

Figure 7.2: Motion dampens out before a new step is taken when movement is at 21 °/s. Escapement mechanism only, tube length is 5 m, as in Figure 6.5.

7.2. RECOMMENDATIONS FOR FUTURE WORK

In order to improve the prototype of the PneuScape, different recommendations for future work are given. The following sections indicate improvement of the performance of the PneuScape on each of the design requirements. At the end of the section, new research directions are stated.

7.2.1. IMPROVING ACCURACY & PRECISION

IMPROVING RATCHET DESIGN

Operation of the ratchets is a dominant factor for the inaccurate movement of the PneuScape. As observed during testing, the ratchets experience friction with the housing of the motor, resulting in unreliable motion. Moreover, the momentum of the ratchets makes the escapement anchors skip steps. Furthermore, the ratchet pawls seem fragile. The design of the ratchets can be improved by allowing more space between the motor housing and the ratchet pawl. A different approach is to choose another method of applying actuating force, preferably a more constant method than the ratchet. This constant method could be a vane as in the integrated concept of the Dual Escapement Mechanism with Vane. However, adding this vane would sacrifice the unlimited range of motion produced by the ratchets.

IMPROVING ESCAPEMENT MECHANISM

The step size of the PneuScape is currently designed on $s_t = 0.83^o$. The design requirements specify a one-sided accuracy of 0.46^o, so there is $2 * 0.46 - 0.83 = 0.09^o$ left as error budget in positioning. Currently, the prototype makes an error in rotation of 1^o to 3^o, which is much larger than the error budget. The first recommendation to improve the accuracy of the PneuScape is to improve the method of fabrication of

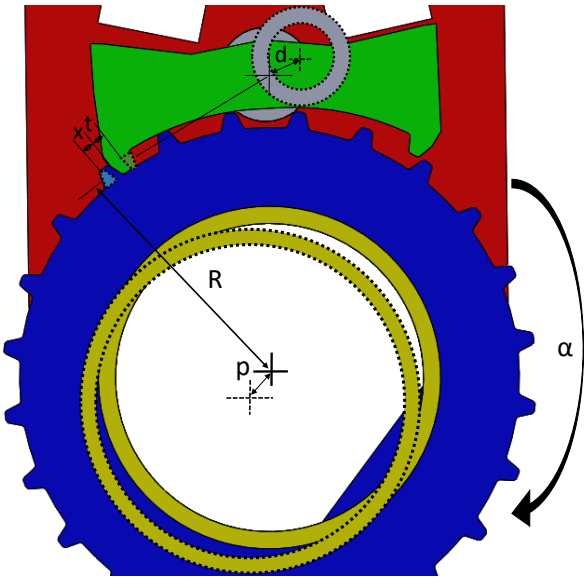

Figure 7.3: Indication of tolerances and geometry variables for error analysis of rotation α. The parts with dashed outer lines indicate parts that are offset within their tolerances. The distance p and d represent the eccentricity of the axes of the gear and anchor. The distance x and t indicate the tolerances of the teeth.

gears and escapement anchors so smaller tolerances can be met. The tolerances in these parts directly influence the accuracy of motion. The worst-case scenario is depicted in Figure 7.3: the gear will make an error α in rotation due to inaccuracies x and t in fabrication of the anchor and gear and eccentric misalignment d and p of their respective axes. An approximation of α is given in Equation 7.1.

$$\alpha = \arctan\frac{x}{R} + \arctan\frac{t}{R} + \arctan\frac{p}{R} + \arctan\frac{d}{R} \approx \arctan\frac{x+t+p+d}{R}. \tag{7.1}$$

An improvement in the tolerances compared to the current prototype can be achieved with more precise laser cutting. Laser cutting of plastics can reach up to 10 μm tolerance [34, 35]. When $x = t = d = p = 10\mu$m, the error $\alpha = 0.15^o$. This error is larger than the error budget of 0.09^o. Different fabrication method can be used to produce smaller tolerances. This would typically increase the costs of production.

As mentioned in Section 6.2.2, re-engagement of the same tooth on the anchor after any number of full rotations results in a precision of 1°. A possible cause for this could be that the teeth and the anchor re-engage at a different place along their edge. When a production method is used that can meet better tolerances, the geometry of the teeth is perfected. Then, the teeth are expected to re-engage closer to the same place, increasing the precision of the movement.

ADDITIONAL MEASURES

There exist additional measures to improve the accuracy and precision of the movement. A decision can be made to design for a smaller step size, in order to leave more error budget. However, smaller step sizes would produce slower motion, so the motor would need to be sped up. Moreover, a smaller step size requires more teeth on the gear, resulting in smaller teeth, which can withstand less torque. The last option is to benefit from the pattern and reproducibility of the error created by the gear as explained in Section 6.2.2. The gear with its errors could be incorporated in the design, and a similar pattern to that of Figure 6.3 could be measured. Since the pattern is known, the error it produces can be compensated for. However, this pattern error measurement would need to be done for every gear produced.

Another solution to increase the accuracy is to add an encoder. The encoder was not yet added in the prototype. The encoder can supply direct feedback on the rotation of the output. When a step is skipped, or any other error is made, the controller knows this and the motor can take compensating steps.

7.2.2. IMPROVING SPEED & TORQUE

If it is wished to improve the speed of the motor, a valve in the motor can be added. A tube with constant pressure runs to the motor, plus a tube that carriers the signal for the anchor. A valve in the motor switches the pressure locally from one piston of the anchor to the other. The air can be exhausted in the motor, and does not need to travel 5 m back to a valve. Furthermore, the pressure in the anchor is build up much quicker, since the valve directs air to the piston from a constant pressure source in the motor. This valve would need to be MR safe and use a pneumatic signal to switch its state.

Furthermore, increasing the speed can be done by increasing the pressure on the ratchets, but the escapement anchors need to be redesigned to withstand the higher momentum of the ratchets. Increasing the pressure on the ratchet also increases the torque the motor can supply. One way to redesign the escapement anchors to withstand a higher torque is to make the angles α_1 and α_2 between the teeth of the escapement and gear in Figure 5.5 larger. This will increase the force F_a the anchor can withstand. Moreover, the pressure on the pistons of the escapement anchors can be increased to make the pistons supply more force.

7.2.3. NEW RESEARCH DIRECTIONS

With the current design with escapement mechanism as a basis, interesting research directions comprise the total number of escapement anchors and gears. What would happen if the PSM uses 3 gears and escapement anchors? Gives this the possibility to have a small step size s_t even with around 10 teeth per gear? What are the effects on the upper bound of rotation of gear 1 ub_1 for this triple gear motor? What happens with s_t and ub_1 when an even larger number of gears is used, for instance; what happens when 10 gears are used?

Another research direction revolves around the following question: is it possible to decrease the number of tubes to the motor, without compromising on speed and resolution of the mechanism? In theory, only 5 different signals are needed to control the motor: step forwards with gear 1, step backwards with gear 1, step forwards with gear 2, step backwards with gear 2 and stop stepping. This requires 3 Boolean signals, which is possible to send through 3 tubes when switching the pressure on and off. The current prototype has 6 tubes, so a reduction could be possible. Implementing less tubes means that a kind of pneumatic valve logic needs to be incorporated in the motor, decrypting the pneumatic signals into the right pneumatic piston actions.

7.3. ADDITIONAL FIELDS OF APPLICATION

The PneuScape was designed with movement of a load of 0.5 kg on 10 cm distance in mind, resulting in 0.5 Nm of torque. This load represents a biopsy module that is moved by rotation of the segments. The PneuScape currently has the smallest designed step size $s_t = 0.83^o$ of any MR safe pneumatic motor. A future version of the PneuScape can be developed expecting to meet the requirements with the recommendations given in this chapter. The motor's main application is in precise needle position. A future version of the PneuScape can be used in other MR safe devices where precise positioning is required, even when a load is applied. These include, among others, MR safe biopsy devices, laser positioning in the MR environment, ultrasound ablation, injection of fluids and medical robotics.

8

Conclusion

A small size, MR safe and high resolution pneumatic stepper motor was designed for operation of the aiming segments of the Needle Placement System (NPS). This motor, called the PneuScape, was designed to fit in the orientation module of the NPS. The PneuScape has a target step size of $s_t = 0.83^o$, which is smaller than the former state-of-the-art MR safe pneumatic stepper motor with $s_t = 2.86^o$. The design of the PneuScape consists of dual gear escapement mechanisms, connected with a differential mechanism. Ratchets apply a torque to move the output either clockwise or counterclockwise and the escapement anchors index the movement, creating a step.

A prototype of the Pneuscape was developed using rapid prototyping techniques and was tested against the design requirements. The total prototype did not meet all requirements, in particular the requirement of maximum positioning error. The ratchets do not work reliably and result in the motor skipping steps, diminishing the motor's accuracy. The escapement anchors however, show promising results in their performance.

Recommendations are given to improve the prototype. A fabrication method for the anchors and gears can be chosen that produces smaller tolerances than the current laser cutting and 3D printing techniques used. Furthermore, a smaller designed step size s_t can be chosen to allow for more errors in the production of the gears and anchors. Moreover, a different method of applying torque can be chosen, or the ratchets' design can be improved. If the prototype is improved with the aid of the recommendations given, a future version of the PneuScape is expected to meet the design requirements. Finally, the work in this thesis has made science take a step towards high resolution MR safe actuation.

BIBLIOGRAPHY

[1] K. A. Smith and J. Carrino, *Mri-guided interventions of the musculoskeletal system,* Magn Reson Med **27**, 339 (2008).

[2] R. Monfaredi, K. Cleary, and K. Sharma, *Mri robots for needle-based interventions: Systems and technology,* Ann Biomed Eng , 1 (2018).

[3] R. H. Taylor, A. Menciassi, G. Fichtinger, P. Fiorini, and P. Dario, *Medical robotics and computer-integrated surgery,* in *Springer handbook of robotics* (Springer, 2016) pp. 1657–1684.

[4] M. M. Arnolli, N. C. Hanumara, M. Franken, D. M. Brouwer, and I. A. Broeders, *An overview of systems for ct-and mri-guided percutaneous needle placement in the thorax and abdomen,* Int J Med Rob Comput Assisted Surg **11**, 458 (2015).

[5] K. Cleary, A. Melzer, V. Watson, G. Kronreif, and D. Stoianovici, *Interventional robotic systems: applications and technology state-of-the-art,* Minim Invasiv Ther **15**, 101 (2006).

[6] American Society for Testing and Materials (ASTM) International DF, *Astm f2503-05, standard practice for marking medical devices and other items for safety in the magnetic resonance environment,* (2005).

[7] F. G. Shellock, T. O. Woods, and J. V. Crues III, *Mr labeling information for implants and devices: explanation of terminology,* Radiology **253**, 26 (2009).

[8] M. Arnolli, *Development of a precision system for image-guided needle placement: from scratch to clinic*, Ph.D. thesis, University of Twente (2017).

[9] R. Moser, R. Gassert, E. Burdet, L. Sache, H. Woodtli, J. Erni, W. Maeder, and H. Bleuler, *An mr compatible robot technology,* in *Robotics and Automation, 2003. Proceedings. ICRA'03. IEEE International Conference on*, Vol. 1 (IEEE, 2003) pp. 670–675.

[10] F. S. Farimani and S. Misra, *Introducing pneuact: Parametrically-designed mri-compatible pneumatic stepper actuator,* in *IEEE International Conference on Robotics and Automation 2018* (2018).

[11] A. Wineland, Y. Chen, and Z. T. H. Tse, *Magnetic resonance imaging compatible pneumatic stepper motor with geneva drive,* Journal of Medical Devices **10**, 020950 (2016).

[12] Y. Wei, Y. Chen, Y. Yang, and Y. Li, *Novel design and 3-d printing of nonassembly controllable pneumatic robots,* IEEE/ASME Transactions on Mechatronics **21**, 649 (2016).

[13] Y. Chen, K.-W. Kwok, and Z. T. H. Tse, *An mr-conditional high-torque pneumatic stepper motor for mri-guided and robot-assisted intervention,* Annals of biomedical engineering **42**, 1823 (2014).

[14] R. Secoli, M. Robinson, M. Brugnoli, and F. Rodriguez y Baena, *A low-cost, high-field-strength magnetic resonance imaging–compatible actuator,* Proceedings of the Institution of Mechanical Engineers, Part H: Journal of Engineering in Medicine **229**, 215 (2015).

[15] B. L. Boland, S. Xu, B. Wood, and Z. T. H. Tse, *High speed pneumatic stepper motor for mri applications,* Annals of biomedical engineering , 1 (2018).

[16] G. Howland, *Pneumatic Nutator Actuator Motor*, Tech. Rep. (BPAD-863-16719R (NASA CR-54788), Bendix Corp, 1965).

[17] S. Oda, K. Suzumori, K. Uzuka, and I. Enomoto, *Development of nutation motors (improvement of pneumatic nutation motor by optimizing diaphragm design),* Journal of mechanical science and technology **24**, 25 (2010).

[18] A. Tantrapiwat and J. P. Coulter, *The development of a pneumatic stepping motor concept for valve based flow control during injection molding,* in *ASME 2007 International Mechanical Engineering Congress and Exposition* (American Society of Mechanical Engineers, 2007) pp. 559–564.

[19] Baumgartner Maschinenbau AG, *Schrittmotor bps,* (2019, accessed 17 January 2019).

[20] V. Groenhuis, F. J. Siepel, and S. Stramigioli, *Dual-speed mr safe pneumatic stepper motors,* in *Robotics: Science and Systems 2018* (2018).

[21] V. Groenhuis and S. Stramigioli, *Rapid prototyping high-performance mr safe pneumatic stepper motors,* IEEE/ASME transactions on mechatronics **23**, 1843 (2018).

[22] D. B. Comber, J. E. Slightam, V. R. Gervasi, J. S. Neimat, and E. J. Barth, *Design, additive manufacture, and control of a pneumatic mr-compatible needle driver,* IEEE Transactions on Robotics **32**, 138 (2016).

[23] D. Stoianovici, A. Patriciu, D. Petrisor, D. Mazilu, and L. Kavoussi, *A new type of motor: pneumatic step motor,* IEEE/ASME Transactions On Mechatronics **12**, 98 (2007).

[24] H. Sajima, H. Kamiuchi, K. Kuwana, T. Dohi, and K. Masamune, *Mr-safe pneumatic rotation stepping actuator,* Journal of Robotics and Mechatronics **24**, 820 (2012).

[25] Z. Guo, T. Lun, Y. Chen, H. Su, D. Chan, and K. Kwok, *Novel design of an mr-safe pneumatic stepper motor for mri-guided robotic interventions,* in *Proceedings of The Hamlyn Symposium on Medical Robotics* (Imperial College London and the Royal Geographical Society London. The . . . , 2016).

[26] Y. Chen, C. D. Mershon, and Z. T. H. Tse, *A 10-mm mr-conditional unidirectional pneumatic stepper motor,* IEEE/ASME Transactions on Mechatronics **20**, 782 (2015).

[27] ASSAG, *Cylkro face gear program,* (2019, accessed 3 September 2019).

[28] Selio, *Gearbox dissection and design, mie243, university of toronto,* (2019, accessed 1 July 2019).

[29] Jahobr, *Harmonic-drive animation (strain wave gear (swg),* (2019, accessed 1 July 2019).

[30] Festo, *Mh2, mh3, mh4 festo,* (2019, accessed 11 July 2019).

[31] Minor Rubber, *Rubber bellow,* (2019, accessed 26 August 2019).

[32] Beckhoff Automation GmbH, *Beckhoff new automation technology,* (2019, accessed 30 August 2019).

[33] Trotec Laser Inc., *Laser engravers and cutters,* (2019, accessed 27 August 2019).

[34] Cam Technologies Inc., *Wire edm cutting vs laser cutting,* (2019, accessed 13 September 2019).

[35] Induflex, *Laser cutting of plastic,* (2019, accessed 13 September 2019).

[36] K. Uzuka, I. Enomoto, and K. Suzumori, *Comparative assessment of several nutation motor types,* IEEE/ASME Transactions on Mechatronics **14**, 82 (2009).

Journal Title
XX(X):1–19

DOI: 10.1177/ToBeAssigned
www.sagepub.com/
SAGE

Actuation principles in the magnetic resonance environment: A review of the patent literature

Stephan Neevel[1], Pieter Wiskerke[2] and Paul Breedveld[1]

Abstract

Interventions done under magnetic resonance (MR) image guidance can benefit from mechatronics. However, conventional electromagnetic actuators often used in mechatronics are not safe for use in the MR environment due to interactions between the magnetic field and the actuators. This review provides an overview of patents on devices and their actuation principles designed for use in the MR environment. The Web of Science Derwent Innovations Index was used to find 113 relevant patents. A systematic classification of actuation principles was proposed. First, a differentiation was made between actuators having their kinetic energy internally induced by a conversion of one form of energy into kinetic energy, versus actuators having their kinetic energy externally induced and transmissioned to the actuator. Second, a differentiation was made on the type of energy being internally converted to kinetic energy and the type of transmission of external kinetic energy. By this top down approach, 15 different types of actuation principles were identified. Next, the classification was applied to the relevant patents. No patents were found for actuation principles using light or chemical energy or heating of a gas or liquid as source of kinetic energy. Furthermore, pneumatic and piezoelectric actuators were used the most in the patents found, as well as in patents which have been commercialized. The insight in the most used and unexplored actuation principles could serve as an inspiration for selecting existing or developing new actuation principles for mechatronic devices in the MR environment. Future work should look into the scientific literature on the found patents for quantitative information on the performance of their actuation principles.

Keywords

MRI, magnetic resonance, actuation, actuator, mechatronics, medical devices, patent

Introduction

Magnetic Resonance Imaging (MRI) is a technique used to capture 3D images of the human body. MRI offers good contrast resolution to accurately detect anatomic features.[1,2] Surgical interventions in the human body can be guided by MRI. These interventions include, among others, MRI-guided brachytherapy, MRI-guided prostate biopsy and MRI-guided neurosurgery.[2] Typically, in such MRI-guided interventions, a needle or instrument has to be placed in the body to reach a specific target, for instance a tumor. It is key that this needle or instrument reaches the target accurately, and mechatronic systems in surgery can significantly improve surgeons' technical capability to perform these interventions.[3] Different types of mechatronic devices have been developed to assist in positioning the needle or instrument. Multiple reviews of the scientific literature on mechatronic devices in MRI-guided surgery have been done.[2,4,5]

MRI scanners consist of electromagnets and Radio Frequency (RF) coils. Scanners with a field strength of 1.5 T to 3 T are typically used in hospitals. However, clinical trials are being conducted with high resolution 7 T scanners. Any instrument or device used in the Magnetic Resonance (MR) scanner room must comply with the electromagnetic effects of the MRI scanner; it must be safe for use in the MR environment. Three terms regarding MR safety have been defined by the ASTM F2503 standard[6]: a device can be MR safe, MR conditional or MR unsafe. As described by Shellock et al.[7]: "A device is MR safe if it poses no known hazards in the MR environment. MR safe devices are nonconducting, nonmetallic, and nonmagnetic. A device may be determined to be MR safe by providing a scientifically based rationale rather than test data." In contrast, a device can also be MR conditional: it poses no known hazards in a specified MR environment. Testing of the device must be performed in order to specify the conditions of usage. For example, conditions can be set on the distance from the device to the MRI scanner, or on the time the device can be used close to the MRI scanner. MR unsafe devices pose safety risks to the patient or user and cannot be used in the MR environment.

Any mechatronic device used to assist in MRI-guided surgery must be MR conditional or MR safe. A key challenge in designing a mechatronic device for the MR environment is selecting MR safe or MR conditional actuators. In conventional mechatronics, electromagnetic motors containing magnetic and conductive materials are often used. These motors are not MR safe, because they will

[1]Delft University of Technology, NL
[2]Demcon Advanced Mechatronics B.V., NL

Corresponding author:
Stephan Neevel, Department of Biomechanical Engineering, Faculty of Mechanical, Maritime and Materials Engineering, Delft University of Technology, Mekelweg 2, 2628 CD Delft, The Netherlands.
Email: XXX@XXX.com

be attracted by the field of the MRI scanner.[8] Furthermore, during operation, these motors will produce artifacts in the MR image, disturbing the image. The artifacts can hinder identification of abnormal tissue or diagnostics with MRI in general. Moreover, Eddy currents in electrically conducting materials will start to flow because of the changing magnetic field in the MRI scanner. This current will heat up the device. Current flowing through the device and heating of the actuator or device can lead to malfunction of the device, and even to injury. Scientific literature on designing and choosing actuators for the MR environment has been published by Fischer et al.[9], Gassert et al.[10] and Yu et al.[11]

Goal of the study

Conventional electromagnetic actuators used in mechatronics are not MR safe. Given the challenges in designing mechatronic devices for the MR environment, insight in the most used and yet unexplored actuation principles could serve as an inspiration for selecting existing or developing new actuation principles for mechatronic devices in the MR environment.

Therefore, the goal of this study is to give an overview of the patent literature on actuation principles used in devices designed for the MR environment. A review of the patent literature has been chosen as patents have not been taken into account in previous reviews in this field yet. To aid the goal, a systematic classification of actuation principles will be made and applied to the devices in the patents. Furthermore, devices will be classified on their MR safety. Moreover, a study will be done to see which patents have been commercialized.

Patent search method

A patent search was done in the Web of Science Derwent Innovations Index (DII). The DII gives the user the ability to perform a ”Topic Search (TS)”. The Topic Search searches in edited abstracts and edited titles, written by a human based on the contents of the patent. Google Patents, Espacenet and Free Patents Online all only allow a search in the regular title and abstract. Since patent abstracts and titles can be ”nonspecific”[12], this Topic Search allows for a more directed search. A full text search, which is possible with Google Patents and Espacenet, would lead to too many irrelevant results.[12]

In order to find actuated devices in the MR environment, a search query was set up. The query contains a part which specifies the patent has to do with magnetic resonance imaging and a part that the patent has to have some sort of actuation. The full query is: *TS=((”magnetic resonance” OR mri OR ”medical imaging”) AND (motor* OR actuat* OR robot*)) AND DC=(P31 OR P32 OR P33 OR P34 OR P35 OR P36 OR S01 OR S02 OR S03 OR S04 OR S05 OR S06)*. The search was restricted to the Health and Amusement section of the General Engineering section (codes: P31 through P36) and the Instrumentation, Measuring and Testing section (codes: S01 through S06) of the DII. The search was conducted in the following patent regions: European, Worldwide, US, China, Korea and Japan.

Eligibility Criteria

Included are all patents that contain a device powered by some sort of motor or actuator and are used in conjunction with an MRI scanner. Excluded are patents of devices that are used with any form of MRI other than that for medical purposes. Duplicates were removed by looking at the title of the patents and checking the inventors and assignees. If multiple patents were found that described the same device, only one patent of that device was included. If one patent described an actuator, and one patent described an application of that actuator in a device, both patents were included.

General results

The query yields 1601 results (26-06-2018). To select relevant patents, all the titles of the patents were inspected and the abstract was read for most patents. When in doubt about the relevance, the patent description itself was read. There were 193 patents selected. Then, exclusion was done based on the criteria mentioned in the previous section. Some patents did not specify which type of actuator was used in the abstract, so the description of these patents was searched for the keyword motor or actuator to identify which type of actuator was used. Patents that still did not specify what type of actuator was used were left out. After further full text inspecting of the patents, 113 relevant patents were found. In Tables 1 and 2 the relevant patents are summarized, showing the inventor(s), assignee, priority date, patent number and the key application of the device described in the patent. Some patents solely describe an actuator, those are indicated as having a key application ’any (actuator)’. Many different devices were found, with applications ranging from actuating microscopes, to drills, needle positioning systems and to inflating medical implants.

Classification of relevant patents

A systematic classification of actuation principles was made. First, a differentiation was made between actuators having their kinetic energy internally induced by a conversion of one form of energy into kinetic energy, versus actuators having their kinetic energy externally induced and transmissioned to the actuator. Second, a differentiation was made on the type of energy being internally converted to kinetic energy and the type of transmission of external kinetic energy. Lastly, the classification was applied to the patents found. This classification is depicted in the tree of Figure 1.

The left branch in the classification tree depicts the first main class of actuators. This class of actuators uses kinetic energy from an external source to act upon its surroundings. To transfer the kinetic energy from the source to the actuator, a type of transmission is used. The classification of the type of transmission is based on the physical state of the particles forming the transmission; gas, liquid or solid. This transmission can thus be pneumatic, hydraulic or mechanic. In the end nodes a distinction was made between linear actuators or rotational actuators. An example of an actuator on the left branch of the tree can be a pneumatic cylinder; in an external compressor kinetic energy is induced in the form of pressurized air. The tube to the cylinder forms

Table 1. Inventor(s), assignee, priority date, patent number and key application of relevant patents. Authors Albrecht - Kwok.

Inventor(s)	Assignee	Pr. Date	Patent Number	Key Application
Albrecht [13]	Siemens AG	10-2009	DE102008034685-A1	Cooling Fan
Backes [14]	Individual	05-1996	WO9745749-A1	Injecting Fluids
Bailey [15]	Intuitive Surgical Operations Inc.	02-2012	US2013211422-A1	Any (actuator)
Barberi et al. [16]	Modus Medical Devices Inc.	01-2016	WO2017120661-A1	Positioning Phantoms
Benitez et al. [17]	Icahn School Medicine	05-2017	WO2017205411-A1	Positiong Body Part
Bergman [18]	General Electric Co	12-1984	US4641823-A	Positioning Patient Bed
Birk et al. [19]	Allergan Inc.	10-2008	US2013253262-A1	Gastric Band
Bosboom et al. [20]	Radboud University	11-2010	WO2012069075-A1	Any (actuator)
Bruce [21]	Devicor Medical Prod Inc.	09-2015	WO2017059134-A1	Positioning Breast for Biopsy
Carreira et al. [22]	Monteris Medical Corp	06-2012	WO2014003855-A1	Laser Ablation Guide (brain)
Chen et al. [23]	Max Planck Ges Foerderung Wissen.	10-2016	EP3315064-A1	Needle guide (rodents)
Christakis [24]	Medsonic Ltd	01-2006	WO2007082495-A1	Ultrasound Ablation
Cinquin et al. [25]	Univ. Joseph Fourier Grenoble	09-2004	US2006058640-A1	Needle Guide
Cinquin et al. [26]	Univ. Autonoma Del Estado Mexicao	07-2008	FR2934487-A1	Needle Guide
Cleary et al. [27]	Childrens Nat Medical	06-2013	US2014371584-A1	Needle Guide (thorax)
Comber et al. [28]	University Vanderbilt	08-2015	US2017036883-A1	Needle Guide
Comber et al. [29]	University Vanderbilt	11-2011	US2013123802-A1	Needle Guide
Consiglio et al. [30]	Koninklijke Philips Electronics N.V.	07-2010	WO2012014119-A1	Paper Feed of Printer
Consiglio et al. [31]	Koninklijke Philips Electronics N.V.	05-2013	WO2014181208-A1	Valve Control
Coppens et al. [32]	Qfix Systems Llc	10-2015	WO2017066616-A1	Positioning Patient Bed
Cowan et al. [33]	Medrad Inc.	01-2006	WO2006078817-A2	Injecting Fluids
Crowley et al. [34]	Siemens Magnet Technology	10-2005	GB2430996-A	Driving Cryocooler of MRI
Damianou et al. [35]	University Cyprus Technology	06-2016	EP3254731-A1	Ultrasound Ablation
Daum et al. [36]	Daum Gmbh	06-2000	DE10029739-A1	Drill
Desai et al. [37]	University Maryland	05-2012	US2013296885-A1	Steerable Probe
Desai et al. [38]	University Maryland	02-2012	US2013218005-A1	Surgery Robot (brain)
DiGiancamillo et al. [39]	University Milano	11-2006	WO2008062493-A1	Positioning Patient Bed
Dirauf et al. [40]	Siemens Healthcare Gmbh	11-2015	DE102015222643-B3	Positioning Patient Bed
Donaldson et al. [41]	Profound Medical Inc.	03-2010	WO2011115664-A2	Ultrasound Ablation
Dong [42]	Individual	04-2007	US2008247059-A1	Any (actuator)
Du et al. [43]	Harbin Inst Technology	01-2015	CN104506080-A	Positioning Antenna
Dubowsky et al. [44]	Massachusetts Inst Technology	05-2002	US2003210811-A1	Any (actuator)
Ehman et al. [45]	Mayo Found. Medical Edu. And Res.	04-2008	US2009295387-A1	Vibrate Tissue Acousticly
Feng et al. [46]	University Soochow	02-2017	CN207270338-U	Positioning of Rodents
Feng W et al. [47]	University Tianjin	11-2011	CN102499726-A	Needle Guide
Fischer [48]	Worcester Polytechnic Inst	11-2009	WO2011057260-A2	Needle Guide
Friebe et al. [49]	Individual	09-2005	DE202005021902-U1	Positioning Laser
Fujimoto et al. [50]	Brigham And Womens Hospital	03-2013	US2014275979-A1	Needle Guide
Goldenberg et al. [51]	Eng Services Inc.	04-2016	US2017290630-A1	Surgery Robot
Goldenberg et al. [52]	Eng Services Inc.	07-2008	WO2009152613-A1	Needle Guide (prostate)
Grady [53]	Individual	04-2014	US2017035377-A1	Fluroscopy
Griffiths et al. [54]	Medrad Inc.	08-2003	US2008056920-A1	Injecting Fluids
Groenhuis et al. [55]	University Twente	08-2017	WO2018038608-A1	Needle Guide
Guettler et al. [56]	Charite University Medizin Berlin	08-2011	WO2013020877-A1	Drill
Hassler et al. [57]	Ethicon Endo-Surgery Inc.	05-2004	EP1600183-A1	Gastric Band
Hiratsuka et al. [58]	Medicaroid Corp	12-2015	WO2017098543-A1	Positioning Patient Bed
Horne et al. [59]	Imaging Solutions Pty Ltd	04-2016	WO2017181230-A1	Positioning Patient Bed
Householder et al. [60]	Devicor Medical Prod Inc.	10-2016	US2018116644-A1	Biopsy Apparatus
Ilan et al. [61]	Individual	04-2002	US2003184296-A1	Positiong Body Part
Illindala et al. [62]	Zoll Circulation Inc.	09-2011	US2013072830-A1	Performing CPR
Iwasa [63]	Canon Inc.	06-2012	JP2014003732-A	Any (actuator)
Janssens [64]	Individual	01-2007	WO2008086817-A1	Biopsy Apparatus
Kan et al. [65]	Ge Medical Systems Technology Co	02-2000	WO200156493-A2	Fan
Kawashima [66]	Canon Inc.	05-2011	JP2012239788-A	Positioning a Visual Stimulus
Keene et al. [67]	Metrasens Ltd	11-2013	WO2015071672-A3	Door of MRI Room
Keibel [68]	Kuka Roboter Gmbh	03-2016	DE102016204271-A1	Surgery Robot
Keidl et al. [69]	Surgi-Vision Inc.	07-2007	US2009112082-A1	Positioning Surgery Camera
Kirschenman [70]	St Jude Medical Atrial Fibrillation Div	12-2011	WO2013101259-A1	Catheter Positioning
Kobayashi et al. [71]	Hitachi Medical Corp.	03-2003	WO2004087033-A1	Positiong Body Part
Kolipaka et al. [72]	Ohio State Innovation Found	11-2014	WO2016077776-A1	MR Elastography
Kroeckel et al. [73]	Siemens AG	12-1998	DE19856803-C1	Any (actuator)
Kwok et al. [74]	University Hong Kong	06-2016	US2017367776-A1	Catheter Positioning

Table 2. Inventor(s), assignee, date, patent number and key application of relevant patents. Authors Lamperth - Zhang.

Inventor(s)	Assignee	Pr. Date	Patent Number	Key Application
Lamperth et al.[75]	Imperial Innovations Ltd	11-2006	WO2008059253-A2	Any (actuator)
Larson et al.[76]	Mri Robotics Llc	04-2008	US2017135779-A1	Needle Guide (breast)
Li Z et al.[77]	Shenzhen Seacrown Elec.mech. Co Ltd	06-2016	CN205903495-U	Injecting Fluids
Li et al.[78]	Individual	11-2014	CN204318757-U	Move Head of Patient
Matchey et al.[79]	Inset Technologies	07-2008	WO2010011499-A1	Injecting Fluids
Matsuwaki et al.[80]	University Kagoshima	08-2015	JP2017047343-A	Vibrator (Nerve Stimulation)
Mcmillan et al.[81]	University Maryland	05-2012	US2013296737-A1	Surgery Robot (brain)
Miller[82]	Suros Surgical Systems Inc.	11-2000	US2009048533-A1	Biopsy Apparatus
Mujica-parodi et al.[83]	University New York State Res Found	06-2015	WO2017004277-A1	Positioning Phantoms
Nakamura et al.[84]	Mitaka Koki Co Ltd	05-2000	EP1657408-A1	Adjusting Microscope
Nakayama et al.[85]	Hitachi Ltd	01-2006	EP1808870-A1	Driving Cryocooler of MRI
Nazim et al.[86]	Sloan Kettering Inst Cancer Res	04-2015	WO2016176683-A1	Catheter Positioning
Nemoto et al.[87]	Nemoto Kyorindo Kk	10-2017	JP2018061836-A	Injecting Fluids
Newman et al.[88]	Individual	09-2015	WO2017048332-A1	Inflating Medical Implants
Oneill et al.[89]	Koninklijke Philips Electronics N.V.	06-2012	WO2013186725-A2	Valve Control
Ono et al.[90]	University Nippon	06-2009	JP2011000183-A	Injecting Fluids
Onuma et al.[91]	Canon Inc.	06-2012	JP2014003734-A	Any (actuator)
Osman et al.[92]	University Johns Hopkins	05-2010	US2011270079-A1	Positioning Breast for Biopsy
Parihar et al.[93]	Devicor Medical Prod Inc.	12-2008	US2013066191-A1	Biopsy Apparatus
Plante et al.[94]	Socpora Sci And Genie Sec	08-2010	WO2012019292-A1	Needle Guide
Rhad et al.[95]	Devicor Medical Prod Inc.	11-2010	US2012109007-A1	Biopsy Apparatus
Roeck et al.[96]	University California	10-2009	US2010264918-A1	Any (actuator)
Rohling et al.[97]	General Electric Co	09-1994	US5443068-A	Ultrasound Ablation
Roozen et al.[98]	Koninklijke Philips Electronics N.V.	12-2000	WO200246783-A1	Counteract Vibrations
Salminen[99]	Koninklijke Philips Electronics N.V.	09-2009	WO2011036607-A1	Ultrasound Ablation
Saloux et al.[100]	University Cent Hospitalier	06-2013	WO2014201571-A1	Positioning Phantoms
Sander[101]	Leica Microsystems Schweiz	06-2010	DE102010030007-A1	Adjusting Microscope
Scantlebury et al.[102]	Midas Rex Pneumatic Tools Inc.	07-1996	US5782836-A	Bone Cutter
Schaerer et al.[103]	Imris Inc.	01-2011	US2012190965-A1	Surgery Robot (brian)
Schwindt et al.[104]	Tissue Extraction Devices Llc	04-2002	US2003199787-A1	Biopsy Apparatus
Shih et al.[105]	Individual	02-2014	US2015234022-A1	Breast Inspection (PET)
Shvartsman et al.[106]	Viewray Technologies Inc.	03-2013	US2017281043-A1	Radiotherapy
Stoianovici et al.[107]	University Johns Hopkins	01-2003	WO2004062517-A2	Robotic Arm
Stoianovici et al.[108]	University Johns Hopkins	12-2005	WO2007065013-A2	Needle Guide
Stoianovici et al.[109]	University Johns Hopkins	08-2005	US2007034046-A1	Any (actuator)
Stoianovici et al.[110]	University Johns Hopkins	05-2016	WO2017192796-A1	Needle Guide (prostate)
Su et al.[111]	Shende Medical Equip Technology	12-2017	CN108042932-A	Ultrasound Ablation
Su X et al.[112]	Jiangsu Glittering Orient Ultrasonic Mot	04-2016	CN205698713-U	Injecting Fluids
Susi[113]	Iradimed Corp	11-2005	US2013281966-A1	Injecting Fluids
Tanaka et al.[114]	University Yamaguchi	12-2003	JP2005185072-A	Needle Puncture
Taracila et al.[115]	General Electric Co	09-2011	US2013076358-A1	Move Head of Patient
Tie et al.[116]	Shenzen Inst Advanced Technology	06-2016	CN206102770-U	Ultrasound Ablation
Tigwell[117]	Siemens Magnet Technology	11-2005	GB2432112-A	Positioning Patient Bed
Tse et al.[118]	University Georgia Res Found Inc.	12-2015	WO2017117382-A1	Needle Guide (prostate)
Tsekos et al.[119]	University Houston	08-2012	WO2014032046-A1	Surgery Robot
Unknown[120]	Aspect Imaging Ltd	08-2013	DE202013103646-U1	Transporting Bio Samples
Vij et al.[121]	Mri Interventions Inc.	03-2014	US2015272596-A1	Drill
Wei et al.[122]	Univ. China Mining And Tech. Beijing	10-2016	CN206365925-U	Needle Guide
Yehezkeli et al.[123]	Insightec Txsonics Ltd	07-2000	WO200209812-A1	Ultrasound Ablation
Yue[124]	Cedars Sinai Medical Cent	07-2015	WO2017019809-A1	Positioning Phantoms
Zhang et al.[125]	University Tianjin	01-2011	CN102113905-A	Needle Guide

the pneumatic transmission. Finally, the pneumatic cylinder converts the kinetic energy of the air into a linear motion. An example in the class of actuators with mechanical transmission can be a Bowden cable. Kinetic energy is induced in the form of a pull motion at an external site and is transferred via the cable to the end effector.

The right branch in the classification tree depicts the second class of actuators; the class that induces kinetic energy by internal conversion of a form of energy to kinetic energy. The forms of energy depicted can controllably be transformed into kinetic energy in order to form an actuator. A distinction has been made between actuators that have their kinetic energy induced by electricity, heat, magnetism, chemical energy or light. An example of an actuator in this class of actuators is an electromagnetic motor, which internally converts electricity into rotational kinetic energy.

The devices in the patents were categorized based upon their actuation principles and the references to the patents were put below the corresponding nodes of the tree. Furthermore, MR safety (MR safe, conditional or unsafe) of

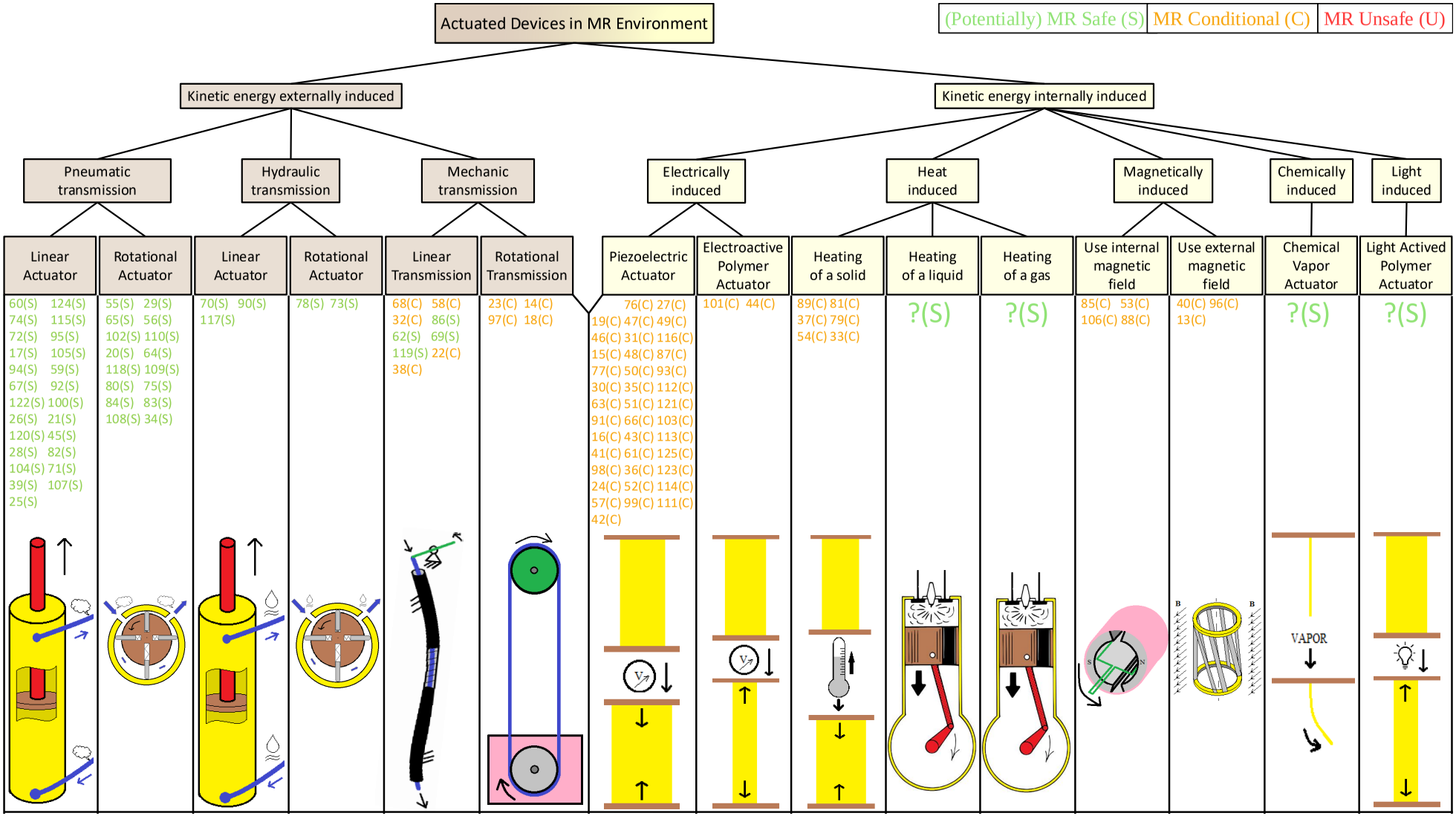

Figure 1. Classification of actuation principles. References to the patents are placed below the nodes of tree. The letters (S) or (C) indicate a device is MR safe or MR conditional, respectively.

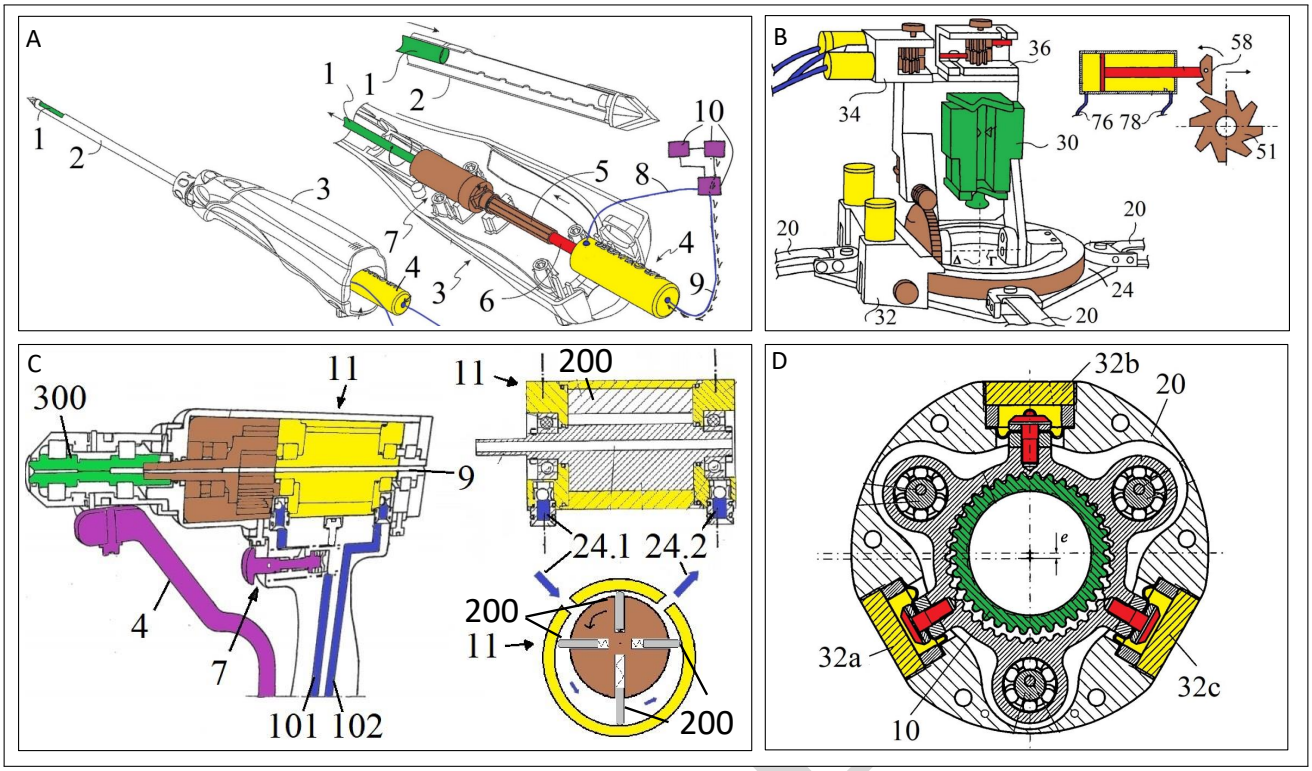

Figure 2. Pneumatic devices. (A) Biopsy device, adapted from Householder and Bruce.[60] (B) Needle placement system, adapted from Cinquin et al.[25] (C) Drill with pneumatic vane motor, adapted from Guettler et al.[56] (D) Pneumatic stepper motor, section view, adapted from Stoianivicie.[109]

each device is indicated in the classification tree. A device is potentially MR safe if it is or can be made entirely out of nonmagnetic and nonconducting materials. A device is MR conditional if it can be used with an MRI scanner, but on certain conditions. A device is deemed MR unsafe if it uses magnetic and conducting materials which are unshielded and used close to the MRI scanner. The pictures below the nodes show an example of the actuator corresponding to that node.

There are six types of actuators on the left branch. On the right branch there are nine different types of actuators. This section continues with a description of one, two or three exemplary patents per type of actuator. There are four types of actuators that have not been used in the patents found; the actuator that uses heating of a gas or liquid to form kinetic energy and actuators that work based on chemical or light energy.

Pneumatic transmission, linear actuator

A pneumatic linear actuator uses compressed air to generate a linear motion. The kinetic energy is transmissioned via tubes to the actuator. Pneumatic cylinders are the dominant form of pneumatic linear actuators, with 25 patents using this type.[17,25,26,28,39,59,60,67,71,72,74,82,92,95,100,104,105,107,115,120,122]

One example of a device using a pneumatic linear actuator in the form of a pneumatic cylinder is the biopsy device of Householder and Bruce.[60] It is used to take tissue samples from the breast of the patient, see Figure 2A. To cut the tissue, the cutter (1) is moved forward and rotated at the same time: the device uses a pneumatic cylinder (4) to apply a linear motion to a rod (6). In the cutter actuation assembly (7), the linear motion of the rod (6) is converted to a linear and rotational motion of the cutter (1). The pneumatic cylinder (4) is connected with a pneumatic transmission in the form of tubes (8, 9) to a control module (10) with valves. The control module (10) can be placed further away from the MRI scanner in order not to let its electronics interfere with the MR image. Since the biopsy device itself can be made of nonmagnetic and nonconducting materials, the device is potentially MR safe. Three patents describing similar biopsy devices with pneumatic linear actuators have been found.[82,95,104]

Another example of a device with pneumatic linear actuators is the instrument placement system of Cinquin et al.[25] With reference to Figure 2B; platform (24) is placed on the body of the patient, an instrument or needle can be held in holder (30) and be inserted in the patient under MRI guidance. Each axis is controlled by an actuator group consisting of two pneumatic linear actuators. The piston works together with a ratchet mechanism. When the piston extends, the pawl (58) turns the gear (51) in clockwise direction, when the piston retracts, the gear (51) does not turn back; there is a one-way motion. To achieve two-way motion of the axis of the gear, a second piston and ratchet mechanism is installed in mirrored configuration, creating an actuator group as (32, 34, 36). Platform (24) can be moved in plane with a similar actuator group via the flexible straps (20). The device is made of nonmagnetic and nonconducting materials, and therefore it is MR safe. There are patents describing similar instrument placement systems with pneumatic linear actuators.[26,28,94,122]

Other types of pneumatic linear actuators are also used: The patent of Plante et al.[94] uses pneumatic muscles. The patents of Bruce[21] and Yue[124] use pneumatic bellows. The

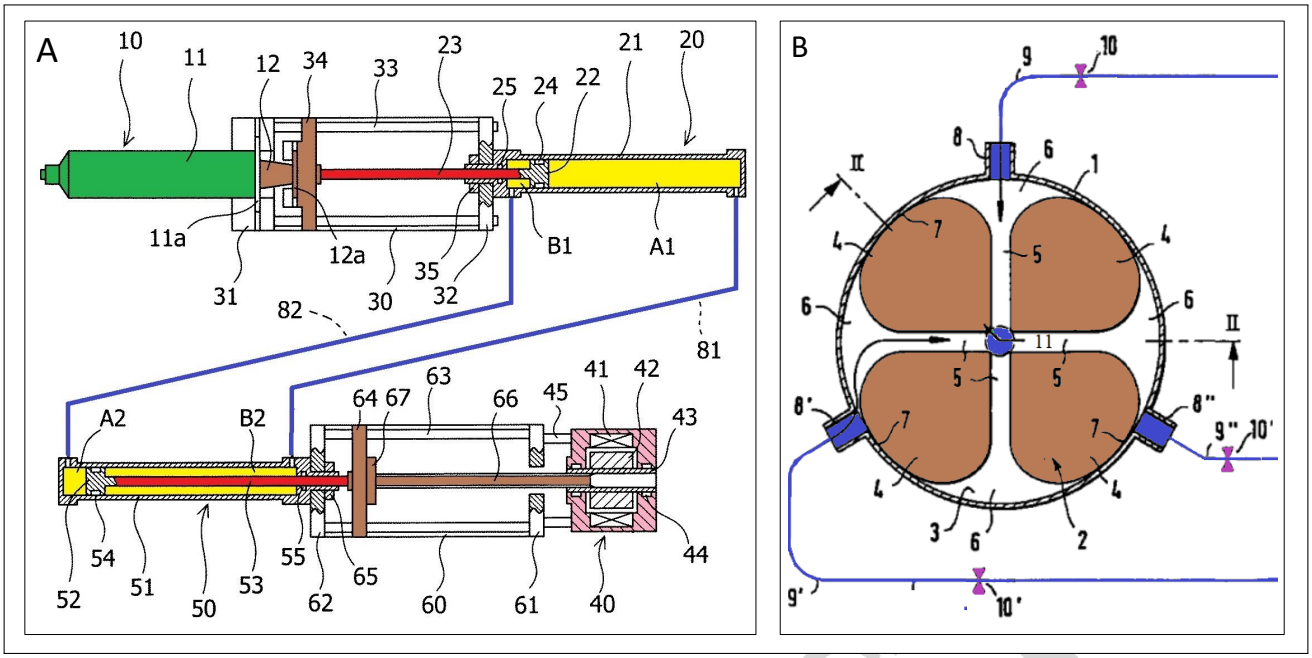

Figure 3. Hydraulic devices. (A) Hydraulic Syringe, adapted from Ono et al.[90] (B) Hydraulic stepper motor, adapted from Kroeckel and Rauh.[73]

patent of Ehman et al.[45] uses air in combination with a sophisticated speaker to generate shear waves to vibrate tissue acoustically.

Pneumatic transmission, rotational actuator

A pneumatic rotational actuator uses compressed air to generate a rotational motion. There are sixteen patents that use a rotational pneumatic actuator. In the patent literature, two types of rotational pneumatic actuators were found, the continuous pneumatic motor, and the pneumatic stepper motor. Continuous pneumatic motors are most frequently used and found in twelve patents.[20,29,34,56,64,65,75,80,83,84,102,118] Guettler et al.[56] describe a drill using a continuous pneumatic motor. This drill is used to drill holes in bones and can also place Kirschner Wires in bones. These Kirschner wires are long rods used to hold bone fragments together. See Figure 2C, clamping of the drill or wire is done by (300). Insertion of the wire is done through opening (9). The actuator used is a pneumatic vane motor (11). Compressed air enters inlet (24.1), drives the vanes (200), and exits via outlet (24.2). An internal planetary transmission (6) reduces the speed of the motor by a factor 5. Handle (4) can be used to apply a clamping force on the drill or wire, in order to transfer torque from the motor to the drill or wire. A throttle valve (7) is used to adjust the speed of the vane motor. The drill can be made out of nonmagnetic and nonconducting materials, so it is potentially MR safe. Pneumatic vane motors are also used in two other patents.[34,65]

Pneumatic stepper motors make discrete steps and are used in four patents.[55,108–110] Stoianovicie et al.[109] describe a pneumatic stepper motor. The motor is depicted in Figure 2D. The stepper motor consists of a hoop gear (20), diaphragm cylinders (32a, 32b, 32c) and a central gear (10). Extending and retracting the diaphragm cylinders one after another in clockwise fashion will make the hoop gear translate in the xy-plane, with its motion describing a circle. This motion of the hoop gear will turn the central gear (10) counterclockwise. A step size of $3.33°$ with a 99% coincidence error of 0.84% is achieved, with speeds in the order of 10^2 steps per second. The total power of the stepper motor is 37 W. The materials used in the stepper motor are plastics, glass, and rubber, which are all MR safe. Therefore, this device is MR safe.

Hydraulic transmission, linear actuator

A hydraulic linear actuator uses a compressed liquid to transmission motion from the compressor to the actuator. Three patents have been published that use a hydraulic linear actuator.[70,90,117] The patents all use hydraulic cylinders. The patent of Kirschenman[70] describes a catheter positioning device. The patent by Tigwell[117] positions a patient bed. Ono et al.[90] have patented a hydraulic syringe. This syringe can be used to accurately inject a dose of liquid, see Figure 3A. The device consists of a syringe side (10) and a power side (50). On the syringe (10), a hydraulic cylinder (21) is connected via piston (23) and mechanism (34) to the syringe cylinder containing the liquid. The syringe side is connected via a hydraulic transmission in the form of tubes (81, 82) to the power side. The power side is placed at a distance from the MRI scanner; for instance outside of the MRI scanner room. The power side is similar to the syringe side; there is a hydraulic cylinder (51), connected to mechanism (60). This mechanism (60) is connected to an electric motor (40). The motor uses thread (43) to move mechanism (60) axially, which will move the pistons (51, 21) to inject the liquid into the patient. The syringe side and the transmission are made out of MR safe materials, and the power side is placed at a distance from the MRI scanner, which makes this device MR safe.

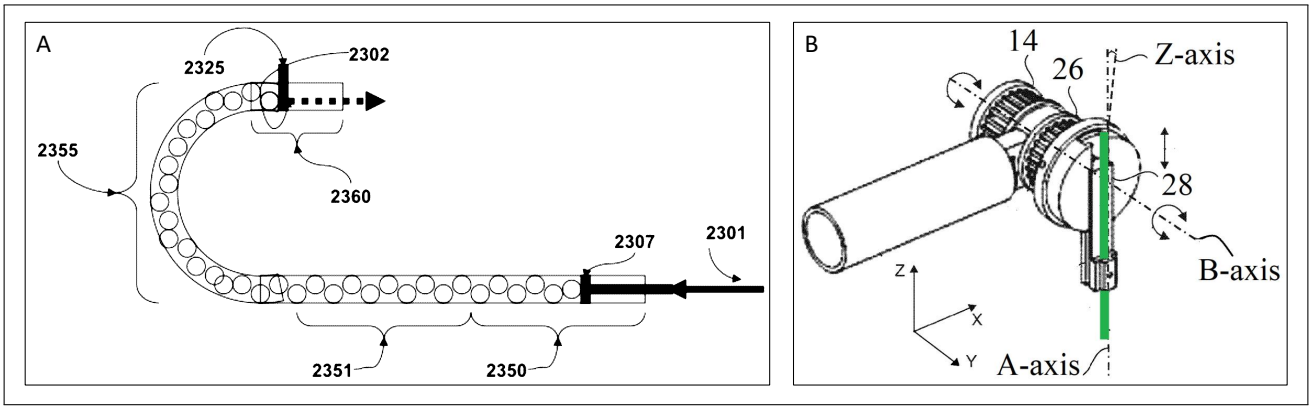

Figure 4. Mechanical transmission devices. (A) Mechanical transmission with solid spheres, from Tsekos.[119] (B) Transmission with belt, adapted from Chen et al.[23]

Hydraulic transmission, rotational actuator

Two main types of hydraulic rotational actuators exist: continuous and stepper motors. The patent of Li et al.[78] uses a hydraulic motor to position a head rest. The hydraulic stepper motor of Kroeckel and Rauh[73] is a patent from as early as 1998 and the oldest patent found that describes an actuator specifically made for the MR environment. A schematic representation of the stepper motor is in Figure 3B. The motor has $n = 3$ inlets (8,8',8"). There are $n + 1 = 4$ rotor segments which are rotating about a central axis. The authors allow for different numbers of inlets n in this design. This central axis is also the outlet of the fluid. The operation of the motor is as follows: as valve (10) is open the motor is in locked state, liquid flows through (8) to the central outlet. With valve (10) in closed state and valve (10') open, liquid will flow through inlet (8') to the central outlet and the rotor segments turn in counterclockwise direction. Afterwards valve (10') closes and valve (10") opens, resulting in the next step. The motor is made out of MR safe materials. The valves (10, 10', 10") are solenoid valves. In essence, solenoid valves are not MR safe, since they rely on electromagnetism to operate. However, the solenoid valves can be placed far away from the MRI scanner, so this stepper motor can be MR safe.

Mechanic transmission, linear transmission

The devices in the category have an actuator placed at a distance from the MRI scanner and transfer the kinetic energy to the device via mechanical means. A form of linear mechanical transmission is used by nine patents. There are four patents that use a cable to transfer kinetic energy.[22,38,69,86] The patents of Hiratsuka et al.[58] and Keibel[68] use a long robot arm to transfer motion to the end effector. The patent of Illindala et al.[62] uses a long rod to position a pneumatic device outside the influence of the MR field. The patent of Coppens et al.[32] describes a motorized patient bed that places electromagnetic components away from the MRI field and uses a scissor linkage to transfer motion.

The device of Tsekos[119] uses an unconventional transmission. The device is used for image guided robotic surgery, and can for instance position a needle inside the body. Motion from electromagnetic motors is transferred via solid spheres inside a tube to the robotic arm. See Figure 4A, a push motion on (2307) pushes the spheres through the tube in clockwise direction. In the patent, multiple concepts are proposed to move the spheres in the other direction, one of which includes running a cable through the center of the spheres and pulling it. Nonmagnetic and nonconducting materials can be used in the mechanical transmission and in the robotic manipulator. All electromagnetic components are placed in a different room than the MRI scanner, so this device is MR safe.

Mechanic transmission, rotational transmission

A transmission of kinetic energy to an actuator via a rotational transmission is used by five devices. All five devices use an electromagnetic motor to induce the kinetic energy externally. The devices[33,97] use a drive shaft as a rotational transmission. The devices[14,18,23] use a driving belt to transfer motion.

The device of Chen et al.[23] is used to insert an instrument into the brain of rodents. The rodent is placed in a small bore MRI scanner. This instrument can be an electrode to record electrochemical signals. An overview of the device is given in Figure 4B. The pulley (14) is used to rotate the end effector over the B-axis. An Archimidean spiral inside the holder (28) turns rotation of the pulley (26) into translation of the end effector over the Z-axis. The pulleys (14, 26) are connected with timing belts to motors. The actuation assembly is positioned at a distance of 4.7 m for 14 T scanners, and a distance of 1.5 m for 9.4 T scanners, in order not to let the motors interfere with the MRI scanner. Since electromagnetic motors are used in the MR room and conditions are set on the distance between the device and the MRI scanner, this device is MR conditional.

Piezoelectric actuator

The piezoelectric actuator is the first actuator on the right branch of the classification tree. These actuators work with a piezoelectric material (frequently a ceramic), that produce a mechanical stress when an electric current is passed through the material. The kinetic energy is induced within the actuator, by transforming electric energy to kinetic energy. There are 39 patents using a form of piezoelectric actuation. Rotational piezoelectric motors are used in many

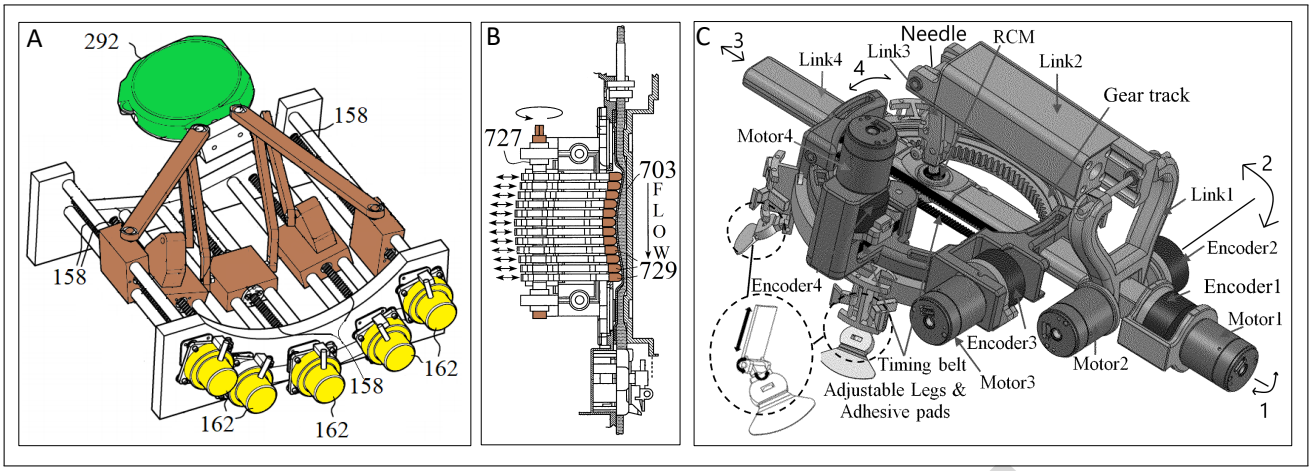

Figure 5. Devices using piezoelectric actuators. (A) Ultrasound transducer positioning system, adapted from Salminen.[99] (B) Internal mechanim of liquid pump, adapted from Susi.[113] (C) Needle placement system, adapted from Cleary et al.[27]

devices.[15,16,19,27,31,35,43,46,50,51,63,76,77,87,91,93,111–113,116,121,123 & 24,30,36,41,42,47–49,52,61,66,99,103,114,125] The patent of Hassler[57] use linear piezoelectric actuators to actuate a fluid pump for inflation of a gastric band. The patent published by Roozen and Van Schothorst[98] uses linear piezoelectric actuators to counteract vibrations of the gradient coil of the MRI scanner.

The patent of Salminen[99] represents a group of seven patents that describes devices to position ultrasound transducers for ultrasound therapy guided by MRI. Ultrasound therapy is used to locally heat tissue. See Figure 5A, in which the transducer is (292). There are five piezoelectric motors (also known as ultrasonic motors) (162), to operate on the threads (158). A mechanical linkage is connected from every thread to the transducer (292). The links are connected using ball joints. The device uses electricity and conducting elements, therefore it is MR conditional. The patent does not report on the generation of noise in the images due to operation of the ultrasonic motors. Other patents describing similar positioning systems for ultrasound therapy are published.[24,35,41,111,116,123]

Another group of four patents which use piezoelectric actuators describes devices for injecting fluids.[77,87,112,113] An example in this group is the peristaltic pump of Susi.[113] The pump can be used in the MR environment, and can be connected to bypass a regular MR unsafe pump. With reference to Figure 5B, the pump uses an ultrasonic motor connected to axis (727). An optical encoder is used to measure the rotation of the motor. As the motor turns, the pump elements (729) push down on the flexible tubing (703) through which the liquid flows. The pump elements create a peristaltic movement, which causes the liquid to be pumped out at a known rate. The pump is made entirely out of nonmagnetic materials. The device has conducting elements so it is MR conditional. The electronics in the device are RF shielded to reduce the interference with the imaging process.

A third group of six patents describes devices to position a needle in the body.[47,48,50,52,76,125] The device of Cleary et al.[27] is used to place a needle in the elbow joint to inject contrast agent. See Figure 5C, the needle is guided by the link indicated 'needle'. The device is placed on the body and secured with the adjustable legs and adhesive pads. The needle is inserted through the ball joint indicated 'RCM'. The needle guide, link 2 and link 1 form a parallelogram. The device uses piezoelectric motors; motor 1 turns link 1 around axis 1. Motor 2 turns link 1 around axis 2. Motor 3 translates over axis 3. Motor 4 rotates the system around 4. There are no ferromagnetic materials used in the device. Since the device uses piezoelectric motors which run on electricity, the device is MR compatible. The patent reports on the artifacts created because of the piezoelectric motors, and states that if the motors are placed more than 2.5 cm away from the target, the artifacts form no problem.

Electroactive polymer actuator

Electroactive polymers are materials that extend when an electric current runs through it. Two patents by Dubowsky et al.[44] and Sander[101] use an electroactive polymer actuator (EAP). The patent of Sander[101] describes a microscope that can safely be used in the MR scanner room. The microscope is attached to a tripod and adjustment mechanism. The tripod can be used to position the microscope and uses EAP actuators to hold position after adjustment. The inside of the microscope is depicted in Figure 6A. EAP actuators (18) and (19) are used to move lens (14) and (15) over axis (17), respectively. The device is made entirely from nonmagnetic materials. The EAP actuators conduct electricity, so the device is MR conditional. The device is not used closely to MR scanner, so it is not expected to produce artifacts in the MR image. Dubowsky et al.[44] describe all kinds of actuator setups with electrostrictive polymer artificial muscle actuators, see Figure 6B for an example of one such actuator.

Actuators making use of heating of a solid

For this type of actuator, the kinetic energy is induced by heating of a solid. There are five patents in this category, all using a shape memory alloy (SMA) actuator. An SMA is a material that forms back to its original form when heat is applied. The patent of Matchey et al.[79] uses an SMA wire that retracts by 3% when a current passes through it and the wire heats up. See Figure 6C, the SMA wires are (312, 322). The device is a fluid pump, to accurately inject medicine into the body. The inlet (140) is connected to an external reservoir, the outlet (150) to the catheter. The device

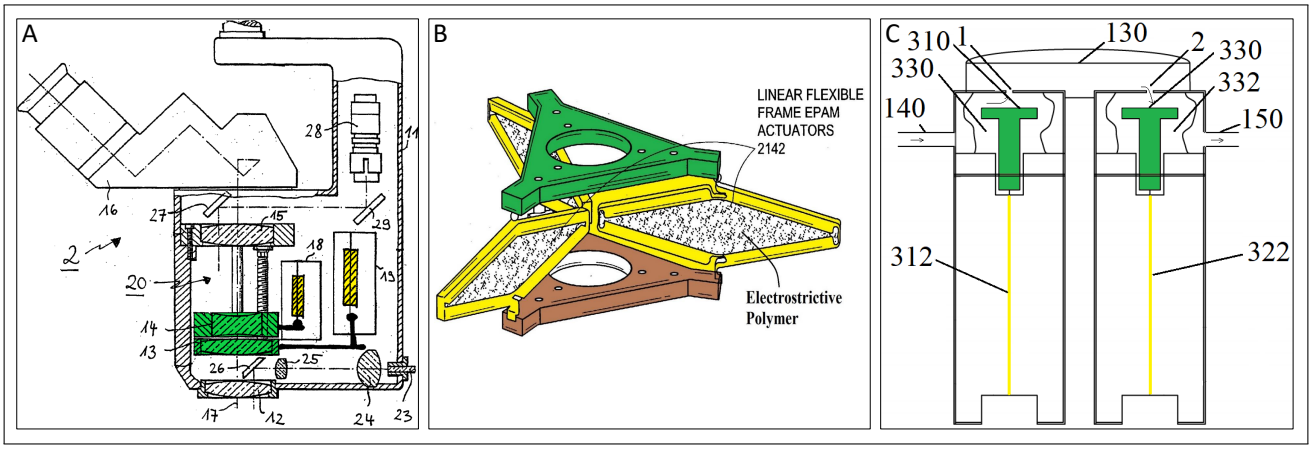

Figure 6. Devices using electroactive polymer actuators and shape memory alloy actuators. (A) Internal view of microscope, adapted from Sander.[101] (B) Electrostrictive polymer artificial muscle actuator, adapted from Dubowsky et al.[44] (C) Valve pump, adapted from Matchey et al.[79]

works as follows: first, the SMA wires are extended, and both plungers (310, 320) are pressed against the openings (1, 2) by elastic material (330, 332) to close the openings. Then, the SMA wire (312) retracts and the inlet plunger opens, filling the accumulator (130). After that, the inlet plunger closes and the outlet plunger opens, letting the fluid run from the accumulator (130) to the outlet (150) by an internal pressure difference. The outlet plunger closes and the cycle can be repeated. The device uses conducting elements, therefore it is MR conditional. The patent does not report on the generation of imaging artifacts due to operation of the SMA wires.

Actuators making use of heating of a liquid or gas

Another type of actuator that works on heat is one that uses expansion of a liquid or gas due to applied heat. An example of such an actuator is a combustion engine. Due to heat released by the reaction of a liquid or gas with oxygen, expansion of that gaseous mixture occurs, which produces a form of kinetic energy. In theory, a combustion engine can be made out of nonmagnetic and nonconducting materials. However, care must be taken to make sure these engines are safe for use during surgical interventions. No hot parts can be exposed, sterilization of the parts must be taken into account and no exhaust gases may escape. No patents have been found using this type of actuator.

Actuators using internal magnetic field

The electromagnetic actuators in this category use a magnetic field in the actuator itself in order to induce kinetic energy. A typical example is a DC motor, it uses permanent magnets to form a stator magnetic field. The rotor of the motor consists of a wire through which electricity runs, resulting in a Lorenz force driving the motor. Since the actuator contains a magnetic field, it will attract to the MRI scanner. Therefore, the actuator must be magnetically shielded to counteract the magnetic field of the actuator. Such magnetic shielding is incorporated in the patent of Nakayama et al.[85] An overview of the device is depicted in Figure 7A. The device is a cryocooler and an integral part of an MRI scanner. The crycooler cools the electromagnets of the MRI scanner in order to make them more efficient. The coolant comes from compressor (13) and runs through tubes (14). The motor (11) acts on crankshaft (17) which translates the piston (10) up and down. An adiabatic cooling process takes place in the internal area (9). The magnetic shielding is incorporated by placing ferromagnetic plates around the device. Since the device uses electricity, but is magnetically shielded, it is MR conditional.

Other patents that use a DC motor are published by Shvartsman et al.[106] and Grady et al.[53] The fourth and last patent of this category by Newman and Horowitz[88] uses an asynchronous squirrel-cage motor to inflate medical implants. The squirrel-cage motor does not contain a permanent magnet, but uses alternating current in the stator to produce a rotating magnetic field. The windings of the motor are also made of nonmagnetic materials.

Actuators using external magnetic field

In contrast to the previous section, the electromagnetic actuators in this category use an external magnetic field to generate motion. The patent of Roeck and Nalcioglu[96] describes an electric motor which uses the static magnetic field of the MRI scanner itself as magnet field in the electric motor. Figure 7B shows the layout of the motor. There are eight copper wire coils on the rotor. Running a current through opposing coils induces a torque on the rotor because of the presence of the magnetic field. The current to the coils is regulated to be positive or negative at the right timing in the cycle. The authors have tested the motor by placing it 1.35 m away from the center of the scanner, where the field strength is 1 T. A no load speed of 196 RPM and stall torque of 1.37 Nm is measured, at 12 V coil voltage. During operation at 1.35 m away from the center, the signal to noise ratio (SNR) of the MRI image drops by 65%. The authors solve this by installing a Faraday cage around the motor, and the SNR only drops by 2%. The motor is made out of nonmagnetic materials, but the motor does contain conductive materials, so the device is MR conditional. The patent of Dirauf et al.[40] uses a similar motor to that of Roeck and Nalcioglu[96] to position a patient bed. The patent of Albrecht[13] uses a motor which makes use of the MRI static magnetic field to actuate a fan for cooling electronics inside the MRI scanner.

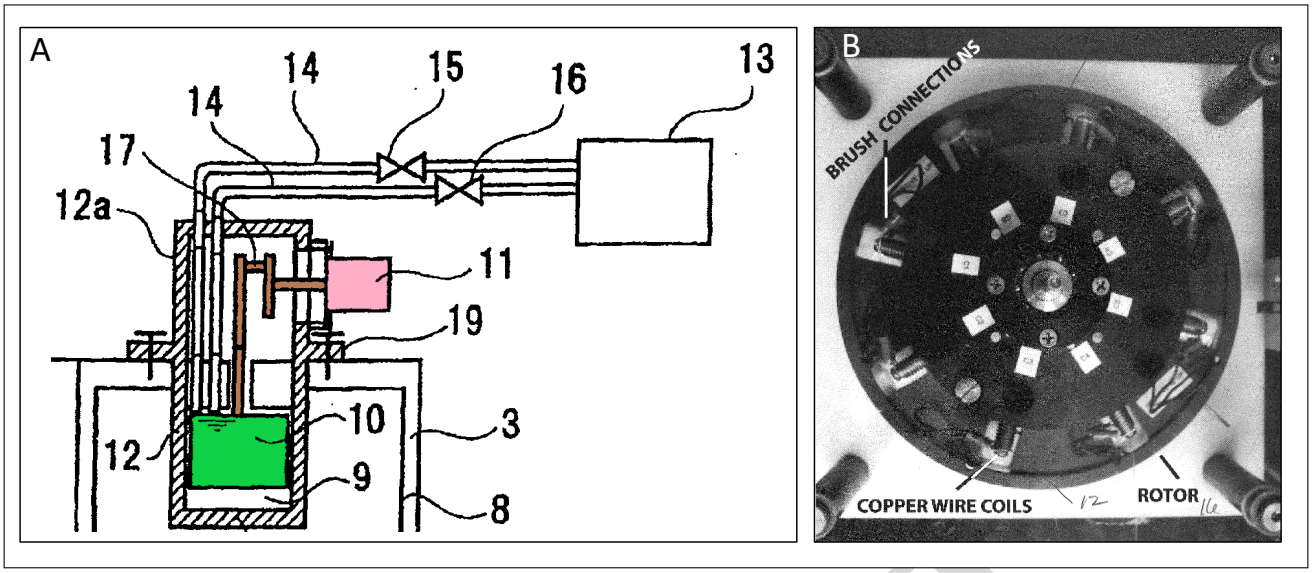

Figure 7. Actuated devices using magnetic field. (A) Cryocooler pump, adapted from Nakayama et al.[85] (B) Ironless DC motor, using static MRI magnetic field, adapted from Roeck and Nalcioglu.[96]

Chemical actuators

Converting chemical energy into kinetic energy is the working principle for a chemo-mechanical actuator. There are no patents of devices found that use this principle. An example of this working principle in scientific literature is the Tunable Polyaniline Chemical Actuator by Gao et al.[126] They constructed polyaniline porous asymmetric membrane strips and exposed them to organic vapors. Due to sorption and desorption of the vapors, the strips bent. A strip of size 40 mm, 2 mm width and thickness 25 μm bends more than 90° in 1.5 s when exposed to tetrahydrofuran. When exposing the strip to air, it bends back in 2.7 s. One could use this principle to construct an MR safe actuator, since no conductive or magnetic materials are used.

Actuators using light

A final actuation principle is the conversion of light into kinetic energy within the actuator. There are no patents found in this study that use this type of actuator. However, an example of this actuation principle can be found in scientific literature: actuators can be made by using laminated layers of light activated polymers (LAPs) that react differently to a light stimulus.[127] It could be an interesting solution for an MR safe actuator, since no magnetic or conductive materials are used. Activation of the LAPs can be done by guiding light through optical fibers to the actuator, which also requires no magnetic or conductive materials.

Commercially available devices

To find patents which have been commercialized, the websites of the assignees of the patents were checked to see if the devices described in the patents could be bought. From the relevant patents, fifteen individual devices have been found that are commercially available. Furthermore, there are sixteen patents owned by large companies such as Siemens, Hitachi, Philips, Canon and General Electronics. These patents describe a small part of a typical machine produced by these companies, and the individual patented part cannot be found on the website of the company. It remains unclear if these patents have been commercialized.

In the group of fifteen individual devices found, the piezoelectric motor is the most used actuator: six devices use piezoelectric motors.[16,19,77,87,113,123] Three devices use a pneumatic transmission with a linear actuator.[21,59,82] Nakamura et al.[84] describe a device that uses a pneumatic transmission with a rotational actuator. There are three devices that use a mechanical linear transmission.[22,32,69] A device described by Cowan et al.[33] uses a mechanical rotational transmission. The device of the patent of Shvartsman et al.[106] uses electric motors in combination with magnetic shielding.

The devices found are used for different kinds of applications, of which the most dominant applications will be discussed next. Four devices are used to inject fluids in the body: the MRIdium (Iradimed Corporation, Winter Springs, FL, USA[128]), Medrad MRXperion (Bayer HealthCare LLC, Pittsburgh, PA, USA[129]), Sonic Shot 7 (Nemoto Kyorindo co., Ltd, Bunkyo-ku, Tokyo, Japan[130]) and the Zenith-C60 (Shenzhen Seacrown Electromechanical Co., Ltd, Shekou, Nanshan Zone, Shenzhen, China[131]). The MRIdium[128] is used to deliver fluids and medication to the patient and is the peristaltic pump of the patent of Susi.[113] In contrast to a regular magnetic peristaltic pump, the fluids can be delivered to the patient when the patient is transferred from the intensive care unit to the MR room. The MRI examination does not have to be delayed until the patient no longer needs fluid delivery, resulting in lower costs.[132] The MRIdium has a nonmagnetic design and uses piezoelectric motors. The device is MR conditional, and is safe to use up to the 10^4 G (1 T) line of a 3 T MRI scanner, so it can be used inside the MR room.

There were two commercial devices found that perform ablation, the Neuroblate System (Monterris Medical, Inc., Plymouth, MN, USA,[133]) and the Exoblate system (InSightec Ltd, Tirat Carmel, Israel,[134]). The Neuroblate system can position laser probes in the human brain to ablate dangerous tissue. The device uses electric motors with a

mechanical linear transmission to drive the probe into the brain. The device is MR conditional.[135] In October 2017, the device was recalled by the US Food and Drug Administration (FDA), because the tip of the laser probe suffered from unexpected heating and damage due to interactions with the MR environment.[136]

The QUASAR MRI4D Motion Phantom (Modus Medical Devices, Inc., London, Ontario, Canada[137]) is used to move a phantom inside the MRI scanner. The phantom is a container filled with a fluid, which can be detected on the MRI scanner. Moving the phantom can help perform quality checks on the MRI scanner. The phantom can be rotated and translated along the medial (central axis) of the MRI scanner and can mimic the respiratory motion of a patient. The device uses piezoelectric motors, with RF noise filtering and shielding. The device is MR safe.

Discussion

This paper provides an overview of patents on actuated devices designed for the MR environment. First, a systematic classification of the actuation principles was made. The actuation principles were differentiated on having their kinetic energy induced externally and transmissioned to the actuator or having their kinetic energy induced internally in the actuator. Within the first group, a differentiation was made between transmission of kinetic energy with a pneumatic, hydraulic or mechanic transmission. The second group has actuators that induce the kinetic energy internally. This induction can be done by conversion of heat, electricity, magnetism, chemical energy or light into kinetic energy. The different types of transmissions and energy conversions to kinetic energy resulted in 15 different types of actuators in the classification tree of Figure 1. Lastly, the classification was applied to the devices described in the relevant patents. An indication was given whether the found patents describe devices which are MR safe, MR conditional or MR unsafe.

MR safety of relevant patents

In terms of MR safety, some types of actuators are intrinsically safe. Pneumatic and hydraulic transmissioned actuators are intrinsically MR safe, since they do not rely on magnetism or electricity to operate. Devices with a mechanic transmission can be MR safe if made out of nonmagnetic and nonconductive materials. A device with a transmission allows for an MR unsafe source of kinetic energy, since this source is placed away from the MR scanner, for instance in the MR control room. If the source of kinetic energy relies on magnetism or electricity and is located closer to the MR scanner, the devices with a mechanic transmission are MR conditional. Devices which have actuators that induce the kinetic energy internally by heat can be MR safe. However, the found patents in this last category all use SMA wires heated by running electricity through the wires, so these devices are MR conditional. Devices that use heating of a liquid or gas, chemical or light energy as a way to induce kinetic energy internally can be MR safe. Devices that use electricity or magnetism to internally induce the kinetic energy are MR conditional. All relevant patents found are either MR safe or MR conditional.

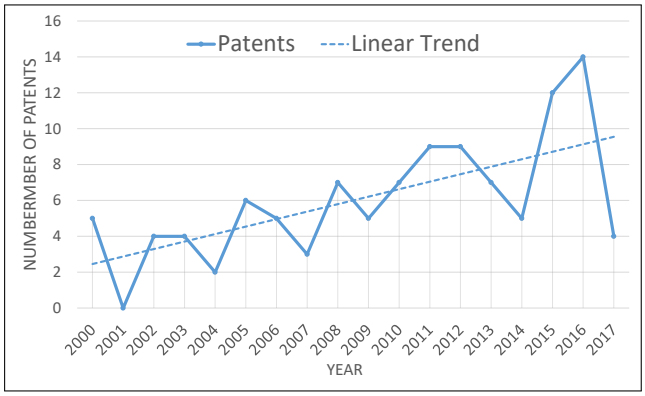

Figure 8. Number of relevant patents published per year, starting from the year 2000. There are five patents published before the year 2000. The dashed line shows an increasing linear trend.

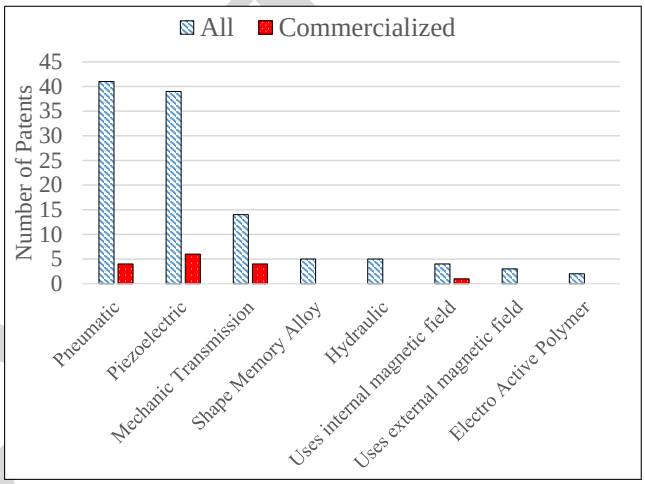

Figure 9. Number of patents published per actuator type.

Comparative analysis

The patent search resulted in 113 relevant patents. In Figure 8 the number of patents published per year is depicted. A linear trend line is fitted on the data, showing an increase in patents published. This may indicate a growing interest in the area of actuated devices used in the MR environment. 60% Of the relevant patents have been published by companies, 31% of patents have been published by academic institutions and 9% by independent assignees. The field does show interest from both companies and academic institutions.

It is of interest to see which actuators have been used frequently in the relevant patents. Figure 9 shows how many patents have been published per type of actuator. In the relevant patents, the piezoelectric and pneumatic actuator have been used the most by far. In the commercial devices, piezoelectric motors were used the most as well. A possible reason for the piezoelectric actuator being used the most is that it is nonmagnetic and commercially available.[138,139] Piezoelectric actuators do contain electrically conductive materials, and will disturb the image in operation. If interleaved imaging and motion of the actuator is allowable for the intervention or use of the device[140], piezoelectric actuators can be used. Possible solutions to reduce image artifacts during operation of the piezoelectric actuators are RF shielding and using special driving electronics[141].

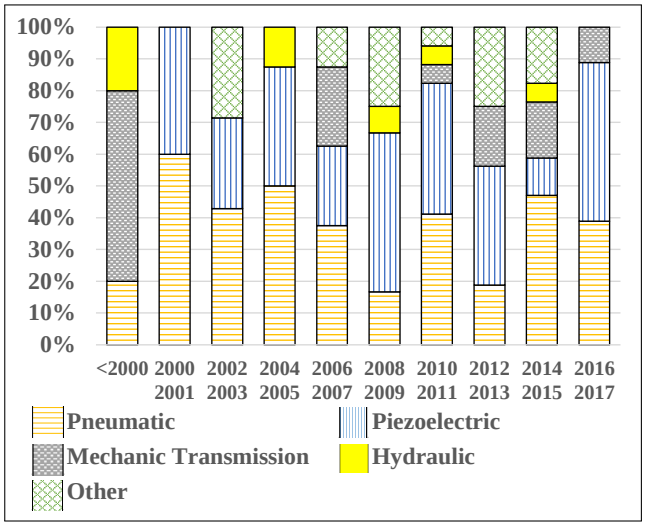

Figure 10. Percentage of type of actuator used in the relevant patents, grouped per two years.

Pneumatic actuators are also used frequently in the relevant patents. A possible reason for their frequent use is that pneumatic actuators are intrinsically MR safe, since they do not rely on magnetism or electronics to operate. Hydraulic actuators are intrinsically MR safe as well, but they can suffer from leakage of fluids. There are four types of actuators in the classification tree that do not have any patents using that type of actuator. Those actuators are the ones that use heating of a liquid and heating of a gas to internally induce kinetic energy and actuators using chemical or light energy.

Also of interest is to see the trend in types of actuators used throughout the years. This could lead to insight into which types of actuators might be used in the future. Figure 10 shows the percentage of type of actuators used. Before the year 2000, solely transmission-based actuators were used; pneumatic, hydraulic and mechanical transmission. After the year 2000, there are more different types of actuators used, including actuators that have their kinetic energy induced internally. However, there is no trend towards the use of a certain type of actuator, both piezoelectric and pneumatic actuators remain more or less dominant throughout the years.

Limitations of this review

A first limitation of this review lies in the search query used. There are patents that describe an actuated device in the MR environment, but do not use the word actuator, motor or robot in the edited title or abstract, but do in the full text. These patents have not been found in this review. The search was also restricted to the 'Amusement and Health' section for the medical domain of the DII and the 'Instrumentation, Measuring and Testing' for the electrical medical equipment domain of the DII. Removing the restriction to these sections results in 2643 patents, instead of 1645, which could yield even more relevant patents in different domains. Secondly, this review only covers patents. Patents seldom describe whether a device works well. Quantified figures regarding SNRs of the MR image during operation of the device as well as accuracy and repeatability of placements of end effectors generally do not appear in the patents. For further research, scientific papers corresponding to the patents could provide performance measures of the devices described in the patents.

Conclusion and future work

This review provides an overview of patents on actuated devices designed for use in the MR environment. A systematic classification of actuation principles has been proposed and applied to the devices described in the patents. By this top down categorization approach, 15 different types of actuation principles have been identified. Pneumatic and piezoelectric actuators were used the most in the patents found, as well as in patents which have been commercialized. No patents were found for actuation principles using light or chemical energy or heating of a gas or liquid as source of kinetic energy. The insight in the most used and unexplored actuation principles could serve as an inspiration for selecting or developing new actuation principles for mechatronic devices in the MR environment. Future work should look into the scientific literature on the found patents for quantitative information on the performance of their actuation principles.

Declaration of conflicting interests

The authors declared no potential conflicts of interest with respect to the research, authorship, and/or publication of this article.

Funding

This work was supported by the Interreg 2 Seas Cooperative Brachytherapy project [CCI: 2014TC16RFCB038], partly funded by the Regional Development Fund (ERDF).

References

1. Smith KA and Carrino J. Mri-guided interventions of the musculoskeletal system. *Magn Reson Med* 2008; 27(2): 339–346.
2. Monfaredi R, Cleary K and Sharma K. Mri robots for needle-based interventions: Systems and technology. *Ann Biomed Eng* 2018; : 1–19.
3. Taylor RH, Menciassi A, Fichtinger G et al. Medical robotics and computer-integrated surgery. In *Springer handbook of robotics*. Springer, 2016. pp. 1657–1684.
4. Arnolli MM, Hanumara NC, Franken M et al. An overview of systems for ct-and mri-guided percutaneous needle placement in the thorax and abdomen. *Int J Med Rob Comput Assisted Surg* 2015; 11(4): 458–475.
5. Cleary K, Melzer A, Watson V et al. Interventional robotic systems: applications and technology state-of-the-art. *Minim Invasiv Ther* 2006; 15(2): 101–113.
6. American Society for Testing and Materials (ASTM) International DF. Astm f2503-05, standard practice for marking medical devices and other items for safety in the magnetic resonance environment, 2005.
7. Shellock FG, Woods TO and Crues III JV. Mr labeling information for implants and devices: explanation of terminology. *Radiology* 2009; 253: 26–30.
8. Moser R, Gassert R, Burdet E et al. An mr compatible robot technology. In *Robotics and Automation, 2003. Proceedings. ICRA'03. IEEE International Conference on*, volume 1. IEEE, pp. 670–675.

9. Fischer GS, Krieger A, Iordachita I et al. Mri compatibility of robot actuation techniques–a comparative study. In *International Conference on Medical Image Computing and Computer-Assisted Intervention*. Springer, pp. 509–517.
10. Gassert R, Yamamoto A, Chapuis D et al. Actuation methods for applications in mr environments. *Concepts Magn Reson Part B* 2006; 29(4): 191–209.
11. Yu N, Hollnagel C, Blickenstorfer A et al. Comparison of mri-compatible mechatronic systems with hydrodynamic and pneumatic actuation. *IEEE-ASME Trans Mech* 2008; 13(3): 268–277.
12. Scali M, Pusch TP, Breedveld P et al. Needle-like instruments for steering through solid organs: A review of the scientific and patent literature. *Proc Inst Mech Eng [H]* 2017; 231(3): 250–265.
13. Albrecht H. Fan device for insertion in scatter field of magnetic field generator of magnetic resonance device, has non-magnetic engine and non-magnetic fan wheel which is actuated by non-magnetic engine. Patent DE102008034685-A1, 2009.
14. Backes CH. Injection appliance for magnetic resonance tomography - has control, electric motor, transmission elements, and housing. Patent DE19621393-A1, 1996.
15. Bailey DW. Compact rotary actuator for use in surgical manipulator for e.g. MRI procedure in e.g. MRI application, has coupling mechanism provides rotation to output shaft from another rotation of input shaft. Patent US2013211422-A1, 2012.
16. Barberi EA, Dietrich JM, Hartman NG et al. Piezoelectric motor assembly for driving e.g. rotational motion of moving insert in MRI motion phantom, has piezoelectric motors mounted on motor frame and biased against outer surface to result in unbalanced net force on circular body. Patent WO2017120661-A, 2016.
17. Benitez CL, Lear C, Potter J et al. Device useful for diagnosing foot injury, preferably lisfranc joint injury of patient comprises main portion to receive and hold foot and lower leg, force application mechanism, and actuators for controllably moving force mechanism. Patent WO2017205411-A1, 2017.
18. Bergman CT. Cradle drive and release mechanism for magnetic resonance scanner - has motor coupled to belt to bidirectionally drive dolly on bridge when clutch pad frictionally engages disc. Patent US4641823-A, 1984.
19. Birk JA, Hoyt RE and Snow S. Implantable device for controlling fluid movement to inflatable portion of gastric band, has microcontroller that controls actuator to apply force to diaphragm based on received telemetric signal from remote transmitter. Patent US2013253262-A1, 2008.
20. Bosboom DGH, Futterer JJ, Barentsz JO et al. Motor system of robot arm device used in e.g. medical MRI application, has control unit that periodically controls each drive unit of each actuator in set of actuators to operate in time-shifted manner with respect to each other. Patent WO2012069075-A1, 2010.
21. Bruce JK. Apparatus for use with e.g. biopsy localization fixture, for positioning breast of patient during biopsy procedure, has support unit positionable between grid plate and medial plate, and actuation device in communication with support unit. Patent WO2017059134-A1, 2015.
22. Carreira DP, Fernandes LFS, Grant MA et al. System for tissue treatment comprises motorless drive mechanism which is compatible with and can operate within an operational field of medical imaging system, base unit and electronic controller including input and output interfaces. Patent WO2014003855-A1, 2012.
23. Chen Y, Yu X and Yu S. Positioning system for MRI device to position insertion element on or in body of animal to treat brain diseases, has belt looped over pulley connected to actuator, where connection between belt and pulley is in form-fit-manner. Patent EP3315064-A1, 2016.
24. Christakis D. Magnetic resonance imaging compatible positioning system for positioning high intensity focused ultrasound transducer, has polyethylene sheet establishing motion in three directions, and four polyethylene angles placed on sheet. Patent WO2007082495-A1, 2006.
25. Cinquin P, Jacquet A and Taillant E. Positioning system for positioning e.g. hollow needle, has actuation system with piston that is adapted for sliding rod, where fluid used by piston is air, and shaft assembled on wheel that comprises dissymmetrical teeth. Patent US2006058640-A1, 2004.
26. Cinquin P, Avila VJC, Vilchis GAH et al. Surgical tool e.g. needle, positioning and/or orienting device for body of patient, has pneumatic actuators with contact surfaces integrated to support, so that internal pressure variation leads to displacement of contact surfaces. FR2934487-A1, 2008.
27. Cleary K, Monfaredi R, Sze R et al. Sterilizable patient mountable robot e.g. fluoroscopy mountable robot, for providing needle guidance at e.g. joint, of body of patient during e.g. biopsy procedure, has actuator attached to robot base that linearly translates base link. Patent US2014371584-A1, 2013.
28. Comber DB, Barth EJ, Slightam JE et al. Apparatus for moving elongate rod relative to ground surface, has locking mechanism for grasping and releasing portion of rod in coordination with motion of rotation part end in chosen one of clockwise and counterclockwise directions. Patent US2017036883-A1, 2015.
29. Comber DB, Barth EJ, Webster RJ et al. Device e.g. stepper motor, for providing motive power to tube of active cannula, has module for providing translational and rotational motions to moved structure, where structure is made from non-ferromagnetic material. Patent US2013123802-A1, 2015.
30. Consiglio RP. Recorder device for recording physiological data from patient has piezoelectric motor that is arranged to feed paper through printer assembly as physiological data from patient in high magnetic field is printed. Patent WO2012014119-A1, 2010.
31. Consiglio RP, Oneill FP and O'Neill FP. Electrically controlled valve for magnetic resonance (MR) system, has valve element that is to be moved by follower against valve seat to restrict fluid flow and to be moved by follower away from valve seat to increase fluid flow. Patent WO2014181208-A1, 2013.
32. Coppens D, Manning J and Ports F. Trolley system for transporting patient within MRI room from trolley, has motor mounted such that elevation of motor is fixed relative to base portion, and trolley system compatible with attraction force less than or equal to certain force. Patent WO2017066616-A1, 2015.
33. Cowan KP, Reilly DM, Fularz JJ et al. Dual syringe injector for use in magnetic resonance environment, has mechanical transmission fabricated from magnetic resonance compatible

components. Patent WO2006078817-A2, 2006.
34. Crowley DM and Crowley D. Cryogenic refrigerator for e.g. indirect cooling of superconductor, has fluid motor constructed of non-magnetic material, and pump operated by electric motor situated remotely from fluid motor to circulate fluid to fluid motor. Patent GB2430996-A, 2005.
35. Damianou C and Yiannakou M. Apparatus for navigating focused ultrasound transducer, has stage dedicated to control position of focused ultrasound transducer source in Z axis, and water container coupling ultrasound to fibroid, breast, abdominal and brain. Patent EP3254731-A1, 2016.
36. Daum W, Winkel A, Guenther T et al. Piezoelectric drive for neuro surgery is non magnetic can be used with NMR is minimally invasive. Patent DE10029739-A1, 2000.
37. Desai JP and Ayvali E. Actuated steerable probe e.g. ultrasound probe, for e.g. MRI machine, has joint assembly comprising actuator with bending element that is configured for movement about and between straight and curved positions in response to actuation. Patent US2013296885-A1, 2012.
38. Desai JP, Ho M, Simard JM et al. Minimally invasive neurosurgical intracranial robot system for use in removal process of tumors, controls rotational motion of adjacent links of one revolute joint, so that robot sub-system is steered relative to target of interest. Patent US2013218005-A1, 2012.
39. Di Giancamillo M and Zani DD. Non-magnetic diagnostic or surgical table for veterinary or medical use, has radio-transparent which is raised with pneumatic system including stabilizer. Patent WO2008062493-A1, 2006.
40. Dirauf F, Gambke G, Koerth M et al. Magnetic resonance tomography system has drive device having rotor which can be flowed through with electrical current and which is connected to bearing plate. Patent DE102015222643-B3, 2015.
41. Donaldson S and Mahon C. Magnetic resonance imaging compatible positioning device for moving thermal therapy applicator of thermal therapy system in patient, comprises mechanical platform for supporting thermal therapy applicator. Patent WO2011115664-A2, 2010.
42. Dong S. Piezoelectric motor for driving a lens in e.g. a cell phone camera has a stator with a piezoelectric ring that includes bottom electrode and segmented top electrode and with the rotor rotatably mounted within the piezoelectric ring. Patent US2008247059-A1, 2007.
43. Du Z, Dong W and Li H. Shearing type piezoelectric ceramic motor used for nuclear magnetic resonance antenna, has two piezoelectric ceramic groups that are connected to positive and negative input ends of signal control module through first and second leads. Patent CN104506080-A, 2015.
44. Dubowsky S, Hafez M, Jolesz FA et al. Actuator for use in magnetic resonance imaging comprises actuator device having elastomeric dielectric film with two compliant electrodes and frame of magnetic resonance bringing device. Patent US2003210811-A1, 2002.
45. Ehman RL, Glaser KJ and Yin M. Stress producing system for use during magnetic resonance elastography scan in MRI system, has strap including inelastic material to convert energy delivered to passive actuator from tube into shear waves with subject. Patent US2009295387-A1, 2008.
46. Feng Y and Huang L. Animal vitro sample MRI driving device, has adjusting bracket whose two ends are extended to end of anesthesia head cover, connecting piece connected with driving rod, and animal head fixing terminal formed with multiple fixing-holes. Patent CN207270338-U, 2017.
47. Feng W, Jiang S, Li W et al. Minimally invasive needle mechanical arm device for nuclear magnetic resonance imaging environment, has translation execution unit and lifting executing unit that are provided to realize surgical needle space position. Patent CN102499726-A, 2011.
48. Fischer GS and Su H. MRI-guided system for interventional needle procedures, such as MRI-guided transperineal prostate biopsy, has fiberoptic force sensor connected to slave robot, and providing data to robot controller. Patent WO2011057260-A2, 2009.
49. Friebe M. Magnetic resonance imaging to show a puncture site for a biopsy in an mri scan. Patent DE202005021902-U1, 2005.
50. Fujimoto K, Arimitsu Y, Hata N et al. Needle placement manipulator for needle positioning system used for imaging modalities, has first and second rotary guides, and needle holder, which have respective rotational axes that cross each other at crossing point. Patent US2014275979-A1, 2013.
51. Goldenberg AA, Yang Y and Ma L. Surgical robot assembly for use with MRI scanner housed in MRI room, has filter operably connected to cables operably connected between motors of surgical robot and controller, and comprising cut off frequency tuned to MRI. Patent WO2017173539-A1, 2016.
52. Goldenberg AA, Haider M, Kucharczyk W et al. Medical robot for use in MRI device for treating prostate cancer, has controller connected to motion joints of horizontal and vertical motion assemblies, where controller is powered off when MRI device collects images. Patent WO2009152613-A1, 2008.
53. Grady JK. Fluoroscopy method involves performing simultaneous imaging by MRI machine and fluoroscopy machine in examination room due to materials which cannot be magnetized. Patent US2017035377-A1, 2014.
54. Griffiths DM, Pomaybo AS and Hirschman AD. Fluid delivery system for use in medical magnetic resonance imaging system, has piston in operative connection with actuator including electroactive material adapted to apply force to piston to pressurize fluid within syringe. Patent US2008056920-A1, 2003.
55. Groenhuis V, Siepel FJ and Stramigioli S. Pneumatic stepper motor used for e.g., magnetic resonance imaging-compatible robotic system, has housing which accommodates rack or geared axle with gear elements, and two pistons which are arranged to cooperate with rack or geared axle. Patent WO2018038608-A1, 2017.
56. Guettler F, Rump J, Seebauer C et al. Medical device i.e. drilling machine, for driving e.g. drill to treat osteitis in human bone or cartilage, has housing, motor and transmission designed to be magnetic resonance tomography-safe and compatible, and radioparent. Patent WO2013020877-A1, 2011.
57. Hassler WL. Implantable device useful in implantable sphincter apparatus e.g. gastric band comprises piezoelectric driver to selectively actuate bellow accumulator between first volume and second volume, and controller to control piezoelectric actuator. Patent EP1600183-A1, 2004.
58. Hiratsuka M, Nakanishi T, Kitano Y et al. Robot arm for intra-operative MRI, has table moving between MRI

imaging position or MRI imaging preparation position and treatment position, by control of control apparatus. Patent WO2017098543-A1, 2015.

59. Horne DJ and Horne J. Support in form of bed for patient, suitable for use with MRI machine, has platform connected to first and second legs, and actuator connected to carriage such that movement of actuator is restrained in horizontal direction. Patent WO2017181230-A1, 2016.
60. Householder RM and Bruce JK. Apparatus for use with biopsy device to promote Magnetic Resonance Imaging (MRI) compatibility, has second cutter drive unit that is associated with case and linear actuator that is configured to drive cutter longitudinally. Patent US2018116644-A1, 2016.
61. Ilan E and Elias I. Passive movement apparatus for use with magnetic resonance tomograph uses ankle joint supports and piezoelectric motors made of non-ferromagnetic materials. Patent US2003184296-A1, 2002.
62. Illindala UKV, Palazzolo JA and Palazzolo J. Compressing chest device e.g. AutoPulse cardiopulmonary resuscitation (CPR) device installed on patient, has linear actuator which is arranged relative to load distributing portion, such that actuator is located outside imaging area. Patent US2013072830-A1, 2011.
63. Iwasa T. Drive device for vibration-type actuator, has elastic element that generates machine vibration as to drive voltage, and correction unit corrects distortion of waveform of machine vibration that arises with press-contacting. Patent JP2014003732-A, 2012.
64. Janssens JP. Device for taking tissue sample has pneumatic driving unit that operates biopsy needle assembly to perform movement of components with respect to each other. Patent WO2008086817-A1, 2007.
65. Kan K and Suga K. Air feed device for use in a magnetic resonance imaging device for feeding air into the image capture space to cool the subject using a fluid motor driving rotating vanes with high efficiency. Patent WO200156493-A2, 2000.
66. Kawashima Y. Visual performance control apparatus for use in magnetic resonance imaging apparatus of magnetoencephalograph for controlling test subject visual performance, has visual performance control unit provided with non-magnetic body. Patent JP2012239788-A, 2011.
67. Keene MN and Goodyear SW. MRI room door assembly for use in protecting entrance to room containing MRI scanner system has door and doorframe with built-in safety system that provides function relating to preventing ferrous objects brought close to MRI machine. Patent WO2015071672-A2, 2013.
68. Keibel A. Medical workplace has lengthening apparatus that is fastened to fastening apparatus in regions outside of prescribed end, and medical robot that is set to move medical instrument into treatment region of magnetic resonance device. Patent DE102016204271-A1, 2016.
69. Keidl C, Peterson DM, Piferi P et al. Magnetic resonance imaging guided interventional system for e.g. use during magnetic resonance imaging guided ablation procedure, has magnetic resonance imaging device whose end is in communication with compatible camera. Patent US2009112082-A1, 2007.
70. Kirschenman MB. Remote guidance system for navigating and steering e.g. ablation catheter within body of human patient for treating heart tissue, has fluid actuator configured such that movement of piston causes movement of medical device within body. Patent WO2013101259-A1, 2011.
71. Kobayashi H, Sato Y, Hiramatsu K et al. Wear-type joint actuation device e.g. for shoulder joint, has control unit to regulate supply and exhaust of fluid to hydraulic actuators so as to expand and contract inner tube. Patent WO2004087033-A1, 2003.
72. Kolipaka A, Arnold JW, Lee FP et al. System for inducing tissue vibration used for magnetic resonance elastography (MRE), has hydraulic drive component to alternately pump hydraulic fluid into hydraulic piston enclosure for linear movement of piston. Patent WO2016077776-A1, 2014.
73. Kroeckel H and Rauh G. Drive for positioning actuators in strong magnetic fields, especially magnetic resonance systems, has fluid stepper motors directly in field region driven via networked magnetic valves. Patent DE19856803-C1, 1998.
74. Kwok KW, Dong Z, Guo Z et al. System for placing catheter for performing interventions remotely on confined anatomy by physician during procedure, has actuators connected to main robot body, and display for providing view from tip of instrument tracked under MRI. Patent US2017367776-A1, 2016.
75. Lamperth MU, Young IR, Elhawary H et al. MRI compatible manipulator for use in MRI scanning system, has series connection of stages which are built to form Cartesian robot having less effect on magnetic fields in scanner bore. Patent WO2008059263-A2, 2006.
76. Larson BT and Erdman AG. Apparatus for medical intervention using tissue-penetrating probe in magnetic-resonance-imaging (MRI) machine, has computer that, based on received user commands, extend tissue-penetrating probe into tissue of patient. Patent US2017135779-A1, 2008.
77. Li Z, Liu K, Xia W et al. High pressure injector, has ultrasonic motor for rotationally driving ball screw to rotate through shaft coupling and driving push rod to move forward or backward attraction, and exhaust pat fixed with test injection part. Patent CN205903495-U, 2016.
78. Li H, Mou X, Sun L et al. Magnetic resonance head elbow bracket, has arm supporting frame whose end is fixed with arm that is connected with wing plate, head support plate provided with neck cushion, and hydraulic pole connected with hydraulic pressure motor. Patent CN204318757-U, 2014.
79. Matchey C, McNally J and Morrison D. Implantable infusion apparatus for delivering medication or other fluids to patient has electronically controlled metering assembly which comprises two valves, each having shaped memory alloy (SMA) wire, fluid chamber, and barrier. Patent WO2010011499-A1, 2008.
80. Matsuwaki H, Shimodozono M, Kawahira K et al. Oscillation apparatus e.g. hand-held massaging device, for use in MRI environment, has rotating shaft accommodated in housing, impeller fixed to rotating shaft accommodated in housing, and outer shell for covering exterior of housing. Patent JP2017047343-A, 2015.
81. McMillan AB, Gullapalli R, Richard HM et al. System for telemetrically controlling e.g. biopsy needle during minimally invasive surgical procedure by neurosurgeon, has navigation sub-system for interfacing with user to receive

user's commands to control interventional device. Patent US2013296737-A1, 2012.
82. Miller ME. Biopsy apparatus for use in taking biopsy for diagnosis and treatment of breast cancer has handpiece which includes magnetic resonance imaging (MRI) compatible devices detachably coupled to inner cannula and comprised with hydraulic motor. Patent US2009048533-A1, 2000.
83. Mujica-Parodi L, Strey H and Dedora D. Dynamic phantom apparatus for use with functional MRI device for obtaining images of e.g. brainstem, has magnetic -resonance-contrast-producing materials for filling space within rotor, and MRI-compatible actuator connected to rotor. Patent WO2017004277-A1, 2015.
84. Nakamura K, Doi M and Nakamura M. Air motor for microscope used in MRI environment, has brake pad for contacting turbine with preset urging force, where brake pad departs from turbine such that brake pad is in non-contact state by using exhausted gas pressure. Patent EP1657408-A1, 2000.
85. Nakayama T, Maeno S, Takeshi N et al. Superconducting electromagnet used in magnetic resonance imaging (MRI) machine, has magnetic shield, which protects motor from magnetic flux of coil, that includes ferromagnetic plates placed opposite each other across the motor. Patent EP1808870-A1, 2006.
86. Nazim K, Vazquez M, Lee J et al. Catheter control apparatus for controlling flexible elongate device e.g. endoscope, has computer arrangement in communication with manipulating arrangement for remotely operating manipulating arrangement, where arrangement includes computer. Patent WO2016176683-A1, 2015.
87. Nemoto S and Hachiya T. Contrast agent injection system for use in e.g. computed tomography (CT) for diagnosing patient, has alarm that is emitted or movement of piston drive mechanism is stopped, when no predetermined range of value is present. Patent JP2018061836-A, 2017.
88. Newman HS and Horowitz MI. Wireless controlled medical implant system, has inflatable medical implant that is connected to fluid reservoir through flexible tubing and is inflated by fluid which is transferred from fluid reservoir through tubing using pump. Patent US2017079760-A1, 2015.
89. Oneill FP, Consiglio RP, Oneill F et al. Valve actuator for actuating magnetic resonance-compatible valve used in e.g. pump, has control circuit providing power signal to shape memory alloy unit to actuate memory alloy unit and maintaining memory alloy unit in active state. Patent WO2013186725-A2, 2012.
90. Ono Y, Hirakawa K, Masuno T et al. Chemical injection device e.g. syringe system pump for use with MRI apparatus has syringe side and motive power side hydraulic-pressure cylinders including hydraulic-pressure chambers connected by pipings, respectively. Patent JP2011000183-A, 2009.
91. Onuma K and Konuma K. Medical manipulator for e.g. medical puncture apparatus utilized in robotics field, has driving circuit connected to vibrating unit, and torque control unit controlling holding torque with which moving unit is held by vibrating unit. Patent WO2013187010-A1, 2012.
92. Osman NF, Jacobs MA, Harouni AE et al. Device for selectively compressing target tissue for MRI of target tissue, has moving mechanism operably coupled to moveable structure member, where mechanism includes set of fluid actuatable devices. Patent US2011270079-A1, 2010.
93. Parihar SK, Dahling TM, Mescher PA et al. Biopsy system used for obtaining biopsy sample, has encoder which operationally coupled with magnetic resonance (MR) compatible motor. Patent US2013066191-A1, 2008.
94. Plante J, Miron G, Proulx S et al. Integrated device e.g. integrated binary elastically averaged pneumatic air muscles manipulator for orienting object, has actuating valves that actuates fluid actuated device to displace supporting element with respect to frame. Patent WO2012019292-A1, 2010.
95. Rhad EA, Hibner JA, Craig HW et al. Biopsy device for use in part of patient's anatomy e.g. prostate, to capture biopsy samples from patient below e.g. stereotactic guidance, has motor operated to actuate firing assembly to retract and fire needle relative to body along axis. Patent US2012109007-A1, 2010.
96. Roeck WN and Nalcioglu O. Magnetic resonance imaging (MRI) compatible electric motor for rotating object e.g. surgical device with respect to MRI field is disposed in portion of MRI field to employ MRI field as internal magnetic field for generation of motive force. Patent US2010264918-A1, 2009.
97. Rohling KW, Cline HE and Abeling WR. Mechanical positioner for magnetic resonance guided ultrasound therapy - has transducer plate constructed of MR compatible material for carrying energy transducer and positioning transducer under control of operator. Patent US5443068-A, 1994.
98. Roozen NB and Van Schothorst G. Magnetic resonance imaging apparatus for medical field, has several suspension elements which are provided with piezo actuator connected in series with resilient element. Patent WO200246783-A1, 2000.
99. Salminen H. High intensity focused ultrasound positioning mechanism for positioning ultrasound transducer, has linear drives that are provided with drive block which form separate ball joint with respect to rod. Patent WO2011036607-A1, 2009.
100. Saloux E and Tournoux F. Heart phantom assembly for use with imagery systems, has phantom interface which is connected to actuators to be displaceable in translational and rotational degree of freedom as function of actuation. Patent WO2014201571-A1, 2013.
101. Sander U. Magnetic resonance-compliant microscope for use in operating microscope system, has actuator for controlling adjustable mechanism of microscope and formed as electroactive polymer actuator. Patent Patent DE102010030007-A1, 2010.
102. Scantlebury TR, Tidwell DG, Umber R et al. Pneumatic resecting tool for dissection of bones - has motor housing, rotor, spindle, and chuck which are made from titanium so as to avoid influence of magnetic field. Patent US5782836-A, 1996.
103. Schaerer S, Alexiuk M, Scarth G et al. Magnetic resonance imaging (MRI) compatible stereoscopic viewing apparatus for observing body part of patient in robotic microsurgical system, has optical assembly, control system, and communication arrangement made compatible with magnet. Patent US2012190965-A1, 2011.
104. Schwindt J. Breast biopsy device, has hollow shaft with cutter end that rotates relative to orifice in cannula to cut tissues, which is drawn through hollow shaft and pneumatic circuit coupled to motor. Patent US2003199787-A1, 2002.

105. Shih M and Huang H. Device for combining MRI and emission tomography for breast examination, has control module for controlling opening process of valve to change gas flows entering into actuator to drive pulley and ropes to allow platform to move up and down. Patent US2015234022-A1, 2014.
106. Shvartsman SM, Dempsey JF and Nicolay D. System for radiotherapy with magnetic resonance imaging, has permanent magnets adjacent drive motors, and oriented to counteract Mill's main magnetic field, and additional conductive elements that are symmetrically disposed around gantry. Patent US2017281043-A1, 2013.
107. Stoianovici D, Wyrobek KA, Mazilu D et al. Medical imaging environment compatible positioning arm for holding device in medical imaging environment workspace has lock that attaches cable and applies tension to cable so as to pull adjoining end faces of links into contact. Patent WO2004062517-A2, 2003.
108. Stoianovici D, Patricui A, Mazilu D et al. Robot for medical image-guided interventions, has several actuators with pneumatic stepper motors for moving medical device mounted platform in desired directions. Patent WO2007065013-A2, 2005.
109. Stoianovici D, Patriciu A, Mazilu D et al. Stepper motor for e.g. magnetic resonance imaging equipment, has fluid pressure applying unit applying fluid pressure driven force on hoop gear so as to cause translational-circular motion of hoop gear. Patent US2007034046-A1, 2005.
110. Stoianovici D, Petrisor D, Jun C et al. Robot for remote center of actuation module, has remote center of motion (RCM) mechanism having parallelogram structure with non-collinear joints instrument for use with robot which is aligned between joint and RCM point of RCM mechanism. Patent WO2017192796-A1, 2016.
111. Su Z, Liu W, Qiao S et al. Ultrasonic probe device for MRI-phased high-intensity focused ultrasound heat treatment system, has probe motor speed changing group connected with probe moving control subassembly by connecting plate to control movement of ultrasonic probe. Patent CN108042932-A, 2017.
112. Su X, Cao J and Su Y. Non-magnetic injection pump for ultrasonic motor, has working table whose end is fixed with injector main body clamp, pushing screw mandrel fixed with round guide rail, and propeller provided with piston rod clamp of syringe. Patent CN205698713-U, 2016.
113. Susi RE. Liquid infusion apparatus for MRI-compatible liquid infusion pump assembly used for infusing e.g. drugs, has housing and door, which are formed of non-magnetic, electrically-conductive material for shielding radio-frequency interference. Patent US2013281966-A1, 2005.
114. Tanaka M, Oka M, Oki T et al. Ultrasonic motor has elastic vibrator provided at side of rotor screwed with female screw, to which piezoelectric elements are attached. Patent JP2005185072-A, 2003.
115. Taracila V, Navarro MA, Gregan DC et al. Adjustable Magnetic Resonance Imaging (MRI) head coil apparatus has actuator mechanism which is configured to adjust relative position of each of multiple plates in order to allow plates to fit a variety of different patient head sizes. Patent US2013076358-A1, 2011.
116. Tie Z, Zou C, Liu X et al. Magnetic resonance guided high-intensity focused ultrasound tumor treating system for small animal, has ultrasound transducer for performing three-dimensional motion by ceramic motor to transmit feedback position signal to driving unit. Patent CN206102770-U, 2016.
117. Tigwell NC. Magnetic resonance imaging scanner for patient during e.g. treatment, has hydraulic cylinder and motor arranged to provide motive force for effecting movement of patient table, and secondary conduits directing fluid to cylinder. Patent GB2432112-A, 2005.
118. Tse TH, Squires A, Xu S et al. Robotic system for guiding needle into prostate of patient in MRI machine, has robot moving guide in left-right and anterior- posterior directions, and rotation unit configured to change yaw angle of guide within coronal plane of patient. Patent WO2017117382-A1, 2015.
119. Tsekos N. Robotic system e.g. MRI guided robot for performing robot-assisted surgical procedure, has computer having network connection that is provided in electronic communication with image-guided robotic manipulator and controlled actuator. Patent WO2014032046-A1, 2012.
120. Unknown. A pneumatic sample supply, which can be embedded in an mri apparatus. Patent Patent DE202013103646-U1, 2013.
121. Vij K, Pandey R and Flores J. Surgical motor-powered driver used in MRI-guided surgery for e.g. drilling into bone, driving screws into bone has handpiece has chuck extending from housing, which holds drill bit and screw driver so as to extend out and rotated by motor. Patent US2015272596-A1, 2014.
122. Wei W, Meng D, Ding X et al. Magnetic resonance compatible pneumatic puncture surgical robot for use by doctor, has puncturing orientation module for adjusting puncture angle of locating needle, and needle module for realizing automatic control and movement of needle. Patent CN206365925-U, 2016.
123. Yehezkeli O, Freundlich D, Magen N et al. Positioning apparatus for a therapy device operated under magnetic resonance imaging guidance has three vibrational motors for adjusting location of therapy device in lateral direction, in longitudinal direction and to adjust roll of device. Patent WO200209812-A1, 2000.
124. Yue Y. MRI-computed tomography (CT) compatible system for kit, has electronic controller that modulates air pressure generated by air pump which in turn modulates position of phantom. Patent WO2017019809-A1, 2015.
125. Zhang Z, Jiang S, Feng W et al. Manipulator for performing acupuncture operation in nuclear magnetic resonance environment, has guide screw slide rail mechanism with slide block whose moving direction is vertical to output axis of ultrasonic motor. Patent CN102113905-A, 2011.
126. Gao J, Sansiñena JM and Wang HL. Tunable polyaniline chemical actuators. *Chem Mater* 2003; 15(12): 2411–2418.
127. Mu X, Sowan N, Tumbic JA et al. Photo-induced bending in a light-activated polymer laminated composite. *Soft Matter* 2015; 11(13): 2673–2682.
128. Iradimed Corporation. 3860+ mri infusion pump. URL http://www.iradimed.com/en-us/products/mridium3860. (2017, accessed 4 October 2018).
129. Bayer Healthcare LLC. Medrad mrxperion mr injection system. URL https://www.radiologysolutions.bayer.com/products/mr/injection/mrxperion/. (2018, accessed 4 October

2018).
130. Nemoto. Sonic shot gx injector for mri. URL http://www.nemoto-do.co.jp/nemoto_en/pr_mr/moreinfo/ss_7.htm. (2018, accessed 4 October 2018).
131. Shenzhen Seacrown Electromechanical Co, Ltd. Zenith-c60. URL http://www.seacrown.cn/en/product/showpro.html?pid=11. (2018, accessed 4 October 2018).
132. Dasta JF, McLaughlin TP, Mody SH et al. Daily cost of an intensive care unit day: the contribution of mechanical ventilation. *Crit Care Med* 2005; 33(6): 1266–1271.
133. Monteris Medical. The neuroblate laser ablation system. URL https://www.monteris.com/neuroblate-system/. (2018, accessed 16 October 2018).
134. Insightec. Insightec for neurosurgery. URL https://www.insightec.com/clinical/neurosurgery. (2018, accessed 16 October 2018).
135. Accessgudid. Neuroblate robotic probe driver. URL https://accessgudid.nlm.nih.gov/devices/00816589020373. (2018, accessed 16 October 2018).
136. US Food and Drug Administration. Monteris medical neuroblate system recalled due to unexpected heating of laser delivery probes. URL https://www.fda.gov/medicaldevices/safety/listofrecalls/ucm602252.htm. (2018, accessed 16 October 2018).
137. ModusQA. Mr safe 4d motion qa for planning, adaptive mrgrt and simulation. URL https://modusqa.com/mri/motion. (2018, accessed 16 October 2018).
138. PiezoMotor. Piezo legs® rotary 50mnm non-magnetic vacuum. URL https://www.piezomotor.com/products/rotary-piezo-motor/rotary-50mnm-non-magnetic-vacuum/. (2018, accessed 17 October 2018).
139. Shinsei Corporation. Non-magnetic model. URL http://www.shinsei-motor.com/English/product/nonmagnetic.html. (2018, accessed 17 October 2018).
140. Krieger A, Song SE, Cho NB et al. Development and evaluation of an actuated mri-compatible robotic system for mri-guided prostate intervention. *IEEE-ASME Trans Mech* 2013; 18(1): 273–284.
141. Wang Y, Cole GA, Su H et al. Mri compatibility evaluation of a piezoelectric actuator system for a neural interventional robot. In *Engineering in Medicine and Biology Society, 2009. EMBC 2009. Annual International Conference of the IEEE*. IEEE, pp. 6072–6075.

B

Overview of the State of the Art in PSMs

Table B.1: State of the art of pneumatic stepper motors, sorted on step size. A '?' indicates the information cannot be found in the literature. Table continues on the next page.

Author	Design	Size (mm)	Step Size (°)	No Load Speed (RPM)	Loaded Speed (RPM)	Torque (Nm) @ Loaded Speed	Power (W)	Pressure (MPa)	MR Safety	Patented
Howland [16]	Nutation	255x255x450	0.25	1.83	2.5	6.7	1.75	0.48	Unsafe	US3486518A
Comber *et al.* [22]	Helical and Linear gears	⌀89x330	0.5	0.83	0.083	0.068	5.9e-4	0.75	Cond.	US2017036883A1
Oda *et al.* [17] & Uzuka *et al.* [36]	Nutation	⌀40x27	0.6	15	7.2	1.8	1.36	0.5	Unsafe	JP4678723B2
Tantrapiwat and Coulter [18]	Nutation	60x60x?	2.4	20	16	1.2	2.01	0.62	Unsafe	No
Groenhuis *et al.* [20]	Spur gear, 4 toothed pistons	⌀30x32	2.86	38.2	4.8	0.072	0.29	0.22	Safe	WO2018038608A1
Farimani and Misra [10]	Scotch Yoke, 3 cylinders	40x25x40 ex. gearbox	3	20	20	0.07	0.15	0.8	Safe	No
Baumgartner Maschinenbau AG [19]	Nutation	⌀62x72.5	3	24	7	2.2	1.61	0.6	Safe	Commercially available

Continuation of Table B.1 from the previous page.

Author	Design	Size (mm)	Step Size (°)	No Load Speed (RPM)	Loaded Speed (RPM)	Torque (Nm) @ Loaded Speed	Power (W)	Pressure (MPa)	MR Safety	Patented
Stoianovici *et al.* [23]	Hoop gear, 3 cylinders	⌀85x35	3.33	180	178	0.14	2.61	0.83	Safe	US10024160B2
Chen *et al.* [13]	Crankshaft, 2 double acting cylinders	95x60x35	3.6	2.4	2.4	0.5	0.13	0.55	Cond.	No
Wineland *et al.* [11]	Continuous motor, 2 cylinder Geneva drive switch	?	3.6	1.02	0.9	0.92	0.09	0.4	Safe	No
Sajima *et al.* [24]	Crown gear, 3 toothed pistons	⌀30x40	4.29	48	35	0.13	0.48	0.8	Safe	JP2011241970A
Boland *et al.* [15]	Crankshaft, 4 cylinders	80x80x80	4.5	400	240	0.016	0.40	0.62	Safe	No
Groenhuis and Stramigioli [21]	Spur gear, 4 toothed pistons	⌀80x37	10	133	91.7	2.6	24.96	0.25	Safe	WO2018038608A1
Groenhuis and Stramigioli [21]	Spur gear, 4 toothed pistons	⌀44x31	10	333	125	0.28	3.67	0.25	Safe	WO2018038608A1
Wei *et al.* [12]	Turbine, push roller in dimpled gear	⌀100x76	18	?	668.8	0.05	3.50	0.2	Safe	No
Guo *et al.* [25]	Crown gear, bidirectional	⌀35x88	30	160	140	0.0032	0.05	0.48	Safe	No
Secoli *et al.* [14]	Crankshaft, 3 cylinders double acting	250x250x50	60	180	72	0.32	2.41	0.4	Cond.	No
Chen *et al.* [26]	Crown gear, unidirectional	⌀10x60	60	90	10	0.0024	0.02	0.45	Safe	No

C

Positioning Error of Aiming Segments

The positioning of the aiming segments must be done with a certain accuracy and precision. There is a maximum error tolerated in positioning the aiming segments, depending on the geometry of the segments. Throughout this appendix, the needle needs to hit a target of 10 mm at 250 mm insertion depth. This is equivalent to a 5 mm one sided positioning error budget. In the current NPS [8], the image registration of the location of the tumor and orientation of the OM causes 0.81 mm error. The physician may rest their hand (1 kg) on the OM, causing a deflection of the body of the NPS. This deflection contributes 0.34 mm error [8]. Furthermore, during insertion the physician could apply a force of 4 N on the aiming segments, deflecting them. This deflection causes 0.43 mm error. The total positioning error budget left for aiming the segments is thus $dp = 5 - 0.81 - 0.34 - 0.43 = 3.42$ mm.

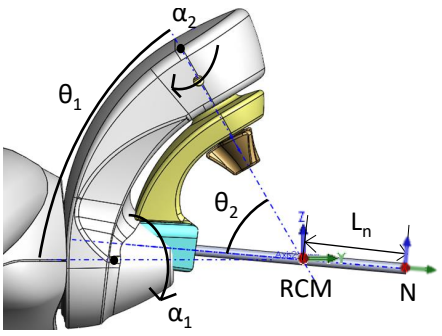

Figure C.1: Geometry of aiming segments. The endpoint N of the needle is L_N mm away from the RCM. In this configuration $\alpha_1 = \alpha_2 = 0°$.

There is a worst-case configuration of the aiming segments; in this configuration the placement of the needle is most sensitive to errors in positioning the aiming segments. The geometry of the aiming segments is depicted in Figure C.1. Equations C.1 through C.3 are used to determine the forward kinematics of the aiming segments, using right-hand rotation matrices R_x and R_y. The positioning error dp between two orientations which are $d\alpha$ apart is determined by Equation C.4. Figure C.2 plots the error sensitivity $dp/d\alpha$, the code used is in Appendix F.6 through F.11. It is observed that error sensitivity is independent of α_1, and that a maximum sensitivity is found for $\alpha_2 = 0°$. Figure C.1 thus depicts a worst-case configuration. The inverse kinematic problem of finding $d\alpha$ for an $dp = 3.42$ mm is solved using an iterative numeric scheme on Equation C.4 with $\alpha_1 = \alpha_2 = 0°$. The latter results in $d\alpha = 0.46°$, so $\alpha_{real} = \alpha_{target} \pm 0.46°$.

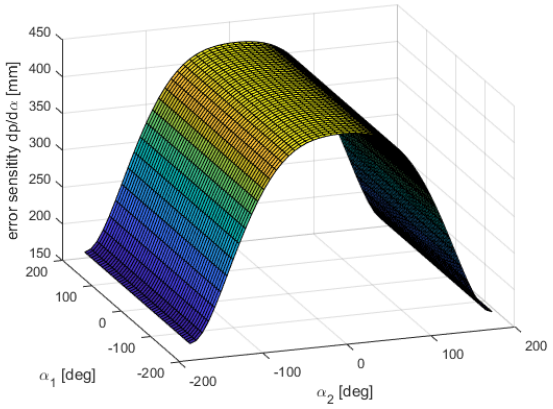

Figure C.2: Error sensitivity $dp/d\alpha$ as function of α_1 and α_2.

$$R_N^{RCM} = R_1^{RCM}(\alpha_1) * R_2^1(\theta_1) * R_3^2(\alpha_2) * R_N^3(\theta_2), \quad \text{(C.1)}$$

$$R_1^{RCM}(\alpha_1) = R_y(\alpha_1), \qquad R_3^2(\alpha_2) = R_y(\alpha_2),$$
$$R_2^1(\theta_1) = R_x(60°), \qquad R_N^3(\theta_2) = R_x(-52.5°), \quad \text{(C.2)}$$

$$\mathbf{p}(\alpha_1, \alpha_2)_N^{RCM} = R(\alpha_1, \alpha_2)_N^{RCM} * \begin{pmatrix} 0 & L_N & 0 \end{pmatrix}^T, \quad \text{(C.3)}$$

$$dp = |\mathbf{p}(\alpha_1 + d\alpha, \alpha_2 + d\alpha)_N^{RCM} - \mathbf{p}(\alpha_1, \alpha_2)_N^{RCM}|. \quad \text{(C.4)}$$

D

Geometry Variables of Escapement Anchors

Table D.1: Geometry variables of escapement anchor 1.

Variable	μ	μ_m	α_1	α_2	β	R	a_1	a_2	b_1	b_2	c	d
Value	0.3	0.25	7.7°	52.85°	10°	19.6 mm	8.03 mm	9.01 mm	4.62 mm	5.11 mm	2 mm	6.6 mm

Table D.2: Geometry variables of escapement anchor 2.

Variable	μ	μ_m	α_1	α_2	β	R	a_1	a_2	b_1	b_2	c	d
Value	0.3	0.25	12.4°	55.8°	12°	17 mm	7.35 mm	8.22 mm	4.87 mm	5.41 mm	2 mm	5.58 mm

E

STEP PLANNING: TABLE OF ACTIONS

Table E.1: Actions that need to be taken to reach the rotation set point when the previous direction of movement was clockwise. Actions depend on the current position p_1 of gear 1, planned positions k_1 and k_2 and on $d = k - p$ of gear 1 and 2. Actions include turn-around compensation. The actions indicate the number of steps to take, together with their direction; CW for clockwise, CCW for counterclockwise. The case ID corresponds to the ID in the Beckhoff code in Appendix G.

Case ID	0	1	2	3	4	5	6	7
$d_1 = k_1 - p_1$	0	>0	>0	≥ 0	0	0	<0	<0
p_1	4	Any	Any	Any	Any	Any	Any	Any
$d_2 = k_2 - p_2$	<0	>0	0	<0	>0	0	≥ 0	<0
First Action	Turn Around	CW $\lvert d_1 \rvert$	CW $\lvert d_1 \rvert$	CW $\lvert d_1 \rvert + 1$	CW $\lvert d_2 \rvert$	Done	CW $\lvert d_2 \rvert + 1$	Turn Around
Second Action	CCW $\lvert d_2 \rvert$	CW $\lvert d_2 \rvert$	Done	Turn Around	Done	Done	Turn Around	CCW $\lvert d_1 \rvert - 1$
Third Action	Turn Around	Done	Done	CCW $\lvert d_2 \rvert - 1$	Done	Done	CCW $\lvert d_1 \rvert - 1$	CCW $\lvert d_2 \rvert - 1$

Table E.2: Actions that need to be taken to reach the rotation set point when the previous direction of movement was counterclockwise. Actions depend on the current position p_1 of gear 1, planned positions k_1 and k_2 and on $d = k - p$ of gear 1 and 2. Actions include turn-around compensation. The actions indicate the number of steps to take, together with their direction; CW for clockwise, CCW for counterclockwise. The case ID corresponds to the ID in the Beckhoff code in Appendix G.

Case ID	14	13	12	10	11	5	9	8
$d_1 = k_1 - p_1$	0	<0	<0	≤ 0	0	0	>0	>0
p_1	-4	Any	Any	Any	Any	Any	Any	Any
$d_2 = k_2 - p_2$	>0	<0	0	>0	<0	0	≤ 0	>0
First Action	Turn Around	CCW $\lvert d_1 \rvert$	CCW $\lvert d_1 \rvert$	CCW $\lvert d_1 \rvert + 1$	CCW $\lvert d_2 \rvert$	Done	CCW $\lvert d_2 \rvert + 1$	Turn Around
Second Action	CW $\lvert d_2 \rvert$	CCW $\lvert d_2 \rvert$	Done	Turn Around	Done	Done	Turn Around	CW $\lvert d_1 \rvert - 1$
Third Action	Turn Around	Done	Done	CW $\lvert d_2 \rvert - 1$	Done	Done	CW $\lvert d_1 \rvert - 1$	CW $\lvert d_2 \rvert - 1$

F

MATLAB Code

Listing F.1: forces_spur_gear.m

```
%%Stephan Neevel
%%Equation of forces on teeth in spur gear
close all
Fi = 10;
R = 0.02;
mu = [0.1 0.3 0.5 0.7 0.9];
alpha_deg = linspace(0,80);
alpha = alpha_deg*pi/180;

figure
hold on
set(gca,'FontSize',15)
xlabel('Angle \gamma [deg]')
ylabel('F_{res}/F_i [-]')
grid on

for i = 1:length(mu)
F(i,:) = Fi./(mu(i)*sin(alpha)+cos(alpha));
Fw(i,:) = mu(i)*F(i,:);
Fres(i,:) = F(i,:).*(sin(alpha)-mu(i)*cos(alpha));
plot(alpha_deg, Fres(i,:)/Fi)
end
legend(['\mu = ',num2str(mu(1))],['\mu = ',num2str(mu(2))],...
    ['\mu = ',num2str(mu(3))],['\mu = ',num2str(mu(4))],...
    ['\mu = ',num2str(mu(5))],'location','northwest')
```

Listing F.2: forces_anchor.m

```
%% Stephan Neevel
%% Calculate forces working on the escapement anchor  when a torque produced by the ...
    ratchet is put on the gear.

p = 0.3; % MPa
mu = 0.3; %[-] friction coefficient between teeth and piston and anchor
mu_m = 0.25; %[-] friction coefficient in axle

%% geometry gear 1 (from CAD)
measured_angle_deg(1) = 97.7; %[deg] measured angle in SolidWorks, first configuration
measured_angle_deg(2) = 142.85; %[deg] measured angle in SolidWorks, second configuration
beta_deg = 10;

R = 0.0196;  a_1 = 8.03; b_1 = 4.62; a_2 = 9.01; b_2 = 5.11; c = 2; d = 6.6;
e = 0.975;

%% uncomment for geometry of gear 2 (from CAD)
```

```
% measured_angle_deg(1) = 102.44; measured_angle_deg(2) = 145.75; R = 0.017; %[m]
% beta_deg = 12; a_1 = 7.35; b_1 = 4.87; a_2 = 8.22; b_2 = 5.41; c = 2; d = 5.58;
% e = 1.34;

%% set up vectors
Fi=zeros(2,1);
Fi_old=zeros(2,1);
err =zeros(2,1);
F =zeros(2,1);
Fn =zeros(2,1);
Mf =zeros(2,1);

%% conversions
alpha_deg = measured_angle_deg -90;
alpha = alpha_deg*pi/180; % 90 is tangent
beta = beta_deg*pi/180;

%% calculation of force of ratchet working on the anchor
A = pi/4*12^2; % [mm^2] area of piston of ratchet
T = p*A*0.022; %[Nm] Torque produced by the ratchet
Fa= T/R;

%% Calculation of forces in first configuration
Fi_old(1) = 10;
Fi(1) = 0;
err(1) = inf;

while err(1) > 0.001
F(1) = (Fa-Fi(1)*sin(beta)+Fi(1)*mu*cos(beta))/(-mu*sin(alpha(1))+cos(alpha(1)));
Fn(1) = Fi(1)*cos(beta)+mu*Fi(1)*sin(beta)+F(1)*(mu*cos(alpha(1))+sin(alpha(1)));
Mf(1) = c.*mu_m.*sqrt(Fa^2+Fn(1)^2);
Fi(1) = 1/((-e-d*mu)*sin(beta)+(e*mu-d)*cos(beta))*(Mf(1) + ...
    F(1)*((-b_1+mu*a_1)*cos(alpha(1))+(mu*b_1+a_1)*sin(alpha(1))));
err(1) = abs(Fi_old(1)-Fi(1));
Fi_old(1) = Fi(1);
end

%% Calculation of forces in second configuration
Fi_old(2) = 10;
Fi(2) = 0;
err(2) = inf;

while err(2) > 0.001
F(2) = (Fa+Fi(2)*sin(beta)-mu*Fi(2)*cos(beta))/(mu*sin(alpha(2))+cos(alpha(2)));
Fn(2) = Fi(2)*cos(beta)+Fi(2)*mu*sin(beta)+F(2)*(mu*cos(alpha(2))-sin(alpha(2)));
Mf(2) = c.*mu_m.*sqrt(Fa^2+Fn(2)^2);
Fi(2) = 1/((-e-d*mu)*sin(beta)+(e*mu-d)*cos(beta))*(Mf(2) + ...
    F(2)*((b_2+mu*a_2)*cos(alpha(2))+(mu*b_2-a_2)*sin(alpha(2))));
err(2) = abs(Fi_old(2)-Fi(2));
Fi_old(2) = Fi(2);
end

%% Outputs
if Fi(1) < 0
  disp(['Situ 1: Zelfremmend!: uitrekkracht = ',num2str(-Fi(1))])
 disp(['diameter = ',num2str(sqrt(-Fi(1)/(pi/4*p)))])
else
  disp(['Situ 1: Lossend!: extra aandrukkracht = ',num2str(Fi(1))])
  disp(['diameter = ',num2str(sqrt(Fi(1)/(pi/4*p)))])
end

if Fi(2) < 0
  disp(['Situ 2: Zelfremmend!: uitrekkracht = ',num2str(-Fi(2))])
  disp(['diameter = ',num2str(sqrt(-Fi(2)/(pi/4*p)))])
else
  disp(['Situ 2 Lossend!: extra aandrukkracht = ',num2str(Fi(2))])
   disp(['diameter = ',num2str(sqrt(Fi(2)/(pi/4*p)))])
end
```

Listing F.3: step_planner.m

```
%% Stephan Neevel
%% Calculate the time it takes to execute movement, and which optimal steps we should ...
    take to get there.
%% the rotation on gear 1 is limited.
% Inputs:
% alpha: scaler of angle to be reached.
% s1: stepsize of first motor stage
% s2: stepsize of second motor stage (stepsize_2>stepsize_1)
% t_step: time to execute one step

% Outputs:
% time: total time to execute movement
% disc_error: absolute discretization error between alpha and the angle that can be ...
    reached by the steps
% steps: 2x1: steps(1): integer of steps with stepsize s1
%             steps(2): integer of steps with stepsize s2

function [time, disc_error, steps] = step_planner(alpha, s1, s2,  t_step)

a = round(alpha/(s2-s1));
angle_disc = a*(s2-s1);
disc_error = abs(alpha-angle_disc);


%use algebraic formula
  d = round(angle_disc/s2);
  steps(1) = cast((d*s2-angle_disc)/(s2-s1),'int8');
  steps(2) = cast(d-steps(1),'int8');

time = t_step*sum(abs(steps)); %total time
end
```

Listing F.4: plot_gear_sizes.m

```
%% Stephan Neevel
%% Dual Speed motor: Plots ub_1: maximum total rotation of gear 1 for different gear ...
    sizes n_1 and n_2. According to n_1 - n_2 = d
% Plots the time needed to make one full rotation for different gear sizes n_1 and n_2

%% user input:
target_s_t = 0.85; %[deg] target step size to reached

t_valve_switch = 0.020; %[s] valve switch time
t_fill = 0.060; %[s] time to fill tubes over 5 meter
t_step = t_valve_switch+t_fill; %total step time

%%%%%%%
n_1 = 20:34; %selection for n1
d = [2,3,4]; % difference vector n_1-n_2 = d
color =['r','b','g']; % colors for the lines in plots
num_plots = 2;

%% set up vectors
ub_1 = zeros(length(n_1),length(d));
bound_step = zeros(length(n_1),length(d));
s_1 = zeros(length(n_1),length(d));
s_2 = zeros(length(n_1),length(d));
s_t = zeros(length(n_1),length(d));
n_2 = zeros(length(n_1),length(d));
end_time = zeros(length(n_1),length(d));
alpha = linspace(0,angle_lim,resolution);
time = zeros(length(p));
steps = zeros(2,length(p));

angle_lim = 360; %[deg] do calcuation of ub_1 for a whole rotation
resolution = 1001; %datapoints on each calculation of ub_1
%% set up figures
close all
```

```
for i =1:num_plots
  figure(i)
  grid on
  hold on
  xlabel('n_1 [-]');
  xticks(n_1)
end
%% Calculations
for j = d-(d(1)-1)  %for all j different lines of n1-n2 = d(j)

  n_2(:,j) =  n_1-d(j); %[deg] calculate n2

  s_1(:,j) = 360./(2*n_1); %[deg] step size gear 1
  s_2(:,j) = 360./(2*n_2(:,j));  %[deg] step size gear 2
  s_t(:,j) = s_2(:,j)-s_1(:,j); %[deg] smallest step size reachable

  for i = n_1-(n_1(1)-1) %for all different n1
    for p = 1:resolution %calculate steps needed take for this n1 and n2 for whole alpha ...
        vector
      [time(p), ~, steps(:,p)] = step_planner(alpha(p), s_1(i,j), s_2(i,j),  t_step);
    end
    end_time(i,j) = time(end); % total time to reach one revolution

    bound_step(i,j) = max(steps(1,:)); %find upper bound on angle of gear 1
    ub_1(i,j) = 2*bound_step(i,j)*s_1(i,j);  %find upper bound on angle of gear 1
  end

  %% plotting
  n_1_temp = n_1(s_t(:,j) <= target_s_t); %all n_1 that have a step size smaller or equal ...
      to target_s_t
  n_1_switch = n_1_temp(1); %the first n_1 that has step size smaller than target_s_t

  ub_1_temp = ub_1(s_t(:,j) <= target_s_t,j);%all ub_1 that have a step size smaller or ...
      equal to target_s_t
  ub_1_switch = ub_1_temp(1); %the first ub_1 that has step size smaller than target_s_t

  end_time_temp = end_time(s_t(:,j) <= target_s_t,j);%all end_time that have a step size ...
      smaller or equal to target_s_t
  end_time_switch = end_time_temp(1);%the first end_time that has step size smaller than ...
      target_s_t

  figure(1)  %ub_1 plot, plot lines that have s_t > target_s_t with striped line, and ...
      lines that have s_t <= target_s_t with solid line
  plot([n_1(s_t(:,j) > target_s_t)'; n_1_switch] ,[(ub_1(s_t(:,j) > target_s_t,j))', ...
      ub_1_switch] ,[color(j),'--*'],'HandleVisibility','off');
  plot(n_1(s_t(:,j) <= target_s_t),ub_1(s_t(:,j) <= target_s_t,j),[color(j),'-*']);

  figure(2)  %time plot, plot lines that have s_t > target_s_t with striped line, and ...
      lines that have s_t <= target_s_t with solid line
  plot([n_1(s_t(:,j) > target_s_t)';n_1_switch] ,[(end_time(s_t(:,j) > ...
      target_s_t,j))', end_time_switch] ,[color(j),'--*'],'HandleVisibility','off');
  plot(n_1(s_t(:,j) <= target_s_t),end_time(s_t(:,j) <= target_s_t,j),[color(j),'-*']);
end

%% final plotting
figure(1)
%plot selection markers
plot(24, ub_1(n_1 == 24, 1),'ko','MarkerSize', 15)
text(24, ub_1(n_1 == 24, 1),'    A')
plot(27, ub_1(n_1 == 27, 2),'ko','MarkerSize', 15)
text(27, ub_1(n_1 == 27, 2),'    B')
plot(34, ub_1(n_1 == 34, 3),'ko','MarkerSize', 15)
text(34, ub_1(n_1 == 34, 3),'C    ','HorizontalAlignment','right')

% extra plot info
ylabel('Maximum total rotation of gear 1 ub_1 [deg]');
set(gca,'FontSize',10)
legend(['n_1 - n_2 = ', num2str(d(1))],...
['n_1 - n_2 = ', num2str(d(2))], ...
['n_1 - n_2 = ', num2str(d(3))], ...
['Selection'],...
```

```
'Location','northoutside','Orientation','horizontal');

figure(2)
%plot selection markers
plot(24, end_time(n_1 == 24, 1),'ko','MarkerSize', 15)
text(24, end_time(n_1 == 24, 1),'    A')
plot(27, end_time(n_1 == 27, 2),'ko','MarkerSize', 15)
text(27, end_time(n_1 == 27, 2),'    B')
plot(34, end_time(n_1 == 34, 3),'ko','MarkerSize', 15)
text(34, end_time(n_1 == 34, 3),'C    ','HorizontalAlignment','right')

% extra plot info
ylabel('Total time for one revolution [s]')
set(gca,'FontSize',10)
legend(['n_1 - n_2 = ', num2str(d(1))], ...
['n_1 - n_2 = ', num2str(d(2))],  ...
['n_1 - n_2 = ', num2str(d(3))],  ...
['Selection'],...
'Location','northoutside','Orientation','horizontal');
```

Listing F.5: show_data.m

```
%% Stephan Neevel
%% Reads out log data from encoder attached to pneumatic stepper motor and
% plots time vs. measured angle and planned angle.
% Also plots angle vs indiviual measured steps

function [PositionPoints,dMeasuredSteps] = show_data(filename,purge_last,suppress_plot,shift)



[data, headers] = readplclogfile(filename); % extract data from log file



%% set up vectors
index = [];
plotje = false;
%% calculations: identify individual steps taken
for i = 1:length(data.BelievedPosition)-1
  if data.BelievedPosition(i+1) ~= data.BelievedPosition(i)
    index = [index;i-1-shift];
  end
end

if ~purge_last
  index = [index;length(data.BelievedPosition)];
  target = data.BelievedPosition(end);
else
  target = data.BelievedPosition(index(end));
end


MeasuredPos = data.MeasuredPosition-data.MeasuredPosition(1);

TimePoints = data.Time(index);
MeasuredSteps = MeasuredPos(index)
PositionPoints = data.BelievedPosition(index);

error_vec = MeasuredSteps-PositionPoints; %calculate error (not used)

dMeasuredSteps = diff(MeasuredSteps); %calculate size of individual measured steps
numsteps = length(dMeasuredSteps); %number of steps

speed = MeasuredPos(end)/data.Time(end); % average speed
disp(['Average Speed =', num2str(speed), 'deg/s']);

designed_stepsize = target/numsteps;
```

```
%avg_y = (dMeasuredSteps(1:2:end) + dMeasuredSteps(2:2:end))/2;
%avg_x = PositionPoints(2:2:end)-designed_stepsize/2;



speed = diff(MeasuredPos)/0.01;


if  target > 300
    plotje = true;
    round(800/target);
end

if ~suppress_plot

  %% plot time vs planned position and measured position
  figure
  set(gca,'FontSize',14)
  hold on
  grid on;
  plot(data.Time,data.BelievedPosition)
  plot(data.Time, MeasuredPos)

  xlabel('Time [s]');
  ylabel('Position [deg]');

  plot(TimePoints(2:end),PositionPoints(2:end),'g*');
  plot(TimePoints(2:end),MeasuredSteps(2:end),'r*');

  legend('Planned Step Pattern','Measured Position',...
  'Planned Position Steps','Measured Position Steps');
  if data.BelievedPosition(end) < 0
    legend('location','northeast');
  else
    legend('location','southeast');
  end

  if plotje
      x1 = 2; %limit for small subplot
      x2 = x1;

      y1 = 1.1*data.BelievedPosition(data.Time==x1);
      y2 = 0.7*target;

      rectangle('Position',[0 0 x1 y1])
      plot([x1 x2],[y1 y2],'k-','HandleVisibility','off')
      axes('position',[0.19 0.6 0.3 0.3])
      box on % put box around new pair of axes
      set(gca,'FontSize',14)
      hold on
      grid on
      ylim([0,y1])
      s = find(data.Time == x1);
      d = find(TimePoints < data.Time(s));
      f = d(end);
      plot(data.Time(1:s),data.BelievedPosition(1:s));
      plot(data.Time(1:s),MeasuredPos(1:s));
      plot(TimePoints(2:f),PositionPoints(2:f),'g*');
      plot(TimePoints(2:f),MeasuredSteps(2:f),'r*');
  end


  %%  plot individual measured step sizes
  figure
  set(gca,'FontSize',14) % Creates an axes and sets its FontSize to 18
  %ylim([1 11]);
  hold on
  grid on
  plot(PositionPoints(1:end-1), dMeasuredSteps,'r-*')
  plot([PositionPoints(1) PositionPoints(end-1)],[mean(dMeasuredSteps) ...
      mean(dMeasuredSteps)],'g-')
```

```
  plot([PositionPoints(1) PositionPoints(end-1)],[designed_stepsize, designed_stepsize],'c-')
  xlabel('Position [deg]');

  ylabel('Step size [deg]');
  legend('Measured Step sizes','Mean Measured Step size','Designed Step ...
      size','location','South');

  %% plot horizontal line to see pattern in position
  if data.BelievedPosition(end) > 360
    xticks([0, 180,360,540,720])
    xlim([0 720])
    plot([360 360],ylim,'k-');
    legend('Measured Step sizes','Mean Measured Step size','Designed Step size','Split ...
        Line','location','South');
  elseif data.BelievedPosition(end) < -360
    xticks(-[0, 180,360,540,720])
     xlim([0 -720])
    plot([-360 -360],ylim,'k-');
      legend('Measured Step sizes','Mean Measured Step size','Designed Step size','Split ...
          Line','location','South');
  elseif data.BelievedPosition(end) == 360
       xticks([0, 180,360])
       xlim([0 360])
  end
 end
```

Listing F.6: plot_error_sensitivity.m

```
%% Stephan Neevel
%% Plot alpha 1 and alpha 2 vs error sensisitivy dp/dalpha of needle positioning.

%% set up vectors
a_1 = linspace(-pi, pi,50);
a_2 = linspace(-pi, pi,50);
dalpha = 0.00001; %small delta alpha
space = zeros(length(a_1),length(a_2));

%% calculations
for i = 1:length(a_1)
  i
  for j = 1:length(a_2)
     space(i,j) = pos_error(dalpha,[a_1(i) a_2(j)])/dalpha;
  end
end

%% plotting
figure
hold on
grid on
surf(a_2*180/pi, a_1*180/pi, space);
xlabel('\alpha_2 [deg]');
ylabel('\alpha_1 [deg]');
zlabel('error sensitity dp/d\alpha [mm]')
```

Listing F.7: find_dalpha.m

```
%% Stephan Neevel
%solve inverse kinematics problem pos_error_target = pos_e(dalpha) for
%dalpha.


%% set up
alpha = [0 0]; % rad
delta_init = 0.001; %pick initial valve for delta alpha
delta = delta_init;
error_target = 3.42; %target error to be reached.
dpos_e = inf;
```

```
%% calculations
while abs(dpos_e) > 0.0001
    pos_e = pos_error(delta, alpha); %calculate position error with current delta
    dpos_e = pos_e-error_target; % calculate difference between target and current value ...
        for position error
    delta = delta -0.1*delta*dpos_e;  %update new delta.
end

%% outputs
delta_deg = delta*180/pi %output found delta in degrees
```

Listing F.8: pos_error.m

```
%% Stephan Neevel
%% Returns euclidian error in mm for small delta difference in alpha
% Input: delta: [rad] small difference in alpha
%        alpha 1x2: [rad] vector of angles
function error = pos_error(delta,alpha)
P_old = coord(alpha);
P = coord(alpha+delta);
error = norm(P-P_old);
end
```

Listing F.9: coord.m

```
%% Stephan Neevel
%% returns coord of needle in mm for rotation of segments
%input: [alpha(1) alpha(2)], [rad] rotation of segment 1 and 2

function P = coord(alpha)
theta_1 = 60*pi/180; %[rad] geometry angle of segment 1
theta_2 = 52.5*pi/180; %[rad] geometry angle of segment 2
l_needle = 250; %[mm] length of needle

R = Ry(alpha(1))*Rx(-theta_1)*Ry(alpha(2))*Rx(-theta_2); %Rotation Matrix
P = R*[0 l_needle 0]'; % coordinates of end effector
end
```

Listing F.10: Rx.m

```
%% Stephan Neevel
%% Rotation matrix around right hand x,
% Input: phi [rad]
function R = Rx(phi)
R = [1 0 0;
     0 cos(phi) -sin(phi);
     0 sin(phi) cos(phi)];
end
```

Listing F.11: Ry.m

```
%% Stephan Neevel
%% Rotation matrix around right hand y,
% Input: phi [rad]
function R = Ry(phi)
R = [cos(phi) 0 sin(phi);
     0 1 0;
     -sin(phi) 0 cos(phi)];
end
```

G

BECKHOFF CODE

Signal logger code made by Rob Reilink is in the Demcon Repository.

Listing G.1: Program definition of Program MAIN

```
// Main program of pneumatic stepper motor
// Stephan Neevel
PROGRAM MAIN
VAR
    // states
    state: States;

    //variables
    planned_step_1: INT;
    planned_step_2: INT;
    max_step_1: INT;
    pos_step_1: INT:=0;
    pos_step_2: INT:=0;
    d_step_1: INT;
    d_step_2: INT;

    t_tot:LREAL; //total step time

    caseID: INT; // caseID for step execution of movement

    // homing
    homing_case:INT:=0; // caseID for homing
    homing_steps_executed: INT:=0;

    // timers
    motor_timer:ton;

    // step executers
    step_1_CW_exe:CW_executer;
    step_1_CCW_exe:CCW_executer;
    n_step_1_executed: INT:=0;

    step_2_CW_exe:CW_executer;
    step_2_CCW_exe:CCW_executer;
    n_step_2_executed: INT:=0;

    // turn around executers
    turn_around:turn_around;
    turned_around: BOOL:=FALSE;

    // logging
    logger:FB_SignalLogger;
    bLogInitDone: BOOL:=FALSE;
END_VAR
```

Listing G.2: Implementation of main.TcPOU

```
CASE state OF
    States.init: //initialize
        IF NOT bLogInitDone THEN    // if logging was not initialized
            init_logger();
            bLogInitDone:=TRUE;
        END_IF
        IF GVL.home THEN  // if homing button was pressed in GUI
            state:=states.homing;
            GVL.home:=FALSE;
        END_IF

    States.homing:      //home: first do 8 steps CCW with gear 1,
                        //then turn around and do 3 steps CW with gear 1
        IF homing_case = 0 THEN
            IF NOT (homing_steps_executed = ABS(8))  THEN // take steps CCW with gear 1
                step_1_CCW_exe(stepsize:=gvl.stepsize_g1,pos_step:=pos_step_1,gear_valve:=
                               gvl.gear_1_valve, n_step_executed:= homing_steps_executed);
            ELSE // done CCW stepping
                homing_steps_executed:=0;
                pos_step_1:=-4;
                pos_step_2:=-1;
                homing_case:=1;
            END_IF
        END_IF

        IF homing_case = 1 THEN //turn around
            IF NOT turned_around THEN
                turn_around(sum_stepsizes:=gvl.stepsize_g1+gvl.stepsize_g2,turned_around:=
                            turned_around,pos_step_1:=pos_step_1,pos_step_2:=pos_step_2);
            ELSE //done turning around
                homing_case:= 2;
            END_IF
        END_IF

        IF homing_case = 2 THEN //steps CW with gear 1
            IF NOT (homing_steps_executed = 3) THEN //step CW with gear 1
                step_1_CW_exe(stepsize:=gvl.stepsize_g1,pos_step:=pos_step_1,gear_valve:=
                              gvl.gear_1_valve, n_step_executed:= homing_steps_executed);
            ELSE //done stepping and homing of gear 1
                gvl.reset_encoder_count:= TRUE; //put encoder to zero
                motor_timer(IN:=TRUE, PT:= T#100MS); // wait for motor to finish its movement
                IF motor_timer.Q THEN //reset used variables and proceed to next state
                    motor_timer(IN:=FALSE);
                    gvl.reset_encoder_count:= FALSE;
                    homing_steps_executed:=0;
                    turned_around:=FALSE;
                    homing_case:=0;
                    gvl.move_button_invisible:=FALSE; //make move button visible
                    state:= states.hold_CW;
                END_IF
            END_IF
        END_IF

        IF GVL.stop_move THEN //stopped moving by user
            IF gvl.direction_CW THEN
                state:= states.hold_CW;  //hold CW position state
            ELSE
                state:= states.hold_CCW; //hold CCW position state
            END_IF
            //reset axis and variables
            step_1_CW_exe.reset(stepsize:=gvl.stepsize_g1,pos_step:=pos_step_1,gear_valve:=
                                gvl.gear_1_valve,n_step_executed:=homing_steps_executed);
            step_1_CCW_exe.reset(stepsize:=gvl.stepsize_g1,pos_step:=pos_step_1,gear_valve:=
                                 gvl.gear_1_valve,n_step_executed:=homing_steps_executed);
            GVL.stop_move:=FALSE;
            homing_steps_executed:=0;
            turned_around:=FALSE;
            homing_case:=0;
        END_IF
```

```
States.hold_CW: //state of holding position with CW ratchet engaged.
                //Check if user want to start moving or do homing.
    gvl.ratchet_CW:= TRUE;
    gvl.ratchet_CCW:=FALSE;
    IF gvl.start_move THEN //if user presses button to start moving
        state:= states.planning;
        gvl.start_move:= FALSE;
    END_IF

    IF GVL.home THEN //if user presses button to home
        state:=states.homing;
        GVL.home:=FALSE;
    END_IF

States.hold_CCW: //state of holding positions with CCW ratchet engaged.
                //Check if user want to start moving or do homing.
    gvl.ratchet_CW:= FALSE;
    gvl.ratchet_CCW:= TRUE;
    IF gvl.start_move THEN //if user presses button to start moving
        state:= states.planning;
        gvl.start_move:= FALSE;
    END_IF

    IF GVL.home THEN //if user presses button to home
        state:=states.homing;
        GVL.home:=FALSE;
    END_IF

States.planning: // step planning
    logger.bEnable := TRUE; //enable logging
    //plan steps
    step_planner(angle:=gvl.des_pos, s_1:= GVL.stepsize_g1, s_2:= GVL.stepsize_g2, k_1 =>
                 planned_step_1, k_2 => planned_step_2, max_step_1 =>max_step_1);

    d_step_1:= planned_step_1-pos_step_1; //d_1 = k_1-p_1
    d_step_2:= planned_step_2-pos_step_2; //d_2 = k_2-p_2

    IF gvl.last_direction_CW THEN // step planning to compensate for turn-around.
        // assign caseID for use in rotate state. CaseID matches with the
        // appendix table step planing and compensation in the report.
        IF d_step_1 > 0 AND d_step_2 > 0 THEN
            caseID:=1;
        END_IF
        IF d_step_1 > 0 AND d_step_2 = 0 THEN
            caseID:=2;
        END_IF
        IF d_step_1 >= 0 AND d_step_2 < 0 THEN
            IF planned_step_1 = max_step_1 AND d_step_1 = 0 THEN
            // special case where gear 1 is in its max position
                caseID:=0;
            ELSE
                caseID:=3;
            END_IF
        END_IF
        IF d_step_1 = 0 AND d_step_2 > 0 THEN
            caseID:=4;
        END_IF
        IF d_step_1 = 0 AND d_step_2 = 0 THEN
            caseID:=5;
        END_IF

        IF d_step_1 < 0 AND d_step_2 >= 0 THEN
            caseID:=6;
        END_IF
        IF d_step_1 < 0 AND d_step_2 < 0 THEN
            caseID:=7;
        END_IF
    ELSE // last direction was CCW
        IF d_step_1 > 0 AND d_step_2 > 0 THEN
            caseID:=8;
```

```
            END_IF
            IF d_step_1 > 0 AND d_step_2 <= 0 THEN
                caseID:=9;
            END_IF
            IF d_step_1 <= 0 AND d_step_2 > 0 THEN
                IF planned_step_1 = -max_step_1 AND d_step_1 = 0 THEN
                // special case where gear 1 is in its max position
                    caseID:=14;
                ELSE
                    caseID:=10;
                END_IF
            END_IF
            IF d_step_1 = 0 AND d_step_2 = 0 THEN
                caseID:=5;
            END_IF

            IF d_step_1 = 0 AND d_step_2 < 0 THEN
                caseID:= 11;
            END_IF
            IF d_step_1 < 0 AND d_step_2 = 0 THEN
                caseID:= 12;
            END_IF
            IF d_step_1 < 0 AND d_step_2 < 0 THEN
                caseID:= 13;
            END_IF

        END_IF
        state:= states.rotate;  //done planning, start rotating

    States.rotate:
        // actions according to appendix table of step planning and compensation
        CASE caseID OF
            0: //turn around, CCW |d_2|, turn around
            IF NOT turned_around THEN
                turn_around(sum_stepsizes:=gvl.stepsize_g1+gvl.stepsize_g2,turned_around:=
                            turned_around,pos_step_1:=pos_step_1,pos_step_2:=pos_step_2);
            END_IF
            IF turned_around THEN
                IF NOT (n_step_2_executed = ABS(d_step_2)) THEN
                    step_2_CCW_exe(stepsize:=gvl.stepsize_g2,pos_step:=pos_step_2,gear_valve:=
                                   gvl.gear_2_valve,n_step_executed:=n_step_2_executed);
                ELSE
                    turned_around:= FALSE;
                END_IF
            END_IF
            1:  //CW |d_1|, CW |d_2|
            IF NOT (n_step_1_executed = ABS(d_step_1)) THEN
                step_1_CW_exe(stepsize:=gvl.stepsize_g1,pos_step:=pos_step_1,gear_valve:=
                              gvl.gear_1_valve,n_step_executed:=n_step_1_executed);
            ELSIF NOT (n_step_2_executed = ABS(d_step_2)) THEN
                step_2_CW_exe(stepsize:=gvl.stepsize_g2,pos_step:=pos_step_2,gear_valve:=
                              gvl.gear_2_valve,n_step_executed:=n_step_2_executed);
            END_IF
            2: //CW |d_1|
            IF NOT (n_step_1_executed = ABS(d_step_1)) THEN
                step_1_CW_exe(stepsize:=gvl.stepsize_g1,pos_step:=pos_step_1,gear_valve:=
                              gvl.gear_1_valve,n_step_executed:=n_step_1_executed);
            END_IF
            3:  //CW |d_1|+1, turn around, CCW |d_2|-1
            IF NOT (n_step_1_executed = ABS(d_step_1)+1) THEN
                step_1_CW_exe(stepsize:=gvl.stepsize_g1,pos_step:=pos_step_1,gear_valve:=
                              gvl.gear_1_valve,n_step_executed:=n_step_1_executed);
            ELSIF NOT turned_around THEN
                turn_around(sum_stepsizes:=gvl.stepsize_g1+gvl.stepsize_g2,turned_around:=
                            turned_around,pos_step_1:=pos_step_1,pos_step_2:=pos_step_2);
            END_IF
            IF turned_around AND NOT (n_step_2_executed = ABS(d_step_2)-1) THEN
                step_2_CCW_exe(stepsize:=gvl.stepsize_g2,pos_step:=pos_step_2,gear_valve:=
                               gvl.gear_2_valve,n_step_executed:=n_step_2_executed);
            END_IF
            4: // CW |d_2|
```

```
IF NOT (n_step_2_executed = ABS(d_step_2)) THEN
    step_2_CW_exe(stepsize:=gvl.stepsize_g2,pos_step:=pos_step_2,gear_valve:=
                  gvl.gear_2_valve,n_step_executed:=n_step_2_executed);
END_IF
5:
//done
6: // CW |d_2|+1, turn around, CCW |d_1|-1
IF NOT (n_step_2_executed = ABS(d_step_2)+1) THEN
    step_2_CW_exe(stepsize:=gvl.stepsize_g2,pos_step:=pos_step_2,gear_valve:=
                  gvl.gear_2_valve,n_step_executed:=n_step_2_executed);
ELSIF NOT turned_around THEN
    turn_around(sum_stepsizes:=gvl.stepsize_g1+gvl.stepsize_g2,turned_around:=
                turned_around,pos_step_1:=pos_step_1,pos_step_2:=pos_step_2);
END_IF
IF turned_around AND NOT (n_step_1_executed = ABS(d_step_1)-1) THEN
    step_1_CCW_exe(stepsize:=gvl.stepsize_g1,pos_step:=pos_step_1,gear_valve:=
                   gvl.gear_1_valve,n_step_executed:=n_step_1_executed);
END_IF
7: // turn around, CCW |d_1|-1, CCW |d_2|-1
IF NOT turned_around THEN
    turn_around(sum_stepsizes:=gvl.stepsize_g1+gvl.stepsize_g2,turned_around:=
                turned_around,pos_step_1:=pos_step_1,pos_step_2:=pos_step_2);
ELSIF NOT (n_step_1_executed = ABS(d_step_1)-1) THEN
    step_1_CCW_exe(stepsize:=gvl.stepsize_g1,pos_step:=pos_step_1,gear_valve:=
                   gvl.gear_1_valve,n_step_executed:=n_step_1_executed);
END_IF
IF turned_around AND NOT (n_step_2_executed = ABS(d_step_2)-1) THEN
    step_2_CCW_exe(stepsize:=gvl.stepsize_g2,pos_step:=pos_step_2,gear_valve:=
                   gvl.gear_2_valve,n_step_executed:=n_step_2_executed);
END_IF
8: // turn around, CW |d_1|-1, CW |d_2|-1
IF NOT turned_around THEN
    turn_around(sum_stepsizes:=gvl.stepsize_g1+gvl.stepsize_g2,turned_around:=
                turned_around,pos_step_1:=pos_step_1,pos_step_2:=pos_step_2);
ELSIF NOT (n_step_1_executed = ABS(d_step_1)-1) THEN
    step_1_CW_exe(stepsize:=gvl.stepsize_g1,pos_step:=pos_step_1,gear_valve:=
                  gvl.gear_1_valve,n_step_executed:=n_step_1_executed);
END_IF
IF turned_around AND NOT (n_step_2_executed = ABS(d_step_2)-1) THEN
    step_2_CW_exe(stepsize:=gvl.stepsize_g2,pos_step:=pos_step_2,gear_valve:=
                  gvl.gear_2_valve,n_step_executed:=n_step_2_executed);
END_IF
9: // CCW |d_2|+1, turn around, CW |d_1|-1
IF NOT (n_step_2_executed = ABS(d_step_2)+1) THEN
    step_2_CCW_exe(stepsize:=gvl.stepsize_g2,pos_step:=pos_step_2,gear_valve:=
                   gvl.gear_2_valve,n_step_executed:=n_step_2_executed);
ELSIF NOT turned_around THEN
    turn_around(sum_stepsizes:=gvl.stepsize_g1+gvl.stepsize_g2,turned_around:=
                turned_around,pos_step_1:=pos_step_1,pos_step_2:=pos_step_2);
END_IF
IF turned_around AND NOT (n_step_1_executed = ABS(d_step_1)-1) THEN
    step_1_CW_exe(stepsize:=gvl.stepsize_g1,pos_step:=pos_step_1,gear_valve:=
                  gvl.gear_1_valve,n_step_executed:=n_step_1_executed);
END_IF
10: // CCW |d_1|+1, turn around, CW |d_2|-1
IF NOT (n_step_1_executed = ABS(d_step_1)+1) THEN
    step_1_CCW_exe(stepsize:=gvl.stepsize_g1,pos_step:=pos_step_1,gear_valve:=
                   gvl.gear_1_valve,n_step_executed:=n_step_1_executed);
ELSIF NOT turned_around THEN
    turn_around(sum_stepsizes:=gvl.stepsize_g1+gvl.stepsize_g2,turned_around:=
                turned_around,pos_step_1:=pos_step_1,pos_step_2:=pos_step_2);
END_IF
IF turned_around AND NOT (n_step_2_executed = ABS(d_step_2)-1) THEN
    step_2_CW_exe(stepsize:=gvl.stepsize_g2,pos_step:=pos_step_2,gear_valve:=
                  gvl.gear_2_valve,n_step_executed:=n_step_2_executed);
END_IF
11: // CCW |d_2|
IF NOT (n_step_2_executed = ABS(d_step_2)) THEN
    step_2_CCW_exe(stepsize:=gvl.stepsize_g2,pos_step:=pos_step_2,gear_valve:=
                   gvl.gear_2_valve,n_step_executed:=n_step_2_executed);
END_IF
```

```
            12: // CCW |d_1|
            IF NOT (n_step_1_executed = ABS(d_step_1)) THEN
                step_1_CCW_exe(stepsize:=gvl.stepsize_g1,pos_step:=pos_step_1,gear_valve:=
                               gvl.gear_1_valve,n_step_executed:=n_step_1_executed);
            END_IF
            13: // CCW |d_1|, CCW |d_2|
            IF NOT (n_step_1_executed = ABS(d_step_1)) THEN
                step_1_CCW_exe(stepsize:=gvl.stepsize_g1,pos_step:=pos_step_1,gear_valve:=
                               gvl.gear_1_valve,n_step_executed:=n_step_1_executed);
            ELSIF NOT (n_step_2_executed = ABS(d_step_2)) THEN
                step_2_CCW_exe(stepsize:=gvl.stepsize_g2,pos_step:=pos_step_2,gear_valve:=
                               gvl.gear_2_valve,n_step_executed:=n_step_2_executed);
            END_IF
            14: // turn around, CW |d_2|, turn around
            IF NOT turned_around THEN
                turn_around(sum_stepsizes:=gvl.stepsize_g1+gvl.stepsize_g2,turned_around:=
                            turned_around,pos_step_1:=pos_step_1,pos_step_2:=pos_step_2);
            END_IF
            IF turned_around THEN
                IF NOT (n_step_2_executed = ABS(d_step_2)) THEN
                    step_2_CW_exe(stepsize:=gvl.stepsize_g2,pos_step:=pos_step_2,gear_valve:=
                                  gvl.gear_2_valve,n_step_executed:=n_step_2_executed);
                ELSE
                    turned_around:= FALSE;
                END_IF
            END_IF
        END_CASE

        gvl.last_direction_CW:= gvl.direction_CW; //update last direction

        IF ((planned_step_1 = pos_step_1) AND (planned_step_2 = pos_step_2))
            OR GVL.stop_move THEN // if done moving or stopped moving by user

            motor_timer(IN:= TRUE, PT:= T#100MS); // set timer
            IF motor_timer.Q THEN // wait for movement to be really settled in the motor.
                motor_timer(IN:=FALSE);
                // set new state, depending on which last direction we moved.
                IF gvl.direction_CW THEN
                    state:= states.hold_CW;
                ELSE
                    state:= states.hold_CCW;
                END_IF
                // reset step counters
                step_1_CW_exe.reset(stepsize:=gvl.stepsize_g1,pos_step:=pos_step_1,gear_valve
                                    :=gvl.gear_1_valve,n_step_executed:=n_step_1_executed);
                step_2_CW_exe.reset(stepsize:=gvl.stepsize_g2,pos_step:=pos_step_2,gear_valve
                                    :=gvl.gear_2_valve,n_step_executed:=n_step_2_executed);
                step_1_CCW_exe.reset(stepsize:=gvl.stepsize_g1,pos_step:=pos_step_1,gear_valve
                                    :=gvl.gear_1_valve,n_step_executed:=n_step_1_executed);
                step_2_CCW_exe.reset(stepsize:=gvl.stepsize_g2,pos_step:=pos_step_2,gear_valve
                                    :=gvl.gear_2_valve,n_step_executed:=n_step_2_executed);
                turned_around:=FALSE;
                GVL.stop_move:=FALSE;
                logger.bEnable:=FALSE; //finish logging
            END_IF
        END_IF
END_CASE

gvl.act_pos:= pos_step_1*gvl.stepsize_g1 + pos_step_2*gvl.stepsize_g2; // update position.
gvl.measured_pos:= (gvl.counter_value-EXPT(2,31))*360/(4*32000);//encoder measured position
// timing delays based on the speed scale in the GUI
gvl.arr_time:=  T#200MS  - (T#200MS-T#1MS)* gvl.speed_factor/100;
gvl.ratchet_time:= 3*gvl.arr_time;
t_tot:= TIME_TO_LREAL(2*gvl.arr_time + 3*gvl.ratchet_time)*0.001; // total time for one step
gvl.speed:= gvl.stepsize_g2/t_tot;

//logging
logger();
```

Listing G.3: Program definition of Method main.init_logger

```
METHOD init_logger : BOOL
VAR_INPUT
END_VAR

VAR
    loggerFileName: STRING(255);
    tempDate: STRING(255);
    loggerDatetime: STRING(255);
END_VAR
```

Listing G.4: Implementation of Method main.init_logger

```
(* Signal logger *)
logger(
    bEnable:= FALSE,
    iDecimation:= 1,
    sFilebasename:=
'C:\Users\sne\Dropbox\Universiteit\Master 3e en 4e jaar\Afstuderen Demcon\Measurements\',
    sFileNameSuffix:= '',
    sHeader:= '',
    bRemote:= FALSE, //remote flag is set from python
    sFilename=> loggerFileName,
    sDatetime=> loggerDatetime
);
// clear all signals
logger.ClearSignals();
// add signals
logger.AddSignal(pAddress:=ADR(gvl.des_pos),iSize:=SIZEOF(gvl.des_pos),
sDescription:='PlannedPosition/f8');
logger.AddSignal(pAddress:=ADR(gvl.act_pos),iSize:=SIZEOF(gvl.act_pos),
sDescription:='ReachedPosition/f8');
logger.AddSignal(pAddress:=ADR(gvl.measured_pos),iSize:=SIZEOF(gvl.measured_pos),
sDescription:='MeasuredPosition/f8');
```

Listing G.5: Program definition of Method main.step_planner

```
//returns number of steps of gear 1 and gear 2 to be taken to reach given angle,
//by taking a minimal amount of steps of gear 1.
// Stephan Neevel
METHOD step_planner
VAR_INPUT
    angle: LREAL; //angle to reach
    s_1: LREAL; //stepsize gear 1
    s_2: LREAL; //stepsize gear 2
END_VAR

VAR
    reverse: BOOL:=FALSE;
    angle_disc: LREAL; //discretized angle reachable by combination of steps
                       //of gear 1 and gear 2
    a: DINT;
    d: DINT;
END_VAR

VAR_OUTPUT
    k_1: INT; //number of steps to be taken by gear 1.
              // A negative number means taking steps backwards.
    k_2: INT;
    max_step_1: INT;
END_VAR
```

Listing G.6: Implementation of Method main.step_planner

```
a:= LREAL_TO_INT(angle/(s_2-s_1)); // round to closest reachable discrete step
```

```
angle_disc:= a*(s_2-s_1); // discretized angle we can reach
d:= LREAL_TO_INT(angle/s_2);

k_1:= LREAL_TO_INT(-(angle_disc-d*s_2)/(s_2-s_1));
k_2:= DINT_TO_INT(d)-k_1;

max_step_1:=LREAL_TO_INT(s_1/(2*(s_2-s_1))); //Only holds for this specific design
```

Listing G.7: Program definition of Function CW_executer

```
// executes steps in CW direction for a given gear valve.
// Return updated position and number of steps
// Stephan Neevel
FUNCTION_BLOCK CW_executer
VAR_INPUT
    stepsize: LREAL;
END_VAR

VAR_IN_OUT
    pos_step: INT;
    gear_valve: BOOL;
    n_step_executed: INT;
END_VAR

VAR
    timer1: TON;
    timer2: TON;
    caseID:INT:=1;
END_VAR
```

Listing G.8: Implementation of Function CW_executer

```
//CW
IF GVL.ratchet_CW_disp < GVL.switch_angle THEN //haven't reached limit of ratchet
    GVL.ratchet_CW:= TRUE; // turn on CW pressure
    GVL.ratchet_CCW:= FALSE;
    IF NOT timer1.IN THEN // if timer hasn't been set
        gear_valve:= NOT(gear_valve); //execute step
    END_IF
    timer1(IN:= TRUE, PT:= gvl.arr_time); // set timer

    IF timer1.Q THEN //wait for execution of step
        pos_step:= pos_step + 1;    // update step counter  with CW step
        n_step_executed:= n_step_executed +1;
        GVL.ratchet_CW_disp:= GVL.ratchet_CW_disp + stepsize;

        timer1(IN:= FALSE); // reset timer
        GVL.direction_CW := TRUE;
    END_IF
ELSE // we have reached limit of ratchet: move back ratchet and re-apply pressure
    CASE caseID OF
        1:  timer2(IN:=TRUE,PT:=gvl.ratchet_time);
            IF timer2.Q THEN
                GVL.ratchet_CW:= FALSE; // turn off counter clockwise pressure
                timer2(IN:= FALSE);
                caseID:= caseID+1;
            END_IF
        2: timer2(IN:=TRUE,PT:=gvl.ratchet_time);
            IF timer2.Q THEN
                GVL.ratchet_CW:= TRUE; // turn on counter clockwise pressure
                timer2(IN:= FALSE);
                caseID:= caseID+1;
            END_IF
        3: timer2(IN:=TRUE,PT:=gvl.ratchet_time);
            IF timer2.Q THEN
                GVL.ratchet_CW_disp:= 0;
                timer2(IN:= FALSE);
```

```
                caseID:=1;
            END_IF
    END_CASE
END_IF
```

Listing G.9: Program definition of Function CCW_executer

```
// executes steps in CCW direction for a given gear valve.
// Return updated position and number of steps
FUNCTION_BLOCK CCW_executer
VAR_INPUT
    stepsize: LREAL; // step size
END_VAR

VAR_IN_OUT
    pos_step: INT;  //current position
    gear_valve: BOOL; //handle to valve to operate on gear
    n_step_executed: INT;   // number of steps executed
END_VAR

VAR
    timer1: TON;
    timer2: TON;
    caseID:INT:=1; //caseID for moving back and re-apply ratchet
END_VAR
```

Listing G.10: Action CW_executer.reset

```
timer1(IN:= FALSE);
timer2(IN:= FALSE);
n_step_executed:=0;
```

Listing G.11: Implementation of Function CCW_executer

```
// CCW
IF GVL.ratchet_CCW_disp < GVL.switch_angle THEN //haven't reached limit of ratchet
    GVL.ratchet_CCW:= TRUE; // turn on CCW pressure
    GVL.ratchet_CW:= FALSE;
    IF NOT timer1.IN THEN // if timer hasn't been set
        gear_valve:= NOT(gear_valve); //execute step
    END_IF
    timer1(IN:= TRUE, PT:= gvl.arr_time); // set timer

    IF timer1.Q THEN //wait for execution of step
        pos_step:= pos_step - 1;    // update step counter  with CCW step
        n_step_executed:= n_step_executed +1;
        GVL.ratchet_CCW_disp:= GVL.ratchet_CCW_disp + stepsize;

        timer1(IN:= FALSE);
        GVL.direction_CW := FALSE;
    END_IF
ELSE // we have reached limit of ratchet: move back ratchet and re-apply pressure
    CASE caseID OF
        1:  timer2(IN:=TRUE,PT:=gvl.ratchet_time);
            IF timer2.Q THEN
                GVL.ratchet_CCW:= FALSE; // turn off counter clockwise pressure
                timer2(IN:= FALSE);
                caseID:= caseID+1;
            END_IF
        2: timer2(IN:=TRUE,PT:=gvl.ratchet_time);
            IF timer2.Q THEN
                GVL.ratchet_CCW:= TRUE; // turn on counter clockwise pressure
                timer2(IN:= FALSE);
                caseID:= caseID+1;
            END_IF
```

```
        3: timer2(IN:=TRUE,PT:=gvl.ratchet_time);
            IF timer2.Q THEN
                GVL.ratchet_CCW_disp:= 0;
                timer2(IN:= FALSE);
                caseID:=1;
            END_IF
    END_CASE
END_IF
```

Listing G.12: Action CCW_executer.reset

```
timer1(IN:= FALSE);
timer2(IN:= FALSE);
n_step_executed:=0;
```

Listing G.13: Program defintion of Function turn_around

```
//executes turn around by moving ratchets. Updates position after turn-around
//Stephan Neevel
FUNCTION_BLOCK turn_around
VAR_INPUT
    sum_stepsizes: LREAL; // sum of step sizes
END_VAR

VAR_IN_OUT
    turned_around: BOOL;
    pos_step_1: INT;
    pos_step_2: INT;
END_VAR

VAR
    timer1: TON;
    timer2: TON;
END_VAR
```

Listing G.14: Implementation of Function turn_around

```
IF NOT GVL.direction_CW THEN //if we last moved CCW, then we now turn around to CW direction
    GVL.ratchet_CCW:= FALSE; // turn off CCW pressure
    GVL.ratchet_CCW_disp:= 0; // reset travelled distance of CCW ratchet
    timer1(IN:= TRUE, PT:= gvl.ratchet_time); // wait for CCW ratchet to move back
    IF timer1.Q THEN    // wait for CCW ratchet to move back
        GVL.ratchet_CW:= TRUE; // turn on CW pressure
        timer2(IN:= TRUE, PT:= gvl.ratchet_time); // wait for CW ratchet to move forward
        IF timer2.Q THEN // wait for CW ratchet to move forward
            timer1(IN:= FALSE); //reset timer
            timer2(IN:= FALSE); //reset timer
            GVL.ratchet_CW_disp:= GVL.ratchet_CW_disp + sum_stepsizes; //update travelled
                                                                       // CW ratchet distance
            GVL.direction_CW := TRUE;   //set last moved direction to CW
            turned_around:=TRUE; //we are done turning around
            pos_step_1:= pos_step_1+1; //update position due to turning around
            pos_step_2:= pos_step_2+1; //update position due to turning around
        END_IF
    END_IF
ELSE //We last moved CW, then we now turn around to CCW direction
    GVL.ratchet_CW:= FALSE; // turn off CW pressure
    GVL.ratchet_CW_disp:= 0;    // reset travelled distance of CW ratchet
    timer1(IN:= TRUE, PT:= gvl.ratchet_time); // wait for CW ratchet to move back
    IF timer1.Q THEN    // wait for CW ratchet to move back
        GVL.ratchet_CCW:= TRUE; // turn on CCW pressure
        timer2(IN:= TRUE, PT:= gvl.ratchet_time); // wait for CCW ratchet to move forward
        IF timer2.Q THEN // wait for CCW ratchet to move forward
            timer1(IN:= FALSE); //reset timer
            timer2(IN:= FALSE); //reset timer
```

```
            GVL.ratchet_CCW_disp:= GVL.ratchet_CCW_disp +sum_stepsizes; //update travelled CCW
                                                                        //ratchet distance
            GVL.direction_CW := FALSE;  //set last moved direction to CCW
            turned_around:=TRUE; //we are done turning around
            pos_step_1:= pos_step_1-1; //update position due to turning around
            pos_step_2:= pos_step_2-1; //update position due to turning around
        END_IF
    END_IF
END_IF
```

Listing G.15: Global Variable List GVL

```
{attribute 'qualified_only'}
VAR_GLOBAL
    act_pos: LREAL:=0;  //currrent position
    des_pos: LREAL:=0; //desired position to reach

    teeth_g1: INT:=27; //number of teeth on gear 1
    teeth_g2: INT:=24; //number of teeth on gear 2
    stepsize_g1: LREAL:= 360/INT_TO_LREAL(2*teeth_g1); //[deg] stepsize of gear 1 (6.666)
    stepsize_g2: LREAL:= 360/INT_TO_LREAL(2*teeth_g2); //[deg] stepsize of gear 2 (7.5)

    ratchet_CW_disp:LREAL:=0; //displacement of CW ratchet
    ratchet_CCW_disp:LREAL:=0; //displacement of CCW ratchet

    last_direction_CW: BOOL:= TRUE; //last direction of movement
    direction_CW: BOOL:=TRUE; //last direction of movement

    arr_time: TIME; //time to wait between steps
    ratchet_time: TIME; //time to wait after ratchet moves back

    // encoder
    counter_value AT %I*: UDINT; //encoder read out value
    reset_encoder_count AT %Q*: BOOL:=FALSE; // bool to reset encoder
    measured_pos: LREAL;    //measured position
    set_counter_value AT %Q*: UDINT:= LREAL_TO_UDINT(EXPT(2,31));

    //GUI buttons and inputs
    start_move: BOOL:=FALSE; //button for start of movement
    stop_move: BOOL:=FALSE; //button for stop of movement
    move_button_invisible:BOOL:=TRUE;
    home: BOOL:=FALSE;
    speed_factor:UINT:=60;
    speed:LREAL:= 0;
    switch_angle: LREAL:=6; //angle after which the ratchets move back to reapply pressure

    //outputs
    ratchet_CW AT %Q*: BOOL:=FALSE; //output ratchet CW valve (true is open)
    ratchet_CCW AT %Q*: BOOL:=FALSE; //output ratchet CWW valve (true is open)
    gear_1_valve AT %Q*: BOOL:=FALSE; // arreteer (false is left locked)
    gear_2_valve AT %Q*: BOOL:=FALSE; // arreteer (false is left locked)
END_VAR
```

Listing G.16: Enumeration States

```
{attribute 'qualified_only'}
{attribute 'strict'}
TYPE States :
(
    init := 0,
    homing,
    hold_CW,
    hold_CCW,
    planning,
    rotate
);
END_TYPE
```

Revision:	Revision description:	Revised by:	Revision date:
A	Initial version	SNE	18-04-2019

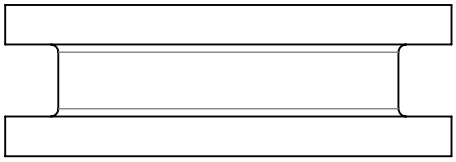

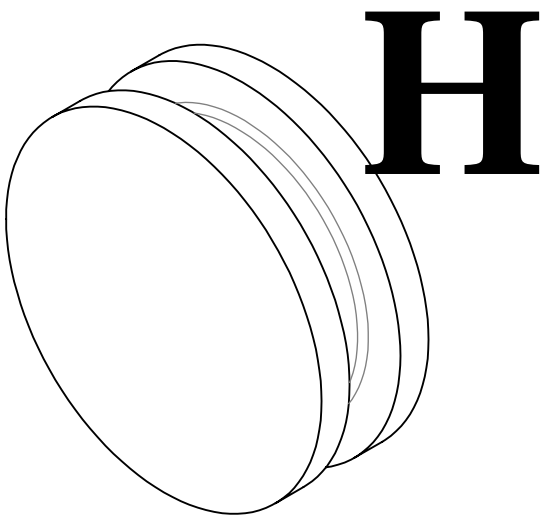

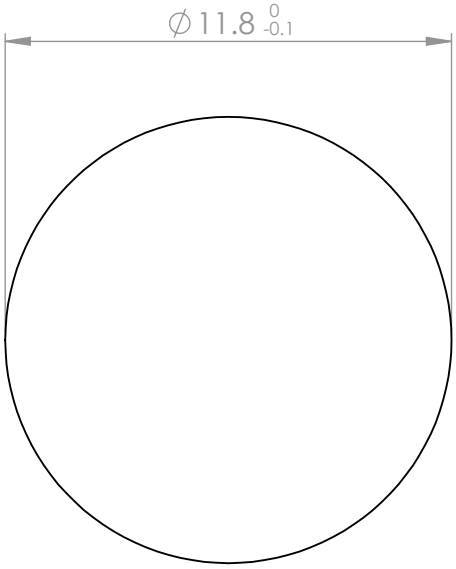

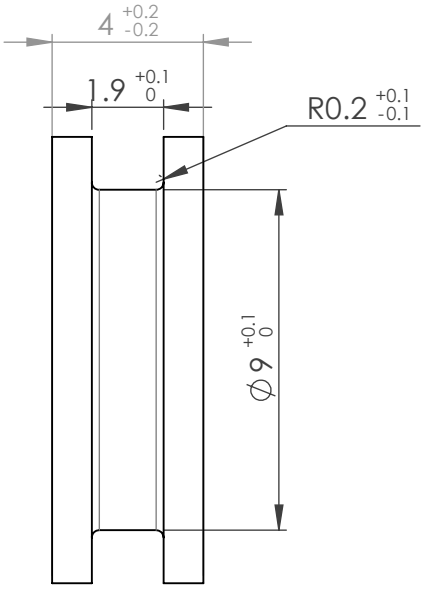

- Geometric tolerancing according to: ISO 1101 - Dimensions on drawing without tolerance indication, tolerances according to: ISO 2768-mK-(E) - Dimensions and tol. of threads according to: BS 3643 - Roughness according to: ISO 1302 - Break sharp edges according to: ISO 13715 - Dimensions apply after surface treatment				Roughness: √Ra 3,2 (3,2)	Treatment: No treatment Material: Acrylic (Medium-high impact) Extruded			
Am. proj.	Scale:	Units:	Sheet:	Format:	Drawn by:	Checked by:	Status:	Released date:
	2:1	mm	1 of 1	A4	SNE	-	Released	25-04-2019

DEMCON
advanced mechatronics

tel. +31 (0)88 115 20 00

Description:
Ratchet Piston Head

Drawing nr.: D208473

Revision: A

Revision:	Revision description:	Revised by:	Revision date:
A	Initial version	SNE	18-04-2019

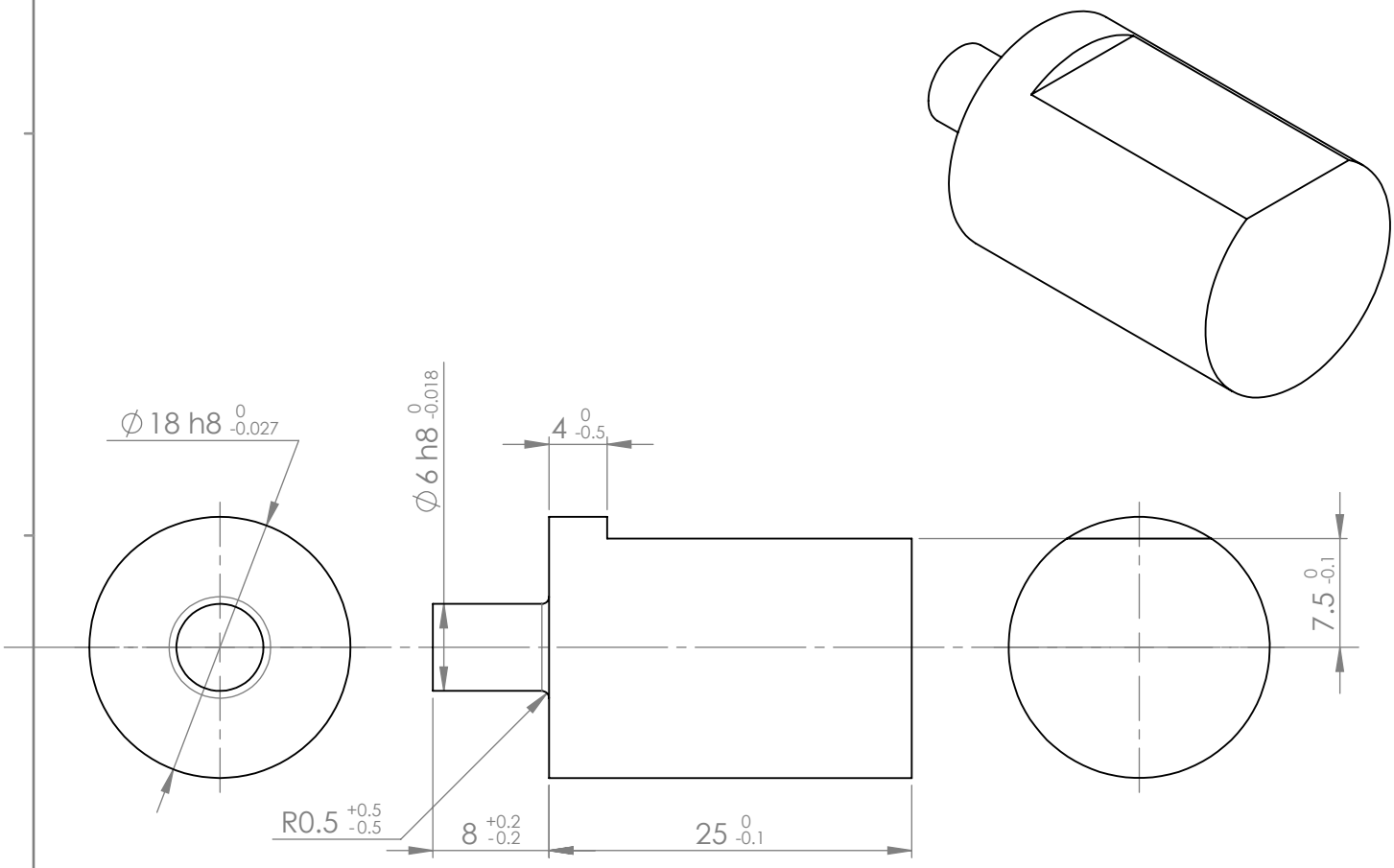

- Geometric tolerancing according to: ISO 1101 - Dimensions on drawing without tolerance indication, tolerances according to: ISO 2768-mK-(E) - Dimensions and tol. of threads according to: BS 3643 - Roughness according to: ISO 1302 - Break sharp edges according to: ISO 13715 - Dimensions apply after surface treatment				Roughness: √Ra 3,2 (3,2)	Treatment: No treatment Material: POM Acetal Copolymer Extruded		
Am. proj.	Scale:	Units:	Sheet:	Format:	Drawn by:	Checked by:	Status:	Released date:
	2:1	mm	1 of 1	A4	SNE	-	Released	19-04-2019

DEMCON
advanced mechatronics

tel. +31 (0)88 115 20 00

Description: Main Axle

Drawing nr.: D208491

Revision: A

Revision:	Revision description:	Revised by:	Revision date:
A	Initial version	SNE	18-04-2019

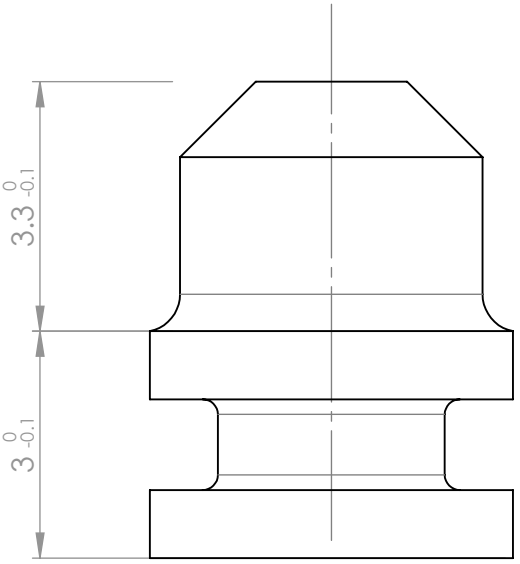

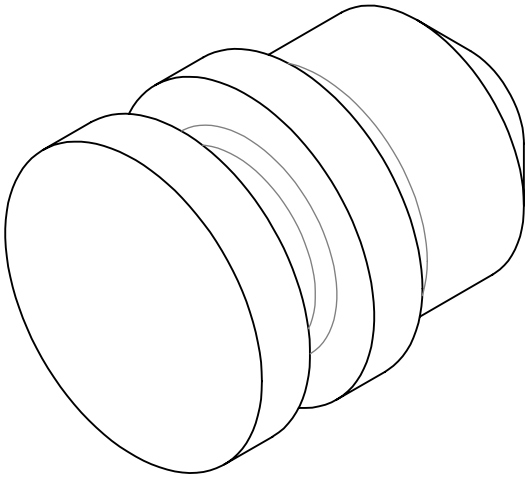

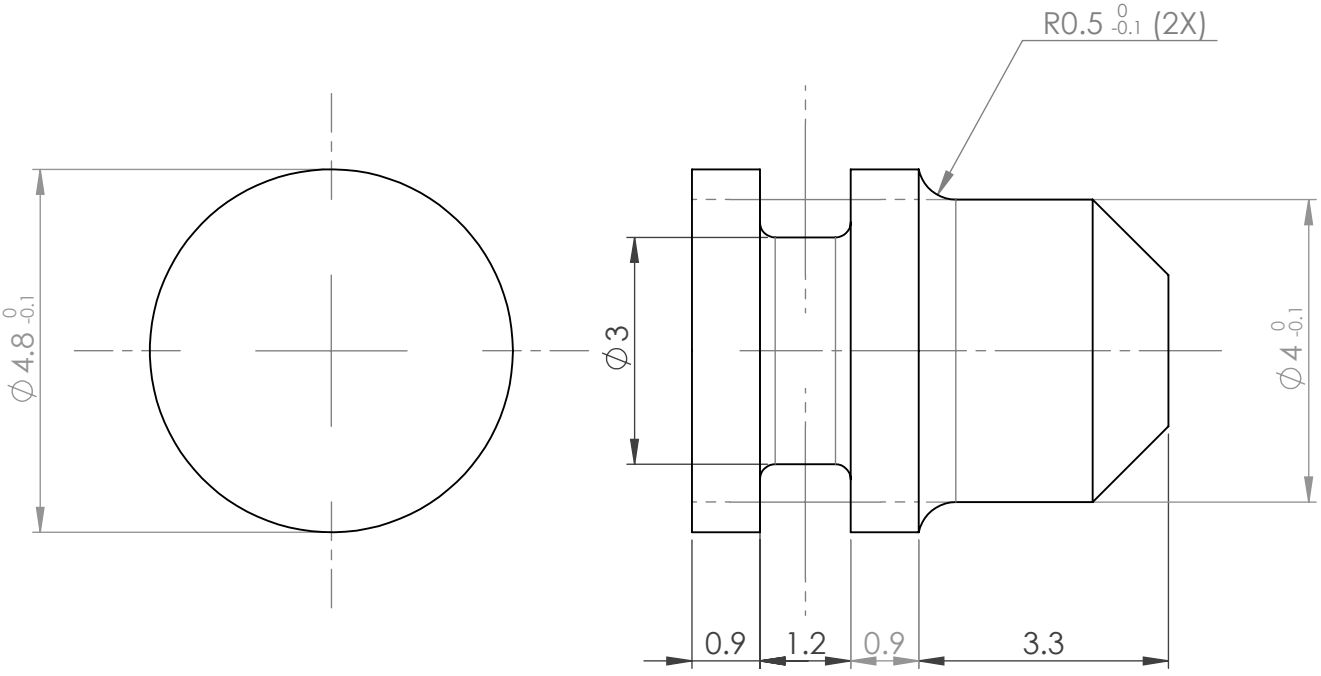

- Geometric tolerancing according to:	ISO 1101	Roughness:	Treatment:
- Dimensions on drawing without tolerance indication, tolerances according to:	ISO 2768-mK-(E)	√ Ra 3,2 (3,2)	No treatment
- Dimensions and tol. of threads according to:	BS 3643		Material:
- Roughness according to:	ISO 1302		POM Acetal Copolymer Extruded
- Break sharp edges according to:	ISO 13715		
- Dimensions apply after surface treatment			

Am. proj.	Scale:	Units:	Sheet:	Format:	Drawn by:	Checked by:	Status:	Released date:
	10:1	mm	1 of 1	A4	SNE	-	Draft	-

DEMCON
advanced mechatronics
tel. +31 (0)88 115 20 00

Description: Small Piston

Drawing nr.: D208507

Revision: A

C B A